



Terms and Conditions of Use of Digitised Theses from Trinity College Library Dublin

Copyright statement

All material supplied by Trinity College Library is protected by copyright (under the Copyright and Related Rights Act, 2000 as amended) and other relevant Intellectual Property Rights. By accessing and using a Digitised Thesis from Trinity College Library you acknowledge that all Intellectual Property Rights in any Works supplied are the sole and exclusive property of the copyright and/or other IPR holder. Specific copyright holders may not be explicitly identified. Use of materials from other sources within a thesis should not be construed as a claim over them.

A non-exclusive, non-transferable licence is hereby granted to those using or reproducing, in whole or in part, the material for valid purposes, providing the copyright owners are acknowledged using the normal conventions. Where specific permission to use material is required, this is identified and such permission must be sought from the copyright holder or agency cited.

Liability statement

By using a Digitised Thesis, I accept that Trinity College Dublin bears no legal responsibility for the accuracy, legality or comprehensiveness of materials contained within the thesis, and that Trinity College Dublin accepts no liability for indirect, consequential, or incidental, damages or losses arising from use of the thesis for whatever reason. Information located in a thesis may be subject to specific use constraints, details of which may not be explicitly described. It is the responsibility of potential and actual users to be aware of such constraints and to abide by them. By making use of material from a digitised thesis, you accept these copyright and disclaimer provisions. Where it is brought to the attention of Trinity College Library that there may be a breach of copyright or other restraint, it is the policy to withdraw or take down access to a thesis while the issue is being resolved.

Access Agreement

By using a Digitised Thesis from Trinity College Library you are bound by the following Terms & Conditions. Please read them carefully.

I have read and I understand the following statement: All material supplied via a Digitised Thesis from Trinity College Library is protected by copyright and other intellectual property rights, and duplication or sale of all or part of any of a thesis is not permitted, except that material may be duplicated by you for your research use or for educational purposes in electronic or print form providing the copyright owners are acknowledged using the normal conventions. You must obtain permission for any other use. Electronic or print copies may not be offered, whether for sale or otherwise to anyone. This copy has been supplied on the understanding that it is copyright material and that no quotation from the thesis may be published without proper acknowledgement.

The Effect *of* Bone Turnover *on* Bone Quality *and* Material Properties

Oran D. Kennedy

BA, BAI

A dissertation submitted to the University of Dublin for the degree of

Doctor in Philosophy

Trinity College Dublin

Supervisors

Prof. David Taylor Prof. Clive Lee Prof. Fergal J. O'Brien

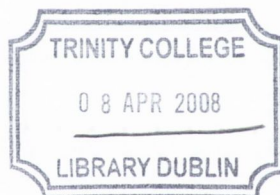
External Examiner

Prof. Mitchell Schaffler

Internal Examiner

Prof. Patrick Prendergast

April, 2007

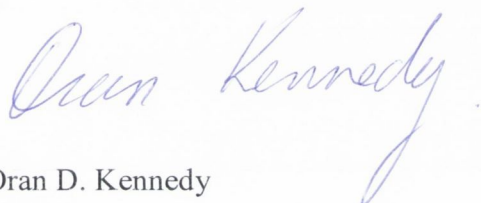


THOS
8340

DECLARATION

I declare that I am the sole author of this thesis and that the work presented here has not previously been submitted as an exercise for a degree or other qualification at any university. It consists entirely of my own work, except where references indicate otherwise.

The Library of Trinity College Dublin may lend or copy this thesis on request.



Oran D. Kennedy

26th April, 2007.

ABSTRACT

Thesis Title: Bone Quality in Osteoporosis

Author: Oran D. Kennedy

Coined in French in the 1820s as a description of a pathological state of bone tissue, the term osteoporosis made its way into the English language only in the 20th century. Unlike other medical concepts, which have not been substantially altered by progress in medical research, the definition of osteoporosis has constantly reflected the state of knowledge on the phenomenon itself (Schapira and Schapira, 1992). Over its 180 years of evolution, this definition has continuously sought to maintain a balance between physiological and clinical criteria. At present the definition, established by the National Institutes of Health (NIH) in 2000, describes osteoporosis as 'a skeletal disorder characterised by compromised bone strength predisposing to an increased risk of fracture'.

It is important to note the subtle downplaying of bone mass in this most recent definition in favour of a more generic statement regarding all of the determinants of bone strength, thereby shifting the emphasis to include bone quality. This study sought to characterise the effect of bone turnover on bone quality and material properties, in an ovariectomised (OVX) ovine animal model at 12 months post-surgery. Animals were intravenously administered five fluorochrome dyes at three-monthly intervals during the study in order to label sites of bone turnover. A study of compact bone turnover and microarchitecture, using epifluorescence microscopy and microCT respectively, was carried out on the left metatarsal. Bone turnover was increased in the OVX group compared with controls. Increased turnover resulted in increased porosity in the OVX group compared to controls. The small reduction in strength resulting from these changes compared well with our calculations which were based on the reduction in load bearing area.

Analyses of fatigue-induced microdamage in control and OVX compact bone samples showed that while numerical crack density was higher in OVX, crack surface density was higher in the controls, due to the presence of more long microcracks. It was also observed that long cracks (>300µm) tended to stop at new (labelled) osteons whereas they tended to penetrate or deflect around older (unlabelled) osteons. This shows that increased turnover has a direct effect on microcrack behaviour in bone.

The lumbar vertebrae are clinically relevant sites in terms of osteoporosis because fractures are often found to occur there. Histomorphometry of the L3 vertebra revealed increased bone turnover in cortical and trabecular compartments in OVX bone compared with controls. The microarchitectural parameters; trabecular number, thickness and separation, relative bone volume and anisotropy were not significantly different in OVX compared with controls. However, these parameters were found to differ significantly between the cranial, mid-vertebral and caudal regions of the vertebra. Biomechanical testing showed that ultimate strength and stiffness were reduced in the OVX group. This group also displayed less plastic strain and more strain due to damage compared with controls. Although no change was found in BMD as measured by DEXA, significant changes were found in bone quality parameters 12 months post-OVX. In conclusion, this study has illustrated the importance of bone turnover in relation to bone quality.

**Dedicated to my Parents,
Aidan and Timmina Kennedy.**

Go raibh mile maith agaibh!

TABLE OF CONTENTS

List of Tables.....	i
List of Figures.....	ii
Acknowledgements.....	vi
Nomenclature.....	viii
Publications.....	x

1. Introduction and literature review

1.1 Introduction.....	2
1.2 Bone types.....	4
1.2.1 Compact bone	4
1.2.2 Trabecular bone	7
1.2.3 Organic and inorganic matrix	9
1.3 Bone cells.....	10
1.3.1 Osteoprogenitor cells	10
1.3.2 Osteoblasts	11
1.3.3 Osteocytes	12
1.3.4 Osteoclasts	12
1.4 Biomechanical properties of bone	13
1.4.1 Fatigue properties.....	16
1.5 Wolff's Law, bone modelling and remodelling.....	17
1.6 Osteoporosis and bone quality	20
1.6.1 Osteoporosis.....	20
1.6.2 Bone quality	21
1.6.3 Bisphosphonates	29
1.6.4 Experimental animal models of osteoporosis	32
1.7 Objectives of this research	39

2. Experimental design, ovariectomy and fluorochrome bone labels

2.1 Introduction.....	41
2.2 Materials and Methods.....	42
2.2.1 Power analysis and sample size calculations.....	42
2.2.2 Sheep.....	43
2.2.3 Ovariectomy.....	46
2.2.4 Fluorochrome dye administration	49
2.2.5 Hormone Assays	53
2.2.6 Sacrifice	54
2.3 Results.....	56
2.3.1 Animal weights	56
2.3.2 Hormone analysis.....	57
2.3.3 Mortality	58
2.4 Discussion	59

3. The effect of OVX on bone turnover and microarchitecture in compact bone

- 3.1 Introduction..... 63
- 3.2 Materials and methods 68
 - 3.2.1 Bone histomorphometry..... 68
 - 3.2.2 MicroCT analysis..... 69
 - 3.2.3 Biomechanical testing..... 70
 - 3.2.4 Statistical analysis..... 71
- 3.3 Results..... 72
 - 3.3.1 Histomorphometric measurements 72
 - 3.3.2 Porosity measured by microCT 77
 - 3.3.3 Biomechanical testing..... 79
- 3.4 Discussion 81
- 3.5 Conclusions..... 86

4. Fatigue induced microdamage in control and OVX compact bone

- 4.1 Introduction..... 88
- 4.2 Materials and methods 94
 - 4.2.1 Sample preparation 94
 - 4.2.2 Fatigue testing..... 95
 - 4.2.3 Histological analysis 96
 - 4.2.4 Statistical analysis..... 98
- 4.3 Results..... 99
 - 4.3.1 Fatigue testing..... 99
 - 4.3.2 Crack density and crack surface density 100
 - 4.3.3 Crack interaction with osteons..... 103
- 4.4 Discussion 108
- 4.5 Conclusions..... 116

5. The effects of osteoporosis on bone quality in ovine vertebrae	
5.1 Introduction.....	118
5.2 Materials and methods	123
5.2.1 Sample preparation	123
5.2.2 DEXA scanning	123
5.2.3 Histological preparation.....	125
5.2.4 Histological analysis	127
5.2.5 MicroCT analysis.....	128
5.2.6 Biomechanical testing.....	129
5.2.7 Statistical analysis.....	131
5.3 Results.....	132
5.3.1 DEXA scanning	132
5.3.2 Histomorphometry	132
5.3.3 MicroCT data	134
5.3.4 Biomechanical testing.....	140
5.4 Discussion	143
5.5 Conclusions.....	153

6. Discussion

6.1 Bone quality and osteoporosis	156
6.2 Ovine animal model	157
6.3 Bone turnover and microarchitecture in compact bone	159
6.4 Fatigue properties and crack behaviour in compact bone.....	161
6.5 BMD, bone quality and bone strength in the vertebral body	164
6.6 Future work	169
6.7 Conclusions.....	173

References.....	175
------------------------	------------

Appendices.....	197
------------------------	------------

LIST of TABLES

Table 1.1:	Strength and elastic modulus data for compact bone in compression, tension and torsion (Reilly, 1974; Burstein, 1976).....	14
Table 1.2:	Microdamage analysis of the 3 rd lumbar vertebra, left ilium, 2 nd thoracic spinous process and right femoral neck (Mashiba et al, 2001).....	32
Table 2.1:	Animal groups, ear-tag numbers and microchip numbers.....	45
Table 2.2:	List of fluorochrome dyes, solution concentrations and dosages...	51
Table 2.3:	Timetable of events and fluorochrome administrations during year 1.....	53
Table 2.4:	Detail of labelling system used to store all of the bones from each sheep.....	55
Table 2.5:	Mean, minimum and maximum levels of P4 and E2 from control and OVX groups.....	58
Table 3.1:	Bone dimensions and resorption cavity number in control and OVX groups.....	72
Table 3.2:	Labelled osteon densities in control and OVX groups at 0,3,6,9 and 12 months post-OVX.....	75
Table 4.1:	Protocol for <i>en bloc</i> staining of compact bone with basic fuchsin.....	96
Table 4.2:	Protocol for the preparation of ground sections of bone for histological analysis.....	97
Table 4.3:	Criteria for identifying microcracks in bone (Lee et al, 1998).....	98
Table 4.4 A:	Relationship between material strength, fibre diameter and spacing, to crack initiation and propagation (Adapted from Martin and Burr, 1989).....	110
Table 4.4 B:	Relationship between control and OVX bone and crack initiation and propagation.	110
Table 5.1:	Mean cortical and trabecular bone area and turnover for L3 from control and OVX sheep.....	133
Table 5.2:	Trabecular parameters Tb.N, Tb.Th and Tb.Sp from our study and others from the literature.	146
Table 5.3:	Trabecular parameters BV/TV and DA from our study and others from the literature.	148

LIST of FIGURES

Figure 1.1:	Coronal section through a human femur showing compact bone at the external surfaces and trabecular or cancellous bone in the internal aspect.....	3
Figure 1.2:	Schematic drawing of the microstructure of compact bone tissue (Junqueira and Carneiro, 1998).....	7
Figure 1.3:	Schematic drawing of trabecular bone tissue in the endosteal region of a long bone and a photograph of trabecular bone structure in the distal end of a human femur (Fleisch, 1997).....	9
Figure 1.4:	Schematic drawing of the activity of osteoclasts, osteoblasts and osteocytes (Junqueira and Carneiro, 1998).....	11
Figure 1.5:	Schematic drawing of a Haversian canal, bone lamellae, osteocytes, lacunae and the cement line (Junqueira and Carneiro, 1998).....	13
Figure 1.6:	Graphical representations of the elastic modulus and the ultimate compressive strength of cortical bone, other tissues and biomaterials (An and Draughn, 2000).....	15
Figure 1.7:	S–N type plot of human vertebral trabecular bone (Haddock, 2000).....	17
Figure 1.8:	Schematic of the major steps in the bone remodelling cycle.....	19
Figure 2.1:	Surgically removing sheep ovaries through a midline ventral laparotomy.....	47
Figure 2.2:	Apparatus for sterilising fluorochrome dyes using a VacuCap ® filtration device.....	52
Figure 2.3:	Box plot of the weights of control and OVX animals at the time of each fluorochrome administration.....	57
Figure 3.1:	Graph of incidence of osteoporotic fracture according to serum carboxyterminal crosslinked telopeptide of type I collagen (S-ICTP) levels and femoral neck BMD. Case-cohort control study of 151 older men from the Dubbo Epidemiological Study (DOES) followed prospectively over 6.3 years (Meier et al 2004).....	64
Figure 3.2:	Cross section through a cortical bone shaft.....	65
Figure 3.3:	Illustration of a full sheep skeleton with the left metatarsal bone highlighted.....	68
Figure 3.4:	Intracortical bone turnover sites labelled with different fluorochrome dyes at X4 magnification from control and OVX bone. Images were viewed using blue epifluorescence ($\lambda=470\text{nm}$).....	73

Figure 3.5:	The number of intracortical labelled osteons in control and control and OVX bone samples at 0, 3, 6, 9, 12 months post-OVX.....	76
Figure 3.6:	μ CT reconstruction of a portion of ovine compact bone from the mid-diaphysis of the left metatarsal.....	77
Figure 3.7:	The intracortical porosity, calculated using μ CT techniques, of control and OVX compact bone samples.....	78
Figure 3.8:	(a) The ultimate compressive strength (b) Young's modulus and (c) work to fracture of control and OVX compact bone samples.....	79
Figure 4.1:	Typical three-phase damage accumulation history as a result of fatigue loading in a composite material (Adapted from Martin and Burr, 1989).....	90
Figure 4.2:	Schematic drawing of the location and dimensions of the beam specimens of cortical bone from the right metatarsal.....	94
Figure 4.3:	Schematic of apparatus used to fatigue-load cortical bone specimens in 3-point bending.....	95
Figure 4.4:	Probability of failure as a function of the number of cycles to failure from fatigue tests of control and OVX bone samples at a stress range of 110MPa.....	99
Figure 4.5:	Graph of total Cr.Dn in control and OVX bone samples.....	100
Figure 4.6:	Graph of Cr.Dn in compressive and tensile regions of OVX and control bone samples.....	101
Figure 4.7:	Graph of Cr.S.Dn in control and OVX bone samples.....	102
Figure 4.8:	Graph of long crack (>300 μ m) density in control and OVX groups.....	102
Figure 4.9:	Microcrack interaction with labelled and unlabelled osteons.....	103
Figure 4.10:	Pooled data from OVX and control groups of microcrack location. Cracks were classified as interstitial, penetrating old (unlabelled) osteons or penetrating new (labelled) osteons.	104
Figure 4.11:	Microcracks viewed using UV epifluorescence in an area of old osteons where cracks are seen to deflect around osteons and in an area of new (labelled) osteons where cracks tend to be attracted towards, and then stopped at the boundary of the osteon.....	104
Figure 4.12:	Schematic diagram of the behaviour of microcracks in relation to old (unlabelled) osteons and new (labelled) osteons.	105
Figure 4.13:	Long microcracks viewed using UV epifluorescence showing cracks deflecting around old (unlabelled) osteons and stopping at the border of new (labelled) osteons.....	106

Figure 4.14:	Graph of the number of crack deflections around old osteons compared with new osteons.....	107
Figure 4.15:	Graph of the number of long cracks that stopped old osteons compared with new osteons.....	107
Figure 4.16:	Experimental data on the fatigue strength of bone from different animals plotted as a function of the stressed volume of the bone or sample (Taylor, 2000).....	113
Figure 5.1:	Image of the apparatus used to carry out DEXA scanning of the L3 lumbar vertebrae.....	123
Figure 5.2:	Schematic diagram of the apparatus used to align vertebrae prior to scanning.....	124
Figure 5.3:	Image of an L3 vertebra clamped in a diamond saw with a 5mm portion being removed from the cranial aspect.....	125
Figure 5.4:	An L3 vertebra with histological sections which have been removed cranially and caudally.....	126
Figure 5.5:	Schematic of the automatic grinding plate used to grind sections down to 150µm thickness.....	127
Figure 5.6:	Histological images showing labelled osteons in the vertebral cortex and labelled bone ‘packets’ in trabecular bone.....	128
Figure 5.7:	Scanned image of a lumbar vertebra divided into 3 regions; cranial, mid-vertebra and caudal.....	129
Figure 5.8:	Typical load-reload force displacement curves for L3 lumbar vertebrae.....	130
Figure 5.9:	Mean BMD data from L3 vertebrae of control and OVX animals as measured by DEXA.....	132
Figure 5.10:	Composite image of a cross-section through an L3 vertebra from control and OVX sheep viewed using blue epifluorescence ($\lambda=470\text{nm}$) at X4 magnification.....	133
Figure 5.11:	Average number of labelled sites of bone turnover in trabecular and cortical bone tissue in control and OVX groups.....	134
Figure 5.12:	Mean Tb.N in three regions of L3, pooled data from both groups.....	134
Figure 5.13:	Mean Tb.N in three regions of L3, from control and OVX groups.....	135
Figure 5.14:	Mean Tb.Th in three regions of L3, pooled data from both groups.....	135
Figure 5.15:	Mean Tb.Th in three regions of L3, from control and OVX groups.....	134
Figure 5.16:	Mean Tb.Sp in three regions of L3, pooled data from both	

	groups.....	136
Figure 5.17:	Mean Tb.Sp in three regions of L3, from control and OVX groups.....	137
Figure 5.18:	Mean DA in three regions of L3, pooled data from both groups.....	138
Figure 5.19:	Mean DA in three regions of L3, from control and OVX groups.....	138
Figure 5.20:	Mean BV/TV in three regions of L3, pooled data from both groups.....	139
Figure 5.21:	Mean BV/TV in three regions of L3, from control and OVX groups.....	139
Figure 5.22:	Ultimate strength of L3 lumbar vertebrae from control and OVX groups.....	140
Figure 5.23:	Percentage stiffness reduction of L3 lumbar vertebrae from control and OVX groups.....	141
Figure 5.24:	Residual strain for L3 lumbar vertebrae from control and OVX groups.....	142

ACKNOWLEDGEMENTS

I was very fortunate to be accepted onto the 'Bone for Life' project to carry out my PhD research between two excellent research institutions; the Trinity Centre for Bioengineering and the Royal College of Surgeons in Ireland. My three supervisors, who encouraged and facilitated my return to academia, will always have my utmost gratitude. Firstly, I would like to thank David Taylor who always offered me help and advice in a patient, encouraging and constructive way. It was a pleasure for me to carry out this research with such supervision. Secondly, I would like to thank Clive Lee for always giving me his time and being an endless source of ideas, discussion, humour and support which I could not have done without. I have learned a great deal about a great deal under Clive's supervision. I would also like to express my very sincere thanks to Fergal O'Brien. I might not have returned from the fine surroundings of British Steel in Sheffield without his encouragement. For continually conveying a sense of enthusiasm about bioengineering research, and for resolute guidance and friendship, I am really very grateful.

Sue Rackard contributed in so many ways to this project that I could not begin to list them all here. Perhaps it will suffice to say that the 'Bone for Life' project would not exist without her input. I would like to thank Sue who is always so generous with her time and expertise among many other things. I should also thank her family for accommodating us hungry and frequent visitors from the nearby Lyons estate during the field-work phase of this project. I spent the majority of my time during this PhD working with Orlaith Brennan, and while I will thank many people for helping me in various ways, to her special thanks are offered. For being ready, willing and able to give time, advice, counsel, coffee, corrections, loans, lifts and all kinds of help in general with everything that I needed to do, or forgot to do, over the years – I am very thankful.

I would like to thank various other members of staff in RCSI including Alice, Tom, Skantha, Jane, Claragh, Farhad, Fadel, Sinead, Peter, Terry, Vincent and, of course John O'Brien. They have all helped make my years as a postgraduate student in the lab thoroughly enjoyable and memorable. Similarly, thanks are due to all the staff in the TCBE particularly Patrick Prendergast, Andrew Torrance, Henry Rice, Joan Gillen and especially Sheena Brown and Peter O'Reilly who have helped me out with so many problems so many times. Also, thanks to all the postgraduate students in TCD that I have worked with over the years, it has always been a pleasure. Others who deserve thanks are Nick Mahony for all his work on the DEXA scanning, everyone in the School of Veterinary Medicine in UCD, especially those based at Lyons Estate; the two Pats, Steven and Patsy. I must also thank Anthony Staines for his help with the statistical analyses which were required at various times during this project.

Thanks to all of my friends in the lab, past and present, especially Mike Jaasma, Matt Haugh, Michael Keogh, Claire Tierney, Ruth Walsh, Niamh Plunkett, Ciara Murphy, Amir Al-Munajjed, Mark Dunleavy, Pdraig Moran, Aileen Gibbons, Cormac Kennedy, Peter Mauer, Jan Hazenberg, Dave Hardiman and Orlaith and John, again. They are a fantastic group of people and have always been a pleasure to work with.

Finally, I would like to thank my family. My parents, Aidan and Timmina who have been so supportive of me, in every way, they are really the ones that made this possible. I could not have done this without their help and encouragement. My brothers Kilian, Lorcan and Ultan, and my new sisters-in-law Francesca and Ruth, have always been a great support to me in everything I have done. Although they may or may not be interested in what it is I actually do, they most certainly help me do it. Others who have helped me in different ways along the journey are Karol, Andy, David, Dave, Richard and many others who are too numerous to mention. Last, but most certainly not least, I would like to thank Elaine for everything over the past few years, merci beaucoup pour tout!

I gratefully acknowledge grant support from the Higher Education Authority, under the Programme for Research in Third Levels Institutes Cycle III, the Health Research Board in Ireland and the Royal College of Surgeons in Ireland.

NOMENCLATURE

2-D	2-Dimensional
3-D	3-Dimensional
BMC	Bone mineral content
BMD	Bone mineral density
BMU	Basic multicellular unit
BV/TV	Bone volume fraction
CD	Connectivity density
CON	Control
Cr.Dn	Numerical microcrack density
Cr.S.Dn	Microcrack surface density
Ct.Ar	Cortical area
Ct.Th	Cortical thickness
d	Delta, change
DA	Degree of anisotropy
DEXA	Dual energy x-ray absorptiometry
E2	Estradiol
E	Young's Modulus
EA	Estimated area
F	Force
F _{max}	Maximum force
FDA	Food and Drug Administration
g	Grams
mg	Milligrams ($\times 10^{-3}$)
ng	Nanograms ($\times 10^{-9}$)
pg	Picograms ($\times 10^{-12}$)
kg	Kilograms ($\times 10^3$)
HCl	Hydrochloric acid
Hz	Hertz
IV	Intravenous
kV	Kilovolt ($\times 10^3$)
λ	Wavelength
l	Litre
ml	Millilitre ($\times 10^{-3}$)
L(V)	Lumbar (vertebrae)
Log	Logarithm to the base 10
Pa	Pascal
MPa	Megapascal ($\times 10^3$)
GPa	Gigapascal ($\times 10^6$)
m	Metre
cm	Centimetre ($\times 10^{-2}$)

mm	Millimetre ($\times 10^{-3}$)
μm	Micrometre/micron ($\times 10^{-6}$)
nm	Nanometre ($\times 10^{-9}$)
mm^2	Millimetres squared
cm^2	Centimetres squared
N	Newton
kN	Kilonewton
N_f	Number of cycles to failure
NaOH	Sodium hydroxide
N.On	Number of osteons
NS	Not significant
O_2	Oxygen
OVX	Ovariectomy
$^{\circ}\text{C}$	Degrees Celsius
P4	Progesterone
p	Probability
π	Pi constant
psi	Pounds per square inch
QCT	Quantitative computed tomography
r	Radius
rBMD	Regional bone mineral density
s	Stress
S	Stress amplitude
sec	Second
SERMS	Selective estrogen receptor modulators
SD	Standard deviation
SMI	Structural model index
S-N	Stress- number of cycles
T(V)	Thoracic (vertebrae)
T-score	Bone mineral density comparison score
Tb.Ar	Trabecular bone area
Tb.N	Trabecular number
Tb.Sp	Trabecular separation
Tb.Th	Trabecular thickness
μCT	Micro computed tomography
UV	Ultra violet
X	Magnification

PUBLICATIONS, PRESENTATIONS and PRIZES

Work arising from this thesis has been published as follows:

O'Brien, F.J.; Brennan, O.; Kennedy, O.D.; Lee, T.C. (2005)

Microcracks in cortical bone: how do they affect bone biology?

Current Osteoporosis Reports 3: 39-45.

Kennedy, O.D.; Brennan, O.; Taylor D.; Rackard, S.M.; O'Brien, F.J.; Lee, T.C. (2006)

Bone for Life: A study of the mechanisms of osteoporosis.

Trinity College Dublin Journal of Postgraduate Research 5: 87-103.

Lee, T.C.; McHugh, P.E.; O'Brien, F.J.; O'Mahony, D.; Taylor, D.; Bruzzi, M. ; Rackard, S.M. ; Kennedy, O.D.; Mahony, N.J.; Harrison, N.; Lohfield, S., Brennan, O.; Gleeson, J.; Hazenberg, J.G.; Mullins, L.; Tyndyk, M.; McNamara, L.M.; Prendergast, P.J. (2004) "Bone for life": osteoporosis, bone remodelling and computer simulation. In: *Topics in Bio-Mechanical Engineering*, P.J. Prendergast and P.E. McHugh (Eds). Trinity Centre for Bio-Engineering, Dublin and National Centre for Biomedical Engineering Science, Galway, Ireland (ISBN: 0 9548583 0 1) pp: 58-93.

The work in this thesis has been presented at the following international and national conferences:

Kennedy, O.D.; Brennan, O.; O'Brien, F.J.; Rackard, S.M.; Taylor, D.; Lee, T.C. (2007). Changes in bone turnover and porosity in ovine compact bone 12 months post OVX. *Transactions of 53rd Meeting of the Orthopaedic Research Society, San Diego, California.*

Kennedy, O.D.; Brennan, O.; Rackard, S.M.; O'Brien, F.J.; Taylor, D.; Lee, T.C. (2007). Fatigue induced microdamage in control and OVX cortical bone. In: *Proceedings of the 13th Annual Conference of the Section of Bioengineering of the Royal Academy of Medicine in Ireland.*

Kennedy, O.D.; Brennan, O.; O'Brien, F.J.; Rackard, S.M.; Taylor, D.; Lee, T.C. (2006). Osteoporotic Compact Bone. In *Proceedings of the 5th World Congress of Biomechanics, Munich, Germany.*

Brennan, O.; Kennedy, O.D.; Mahony, M.J.; Lee, T.C.; Rackard, S.M. and O'Brien, F.J. (2006). BMD measurements do not adequately assess the onset of osteoporosis. In: *Transactions of 52nd Meeting of the Orthopaedic Research Society, Chicago, Illinois: 1795.*

Kennedy, O.D.; Brennan, O.; Rackard, S.M.; O'Brien, F.J.; Taylor, D.; Lee, T.C. (2006). The effect osteoporosis on compact bone. In: *Proceedings of the 12th Annual Conference of the Section of Bioengineering of the Royal Academy of Medicine in Ireland*.

Mauer, P.; Kennedy, O.D.; Brennan, O.; Rackard, S.M.; Taylor, D.; O'Brien, F.J.; Lee, T.C. (2006). Manufacturing mm-scale ovine cortical bone specimens for mechanical testing. In: *Proceedings of the 12th Annual Conference of the Section of Bioengineering of the Royal Academy of Medicine in Ireland* – P. McHugh, D. O'Mahoney and D.P. FitzPatrick, (Eds) NUI Galway and University College Dublin (ISBN 1 905254 075): 85.

Kennedy, O.D.; Brennan, O.; O'Brien, F.J.; Taylor, D.; Rackard, S.M.; Lee, T.C. (2005). The contribution of intracortical bone turnover to bone quality in osteoporosis. In: *Proceedings of the 2005 Summer Bioengineering Conference*, Vail, Colorado: II-85.

Kennedy, O.D.; Brennan, O.; O'Brien, F.J.; Taylor, D.; Rackard, S.M.; Lee, T.C. (2005). Increased bone turnover and porosity in osteoporosis: the effect on bone quality. In: *Proceedings of the 25th Meeting of the Northern Ireland Biomedical Engineering Society*, Belfast, Northern Ireland: 31.

Kennedy, O.D.; Brennan, O.; O'Brien, F.J.; Taylor, D.; Rackard, S.M.; Lee, T.C. (2005). The effect of osteoporosis on compact bone and some applications of biomechanics to the forensic sciences. In: *Proceedings of the British Association for Human Identification, 7th Annual Conference*, Dublin, Ireland.

Kennedy, O.D.; Brennan, O.; O'Brien, F.J.; Taylor, D.; Rackard, S.M.; Lee, T.C. (2005). The contribution of bone turnover to reduced bone quality in osteoporosis. In: *Proceedings of the 11th Annual Conference of the Section of Bioengineering of the Royal Academy of Medicine in Ireland* - D.P. FitzPatrick, and M. Senouchi, (Eds) University College Dublin: 22.

Prizes arising from this work are as follows:

Awarded 3rd prize in the Orthopaedic Category at the 12th Annual Conference of the Section of Bioengineering of the Royal Academy of Medicine in Ireland, Galway, 2006.

Awarded the One-Year Postgraduate Research Prize for Continuing Students 2006/07, from the Graduate Studies Committee, Trinity College Dublin.

Selected as a Ph.D. level finalist for the Student Paper Competition at the 2005 Summer Bioengineering Conference of the American Society of Mechanical Engineers (ASME).

Awarded 2nd prize at the Royal College of Surgeons in Ireland Research Day, Dublin, 2005.

Awarded 2nd prize at the 7th Annual Conference of the British Association for Human Identification, Dublin, 2005.

Awarded 2nd prize at the 11th Annual Conference of the Section of Bioengineering of The Royal Academy of Medicine in Ireland, Dublin, 2005.

Awarded the Postgraduate Travel Bursary 2004/2005 from the Graduate Studies Committee, Trinity College Dublin in order to present my paper at the ASME Summer Bioengineering Conference in Colorado, USA.

Awarded 1st prize in the Biological Category at the 28th Annual Symposium of the Microscopical Society of Ireland, Dublin, 2004

Chapter 1

Introduction and Literature Review

1.1	Introduction	2
1.2	Bone types	4
1.2.1	Compact bone	4
1.2.2	Trabecular bone	7
1.2.3	Organic and inorganic matrix	9
1.3	Bone cells	10
1.3.1	Osteoprogenitor cells	10
1.3.2	Osteoblasts	11
1.3.3	Osteocytes	12
1.3.4	Osteoclasts	12
1.4	Biomechanical properties of bone	13
1.4.1	Fatigue properties	16
1.5	Wolff's Law, bone modelling and remodelling	17
1.6	Osteoporosis and bone quality	20
1.6.1	Osteoporosis	20
1.6.2	Bone quality	21
1.6.3	Bisphosphonates	29
1.6.4	Experimental animal models of osteoporosis	32
1.7	Objectives of this research	39

1.1 Introduction

Bone is an extraordinary dynamically adaptable material which is in a continual state of remodelling in order to conform to its function. It is this 'form-function' relationship that is the key to understanding the material properties and behaviour of bone (Katz, 1980). It is not known what the original structure of bone was or how it was deposited when it first appeared in the earliest vertebrates. It has been argued that initially, bone was formed to act as an osmotic barrier. It was also suggested that it was solely a means of storing calcium and phosphate. Others postulated that it evolved as defensive armour against predators (Reisz, 2004). However, bone would not be an effective osmotic barrier as the gills of fish let dissolved salts enter the body and in relation to the second hypothesis, salts could be stored elsewhere in the body and would not require such an elaborate structure (Sansom, 1992). The most feasible argument is that initially, bone served as superficial armour and was found in the dermis of the skin.

Mammalian bone arises from the differentiation of pluripotential embryonic tissues (Scheuer and Black, 2004). At some sites bone is formed by the replacement of cartilaginous 'models' through a process called endochondral ossification while at other sites, bone formation occurs within a membranous, condensed plate of mesenchymal cells through a process called intramembranous ossification. There are two distinct types of intramembranous or mesenchymal ossification. Firstly, that which is considered to be more phylogenetically ancient and gives rise to dermal bones, which are generally held to be indicators of an evolutionarily distant exoskeleton or armour (Carter and Beaupré, 2001) and secondly, perichondral bone that is formed in the

immediate vicinity of the highly vascular perichondrium by direct apposition from perichondral osteoblasts (Scheuer and Black, 2004).

It is not fully understood why certain bones preform in cartilage and others develop directly in intramembranous fashion. However, although the resultant material is virtually identical there are distinct differences in structure and morphology. Endochondral ossification results in trabecular or cancellous bone formation which is found in the internal aspect of some bones whereas intramembranous ossification results in dense, regularly organised compact bone which is exposed on the external surface (Fig. 1.1)

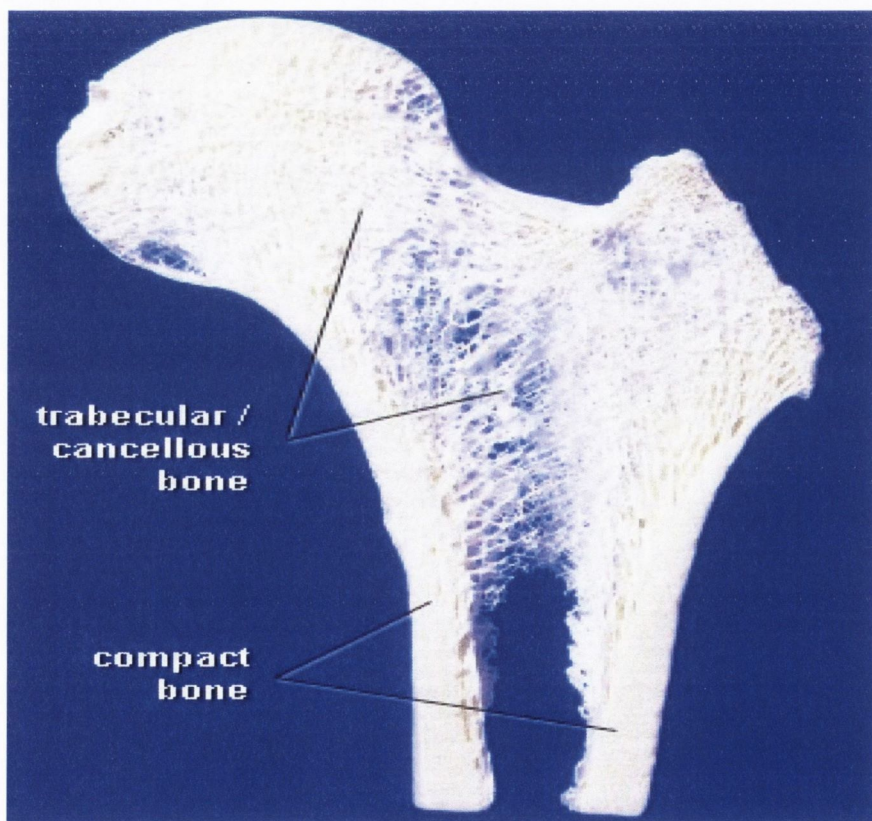


Figure 1.1: Coronal section through a human femur showing compact bone at the external surfaces and trabecular or cancellous bone in the internal aspect.

<http://www.lab.anhb.uwa.edu.au/mb14/CorePages/Bone/Bone.htm#intramembranous>

1.2 Bone types

As mentioned in the previous section, bone tissue can be categorised morphologically into two distinct groups; compact and trabecular. Compact bone is, as the name suggests, a compacted and stiff material with a relatively low porosity. Trabecular bone is a more porous structure comprised of small struts and plates called trabeculae. These two types of tissue can be classified on the basis of porosity and the unit microstructure. Cortical bone has a porosity ranging between 5% and 10% while the porosity of trabecular bone ranges from 50% to 90%. At the tissue level, it is thought that the two bone types are identical.

1.2.1 Compact bone

Compact bone forms the shaft of long bones and the cortices or outer shell of other bones. The outer surface is called the periosteal surface while the inner is called the endosteal. This type of bone comes in four main forms: woven bone, plexiform bone, primary bone, and secondary bone. Woven bone is characterised by the appearance and arrangement of its collagen fibres which are coarse and loosely packed giving it a non-lamellar tissue structure. This type of bone can be laid down rapidly and can be deposited *de novo*, without any previous hard tissue or cartilaginous model. For this reason it is found to form the callus at sites of bone fracture healing (Martin and Burr, 1998). It is an immature type of developing bone and is also found in young foetal skeletons. Woven bone generally contains more bone cells than other types of bone tissue, has a poorly organised structure with large vascular spaces and is thus relatively weak.

Plexiform bone is also formed rapidly in comparison to primary or secondary bone tissue. It has been described as an intermediate tissue type which lies in between non-lamellar and lamellar bone, thus is known as fibrolamellar bone. This form of bone is primarily found in large rapidly growing animals such as cows or sheep and is rarely seen in humans. It is formed from mineral buds which grow first perpendicular and then parallel to the outer bone surface (Martin and Burr, 1998). This growing pattern produces the 'brick-like' structure characteristic of plexiform bone with each 'brick' measuring approximately 125 μ m in length. While this bone type tends to be stiffer than primary or secondary cortical bone, it lacks the crack arresting properties which would be desirable for more active species like canines and humans (Martin and Burr, 1998).

Haversian systems, which were first identified by Clopton Havers in 1691, develop almost exclusively in compact bone (Cohen, 1958). They contain blood vessels which are surrounded by concentric layers (or lamellae) of well organised bone tissue. The structure, including the central blood vessel and surrounding concentric lamellae, is called an osteon. Typically, an osteon has a diameter of 150-200 μ m. What differentiates primary osteonal bone from secondary osteonal bone is the way in which the osteon is formed and also some subtle differences in the resulting structure. Primary osteons are formed by mineralisation of cartilage, thus being formed where bone was not present (Martin and Burr, 1998). As such, they do not contain as many lamellae as secondary osteons. Also, the vascular channels within primary osteons tend to be smaller than those of secondary osteons. For this reason, it is thought that primary osteonal cortical bone may be mechanically stronger than secondary osteonal cortical bone. The creation of secondary osteons is carried out by the remodelling process which is the replacement of older tissue with new tissue. This process is well described in the literature (Jaworski,

1980; Frost, 1991) and is summarised in Section 1.5 of this chapter. In adult humans, most compact bone is entirely composed of secondary bone which includes whole osteons and also the remnants of older osteons that have been partially resorbed, this is called interstitial bone. The microstructural features of Haversian systems and secondary compact bone are illustrated in Figure 1.2.

Research on the biomechanical characteristics of compact bone over the last century has yielded much information about its properties and behaviour. To summarise some of these findings it can be said that compact bone is an elastic, heterogeneous and composite material. The determinants of its mechanical properties include density (apparent density and mineral density), porosity, microstructure (primary and secondary osteons), osteonal structure (composition of lamellae with different collagen fibre arrangement) and collagen fibre orientation. However, a complete understanding of failure criteria, robust fracture mechanics and the general mechanical properties of the tissue at the nanoscale remain to be obtained (Currey, 2004). A better understanding of these issues would allow for more accurate assessment of fracture risk and more effective treatment of bone diseases such as osteoarthritis and osteoporosis.

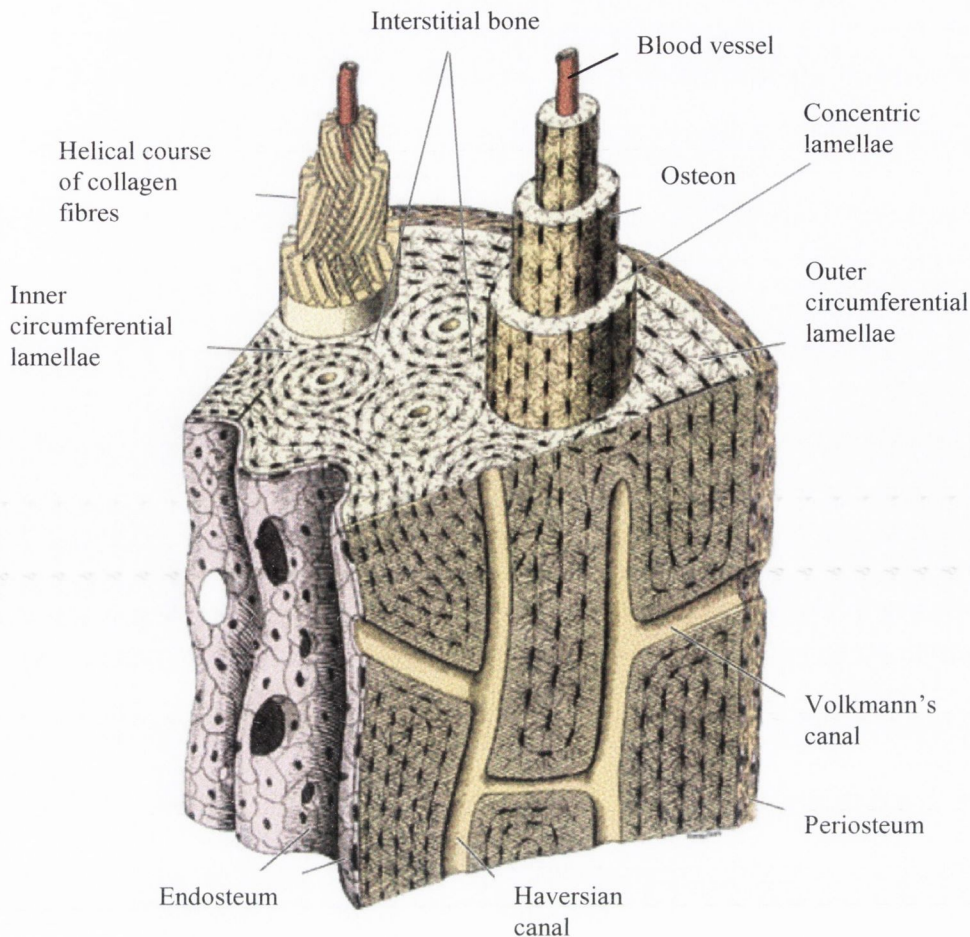


Figure 1.2: Schematic drawing of the microstructure of compact bone tissue (Junqueira and Carneiro, 1998).

1.2.2 Trabecular bone

Trabecular bone (also known as cancellous or spongy bone) has a porous structure consisting of 'rod' or 'plate-like' struts called trabeculae (Figure 1.3). Each strut and plate is composed primarily of lamellar bone and occasionally trabecular plates made up of osteonal bone can be found. Trabecular bone is found in the medullary cavity of flat and short bones, and in the epiphysis and metaphysis of long bones. The microarchitecture of trabecular bone appears random, however the connections and orientation of the trabeculae are found to have precise patterns which are thought to be related to the specific mechanical properties of the bone (Wolff, 1892). The structure of the trabecular bone network in the femoral head and neck is classically put forward as

an example of the correlation between the orientation of the trabeculae and the distribution of the principal forces during load bearing; this is known as the stress trajectorial theory (Bell, 1956).

The primary difference between the mechanical properties of trabecular and cortical bone is their effective stiffness at the macroscale level. Trabecular bone is more compliant than cortical bone and it is believed that it distributes and dissipates the energy from articular contact loads. Trabecular bone contributes approximately 20% of the total skeletal mass within the body while cortical bone contributes the remaining 80%. However, trabecular bone has a much greater surface area than cortical bone. Within the skeleton, trabecular bone has a total surface area of $7.0 \times 10^6 \text{ mm}^2$ while cortical bone has a total surface area of $3.5 \times 10^6 \text{ mm}^2$.

There are no blood vessels within trabeculae but the pores in the structure are filled with red marrow which provides the vital nutrients that bone requires. As with compact bone, a lot of research has been carried out on trabecular bone in recent decades (Carter, 1976; Gibson, 1985; Kaplan, 1985; Goldstein, 1987; Keaveny, 1994). However, there is a lot that has yet to be defined and understood about the behaviour of trabecular bone such as the reaction to tension and shear stresses, the behaviour of individual trabeculae and the interaction between compact and trabecular bone.

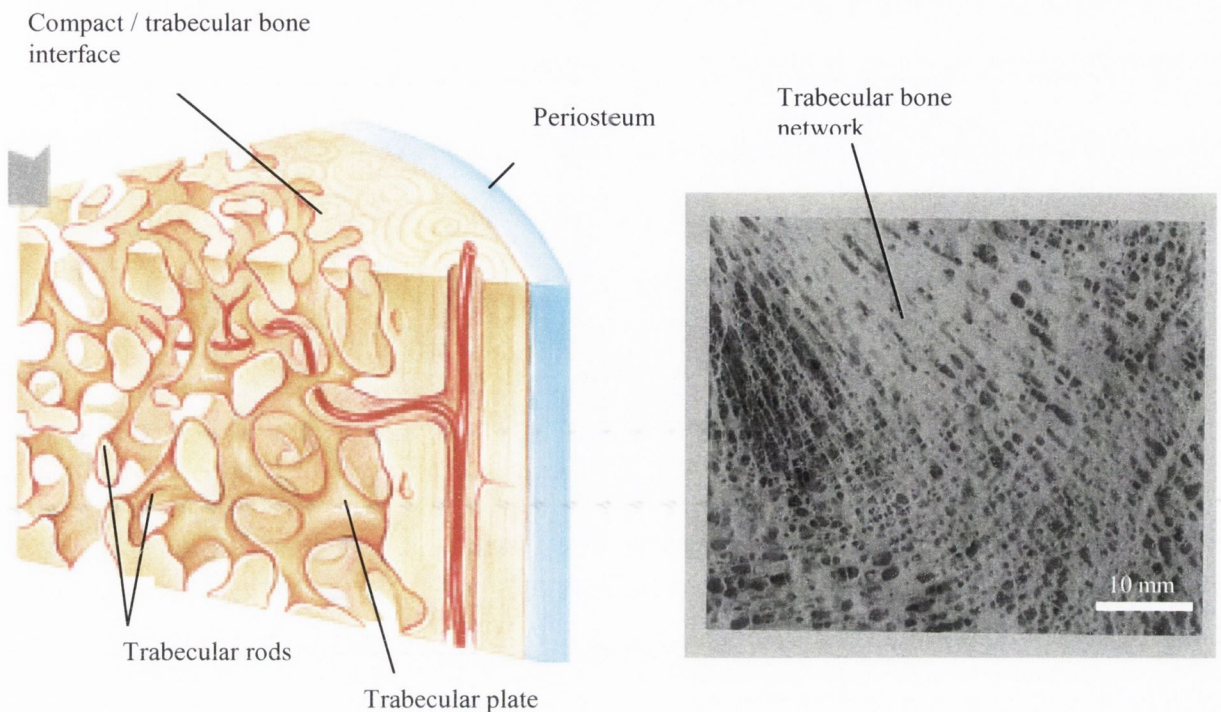


Figure 1.3: Schematic drawing of trabecular bone tissue in the endosteal region of a long bone and a photograph of trabecular bone structure in the distal end of a human femur (Fleisch, 1991).

1.2.3 Organic and inorganic matrix

At the molecular level, bone is one of the few materials in the body that contains a mineral-like component in addition to the organic components, others include dentin and enamel. As a result, bone can be thought of as a simple composite material which has an organic phase (mainly Type-I collagen) and an inorganic or mineral phase (hydroxyapatite). In mature bone, 10-20% by weight of the matrix is water. Dried bone consists of about 70% inorganic matrix and 30% organic matrix by weight. The organic matrix is 90-95% collagen fibres with the remainder being a homogenous ground substance. The ground substance consists of proteoglycans, in particular decorin and biglycan. Collagen molecules, which are approximately 1nm in diameter and 300 nm in length, are bound together by bone mineral crystals. The resulting structure is a collagen fibril; this fibril has a diameter of approximately 5 μ m. Groups of fibrils are referred to

as fibres, and the orientation of these fibres in bone is thought to affect the mechanical properties of the tissue. In woven bone the collagen fibres are randomly organised and loosely packed as a result of the rapid manner in which it is laid down. In lamellar bone the fibres are laid down in a more organised fashion and as a result have superior mechanical properties.

1.3 Bone cells

There are four main cell types in bone tissue; the osteoprogenitor cell, the osteoblast, the osteocyte and the osteoclast (Figure 1.4). Each of these cells resides within the bone matrix.

1.3.1 Osteoprogenitor cells

The osteoprogenitor cell is a primitive cell derived from the mesenchyme. It forms in the inner layer of the periosteum and lines the marrow cavity as well as Haversian and Volkmann's canals of compact bone. During periods of growth and remodelling these cells are stimulated to differentiate into osteoblasts that lay down new bone. They can also differentiate into other cell types such as fibroblasts, chondroblasts and adipose cells during bone loss (Ross et al, 1994). In mature bone that is not actively remodelling, these cells are quiescent and are called bone lining cells. Bone lining cells are generally inactive and have very few cytoplasmic organelles. The full extent of the behaviour and function of these cells is not known at present. Their processes extend through canaliculi to neighbouring cells which suggests that they may be involved in mechanotransduction and cellular communication.

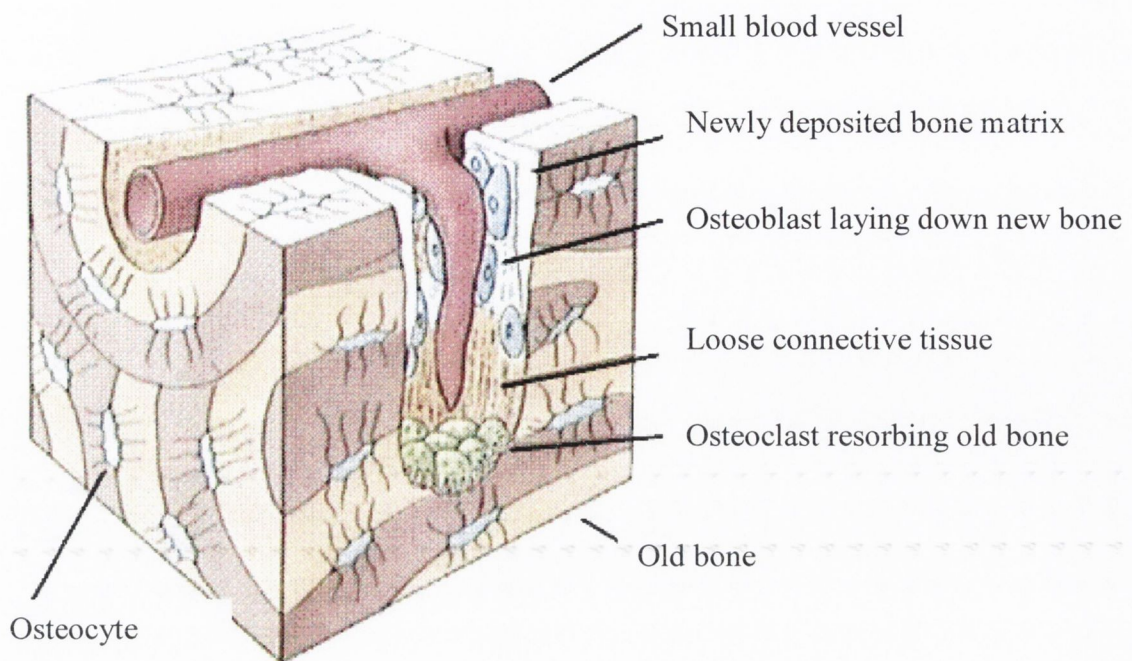


Figure 1.4: Schematic drawing of the activity of osteoclasts, osteoblasts and osteocytes (Junqueira and Carneiro, 1998).

1.3.2 Osteoblasts

Bone lining cells have the potential to be activated so that they differentiate into osteoblasts. Osteoblasts are cells which are responsible for the production of organic bone matrix. These cells synthesize and secrete small vesicles into the existing bone. These matrix vesicles are formed by pinching off portions of the plasmalemma and contain enzymes, including alkaline phosphatase, which load the vesicle with calcium (Junqueira and Carneiro, 1998). Rupture of these vesicles initiates local mineralisation by releasing calcium and by negating local inhibiting mechanisms. Deposition of mineral makes the bone matrix stiffer, impermeable and more capable of bearing loads.

1.3.3 Osteocytes

Osteocytes are the most abundant cells in the bone matrix and are mature osteoblasts that have been 'walled-in' by the bone tissue which has been laid down around them. Approximately 10% of all active osteoblasts are converted into osteocytes. The full role of these cells is still not known however, they are thought to have mechanosensory and chemosensory regulatory roles. Osteocytes are a candidate mechanosensory cell type because they are ideally situated to sense mechanical stimulation such as strain or interstitial fluid flow. These actions are caused by mechanical loading and thus osteocytes are thought to be in some way responsible for bone adaptation and remodelling (Hazenbergh, 2007). Osteocytes maintain healthy tissue by secreting enzymes and controlling the bone mineral content, they also control the calcium release from the bone tissue to the blood. These cells are lenticular in shape and have few cytoplasmic organelles. Every osteocyte occupies a space, or lacuna, within the matrix (Figure 1.5) and extends processes through canaliculi in the matrix to contact processes of adjacent cells by means of gap junctions.

1.3.4 Osteoclasts

Osteoclasts are large multinucleate cells that break down bone tissue. They are derived from the mononuclear phagocytic lineage of the haemopoietic system. They are formed by monocytes either by the fusion of several cells or by DNA replication without cell division in response to stimuli from osteoblasts, osteocytes and hormones. When these cells are active they rest directly on the bone surface in a resorption bay or a Howship's lacuna. They are characterised by two easily identifiable features; the 'ruffled border' which is an infolded plasma membrane where the resorption takes place, and the 'clear

zone' which is the point of attachment of the osteoclast to the underlying bone matrix (Ross and Romrell, 1989).

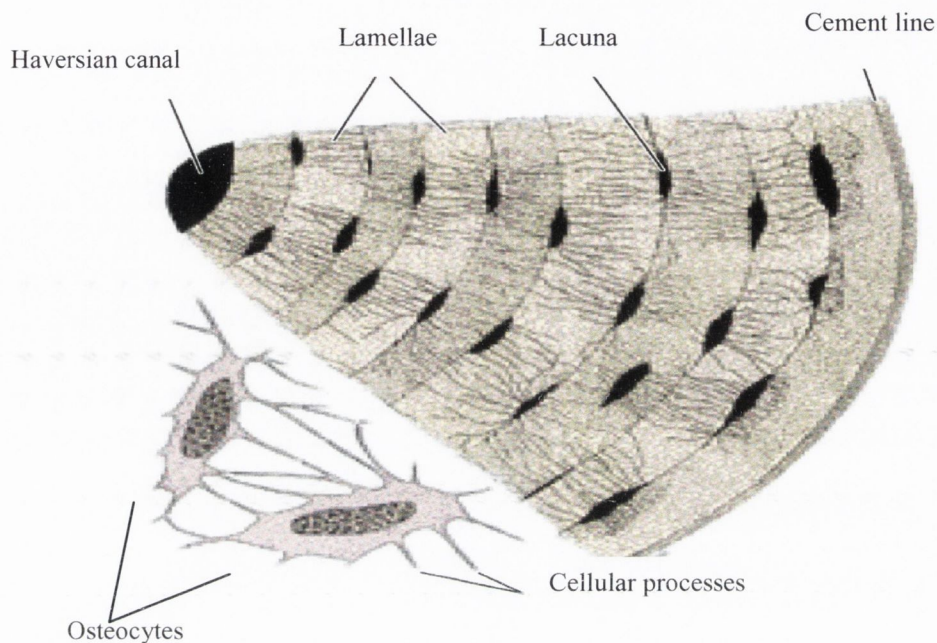


Figure 1.5: Schematic drawing of a Haversian canal, bone lamellae, osteocytes, lacunae and the cement line (Junqueira and Carneiro, 1998).

1.4 Biomechanical properties of bone

The biomechanical properties of bone are the basic parameters which reflect its structure and function and can be measured by testing either whole bones or specimens which are prepared to isolate particular structural components.

Bone is a viscoelastic, anisotropic and heterogeneous material and as such is complex to analyse mechanically. The inherent ability of bone to adapt continually to metabolic and environmental changes *in vivo* creates an even more complex system. The purpose of studying the biomechanical properties of bone is to characterise and better understand the relationship between its structural, material and mechanical behaviours.

The mechanical behaviour of bone depends on various different factors including the stiffness, porosity, orientation of the microstructure and the degree of mineralisation (Sevostianov, 2000). The mechanical strength of bone also depends on the type of load and the loading direction. Figure 1.6 shows some typical values of the elastic modulus and the ultimate compressive strength of cortical bone alongside other tissues and biomaterials. For compact bone, the strength and elastic modulus data from compression, tension and torsion tests are summarised below in Table 1.1.

Table 1.1: Strength and elastic modulus data for compact bone in compression, tension and torsion (Reilly, 1974; Burstein, 1976).

	Strength (MPa)	Elastic Modulus (GPa)
Compression	133 - 295	15 - 34
Tension	92 - 188	7 - 28
Torsion	53 - 76	3 - 5

The term ‘mechanical properties of trabecular bone’ really refers to the structural properties of the tissue due to its architecture of struts and plates. It has been shown that the strength and elastic properties of trabecular bone found by tensile testing are smaller than those found using compressive tests. Kaplan et al (1985) reported that the strength by tensile test is approximately 60% of the value by compression, and the elastic modulus by tensile tests is approximately 70% of the value by compressive testing (Keaveny, 1994). According to data from the literature the values of strength and elastic

moduli of trabecular bone are 1.5 to 38 MPa and 10 to 1570 MPa respectively (An and Draughn, 2000) .

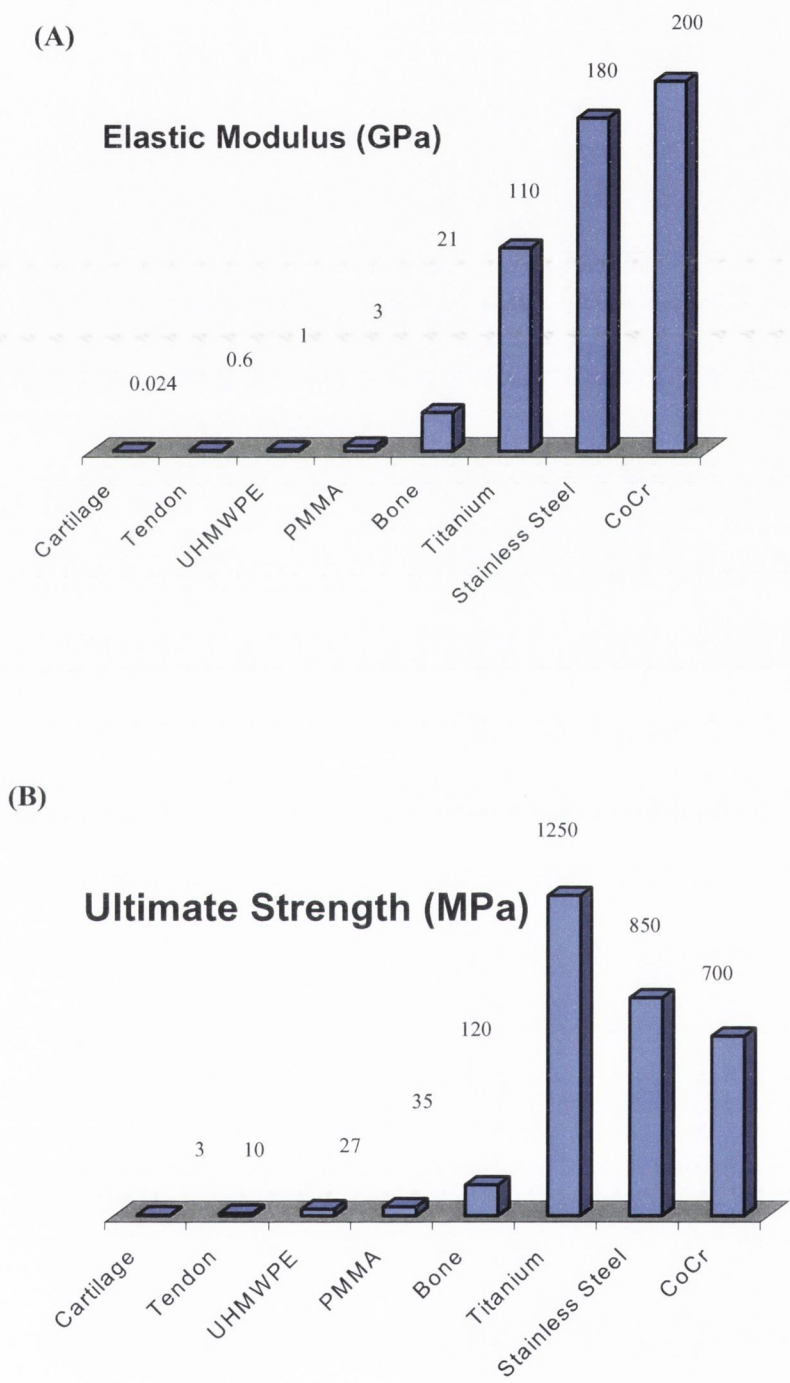


Figure 1.6: Graphical representations of (A) the elastic modulus and (B) the ultimate compressive strength of cortical bone, other tissues and biomaterials (An and Draughn, 2000).

1.4.1 Fatigue properties

Fatigue failure refers to the failure of materials under the action of repeated or cyclical stresses. Fatigue damage causes progressive and localised structural damage through crack initiation and subsequent propagation. It is not fully understood how cracks initiate in bone except that they form at the level of the lamellae and probably by inter-lamellar separation.

An S-N curve is often used to characterise the behaviour of a material under fatigue loading conditions, it is comprised of a graph which displays stress amplitude, S versus number of cycles to failure, N_f for a fatigue test. Some materials, such as low carbon steels, exhibit a fatigue limit below which, in theory, failure should never occur. Figure 1.7 shows an S-N curve for human trabecular bone, the data in this graph exhibit considerable scatter which is not unusual in fatigue test data, the S-N curve is a 'best-fit' curve. Fatigue testing and analysis normally involves the study of crack initiation and subsequent crack behaviour. Compact bone can be viewed as a composite material in which the Haversian systems along with the other microstructural features can affect crack initiation and growth. In compact bone, discontinuities in the form of resorption spaces, osteons, laminae etc. may cause stresses in the bone to concentrate and thus initiate cracks, however they may also serve to increase toughness and fatigue resistance by inhibiting crack growth.

In a study by Choi and Goldstein (1992) trabecular bone specimens were shown to have significantly lower fatigue strength than cortical bone specimens with the same dimensions despite their higher mineral density values. Fracture surface and microdamage analyses illustrated different fracture and damage patterns between trabecular and cortical bone tissue, depending on their microstructural characteristics.

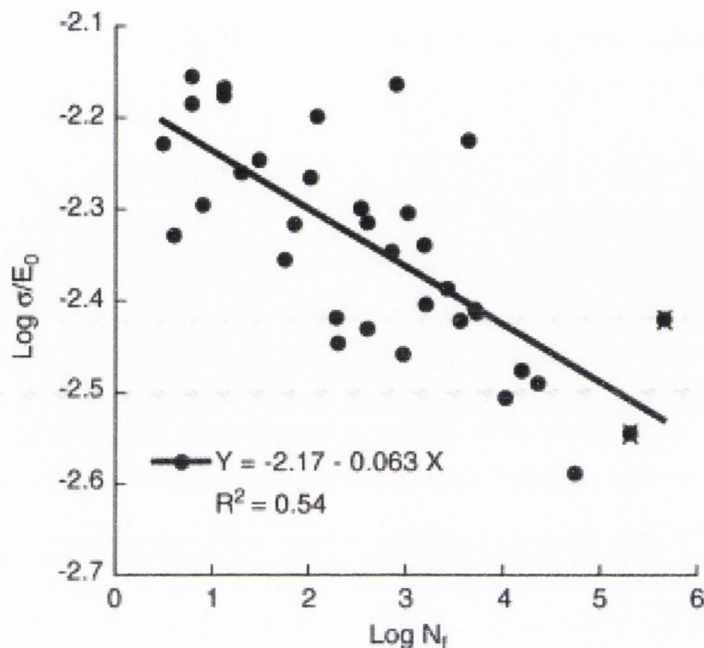


Figure 1.7: S–N type plot of human vertebral trabecular bone (Haddock, 2000).

1.5 Wolff's Law, bone modelling and remodelling

The fundamental ideas on which much orthopaedic research is based date back to the early scientists. One of the recurring arguments of Aristotle, the Greek philosopher, was that the form (of for instance, an animal) is determined by its function or 'telos'. Julius Wolff and Wilhelm Roux further developed with respect to bone mechanics in the late 19th century. The law that describes the relationship between the structure and function of bone is named after the former and is known as Wolff's Law.

Wolff's Law states that 'every change in the form and the function of a bone, or in its function alone, is followed by certain definite changes in its internal architecture and

secondary alterations in its external conformation'. In simple terms, this principle of functional adaptation states that mechanical stress is responsible for determining the internal architecture of bone (Forwood, 1995).

Functional adaptation can occur in a variety of situations, such as during immobility, space flight and extended periods of bed rest, when bone is lost. It may also occur in situations of overloading, such as sudden and extended periods of vigorous exercise, which causes an increase in bone mass. There are other situations where this phenomenon can be observed such as natural growth, fracture healing and implant incorporation. The ability of bone to adapt to its mechanical environment is brought about by continuous bone resorption and formation. When these processes occur at different sites, which is the case in most of the above examples, the bone morphology is altered. Harold Frost defined this as *modelling*, some of the key characteristics of modelling are that osteoclasts and osteoblasts act independently of each other, changes in bone size and/or shape usually results, the rate of modelling is greatly reduced after skeletal maturity and modelling at particular sites is continuous and prolonged.

In the idealised case of homeostatic equilibrium, bone resorption and formation are balanced. In this case, old bone is continuously replaced with new tissue and the mechanical integrity is maintained but no global change in bone morphology occurs. Frost described this process as *remodelling*, some of the key characteristics of remodelling are that osteoclasts and osteoblasts act in a coupled fashion, no change in bone size or shape occurs, the rate of remodelling remains relatively high even after growth stops and finally that remodelling at a particular site is episodic, with each episode having a definite beginning and ending.

Examples of the phenomenon of remodelling (Figure 1.8) can be found in everyday life, in particular in the sporting field. Young soccer players have been found to have a larger bone mass compared with non-players, the soccer players had significantly higher BMD of the total body (2.7%), lumbar spine (6.1%), and the dominant and nondominant hip. The largest increases were found in the femoral greater trochanter on both sides (dominant, 16.5%, nondominant, 14.8%) (Soderman, 2000). It was also shown that the playing arm in adult tennis players had thickened trabeculae compared to non-players (Ashizawa, 1999). At the opposite end of the scale remodelling is also at work, studies on space flights lasting more than 12 months have shown that due to weightlessness, astronauts on long missions may lose as much as 20% of their bone mass (Turner, 2000).

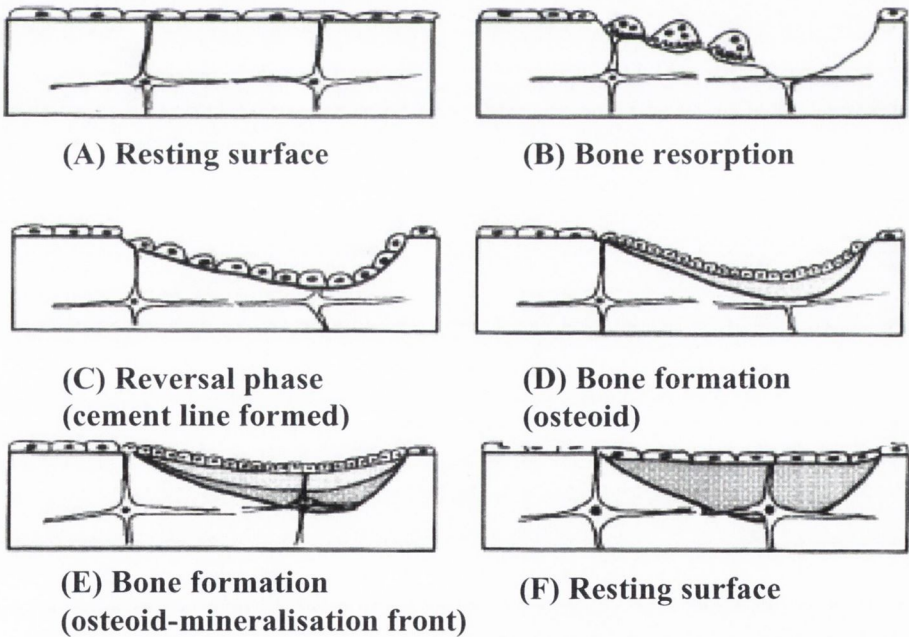


Figure 1.8: Schematic of the 6 major steps in the bone remodelling cycle. Each remodelling process is initiated by activation at a resting surface (A) by which osteoblastic lineage cells start to secrete collagenase which removes the thin layer of unmineralised bone typical of a resting bone surface. This exposes the mineralised bone underneath to the multinucleated mobile, osteoclasts. During osteoclastic bone resorption (B), Howship's lacunae are excavated to a maximum depth of 50-60 μm . A short reversal phase follows, when the cement line is formed (C). Then bone formation begins (D). Osteoblasts produce osteoid at a rate of 0.5-1.0 μm per day. When the osteoid thickness has reached approximately 12-15 μm , mineralisation begins from the bottom (mineralisation front) (E). At the termination of each remodelling process, the bone surface is again covered by an extremely thin layer of non-mineralised bone and a layer of flat lining cells. The bone is again converted into a resting surface (F).

1.6 Osteoporosis and bone quality

1.6.1 Osteoporosis

Osteoporosis can be defined as ‘a skeletal disorder characterised by compromised bone strength predisposing a person to an increased risk of fracture. Bone strength primarily reflects the integration of bone mineral density (BMD) and bone quality (Klibanski, 2001). In clinical practice, dual energy X-ray absorptiometry (DEXA) scanning is the most common way of measuring BMD levels and is the current gold standard for diagnosing and monitoring osteoporosis. ‘Normal’ bone density is considered to be that of a healthy young adult, in DEXA scanning terms the method of comparing individual BMD measurements to the normal is called the ‘T-score’ system. A T-score of -1.0 or higher is considered to be in the normal healthy range. A score between -1.0 and -2.5 means that BMD is borderline for osteoporosis, this condition is called osteopenia. A score of -2.5 or more indicates osteoporosis and is associated with increased fracture risk. BMD is calculated as the mass of mineral per unit area and is normally quoted as ‘areal density’, this is a 2-D measurement of a 3-D property and as such it is thought to be a limiting factor for this technique. Currently, there is no accurate clinical measurement of overall bone strength *in vivo*. In a study by Rice et al (1988), a statistical analysis of the pooled data from a number of previous experiments concerning the dependence of the Young's moduli and strength of cancellous bone tissue upon apparent density was carried out. This study concluded that BMD accounts for approximately 60-70% of strength, and thus can be considered a proxy measurement. Bone quality is thought to account for the remainder.

The term osteoporosis was first used by the French pathologist Lobstein in the 1820's but it was not until 1940s when the American endocrinologist Fuller Albright defined the clinical syndrome of the disease (Reifenstein and Albright, 1947). Since then, and particularly in the last 15 years, there have been major developments in our understanding of the aetiology and pathophysiology of osteoporosis. Estimates were made in the mid 1990s of the prevalence of osteoporosis based on measurements using DEXA and the world health organisation (WHO) classification criteria. Results suggested that 30% of postmenopausal Caucasian women have osteoporosis at the hip, lumbar spine or mid-radius (Melton, 1995). This number is set to rise with the world's increasing elderly population. In the year 2000 there were an estimated 9.0 million osteoporotic fractures globally, of which 1.6 million were at the hip, 1.7 million at the forearm and 1.4 million were clinical vertebral fractures. The greatest number of reported osteoporotic fractures occurred in Europe (34.8%). World-wide, osteoporotic fractures accounted for 0.83% of the global burden of non-communicable disease and were 1.75% of the global burden in Europe (Johnell, 2006). Thus, it is clear that a better understanding of the pathophysiology of osteoporosis, specifically the parameters that affect bone quality, is essential in order to develop better tools for diagnosis and treatment of the disease.

1.6.2 Bone quality

Bone quality is a primary contributor to bone strength. Although a precise definition of bone quality remains elusive, characteristics other than BMD such as bone turnover, microarchitecture and mineralisation of the bone matrix are important factors in the pathophysiology of osteoporosis and the mechanisms that underlie fracture (Bouxsein,

2003). Clinical trials have shown that the risk of fracture in a 75 year old woman is 4-7 times that of a 45 year old woman with an identical bone mass (Hui, 1988).

It has also been shown that after therapeutic intervention the resulting changes in BMD explain only a small proportion of the variance in fracture risk. Often in these cases the reductions in fracture risk are evident long before changes in BMD are observed (Bouxsein, 2003). The most common clinical treatment for osteoporosis is the use of a group of anti-resorptive agents (also known as anti-catabolic agents) called bisphosphonates. These act by reducing the osteoclasts ability to adhere to the bone surface which suppresses the resorption phase of the remodelling cycle thus preserving bone mass. Recent observations have shown that different bisphosphonates can have up to a 7-fold difference in their effect on maintaining BMD and yet have a similar fracture efficacy (Burr, 2004). This further illustrates the importance of bone quality in determining fracture risk. In fact, some researchers have taken this idea further to say that bone fragility is the disease and osteoporosis is just one risk factor (Riggs and Parfitt, 2005).

1.6.2.1 Bone turnover

The rate of bone turnover is an important parameter which can affect bone quality. The bone turnover cycle begins with activation of osteoclasts and their precursors to carry out bone resorption. Matrix components such as TGF-beta, IGF-I, collagen, osteocalcin and other protein and mineral components, are then released into the micro-environment. Growth factors released by resorption contribute to the recruitment of new osteoblasts to the bone surface, which begin the process of collagen synthesis and biomineralisation. In healthy adults, as many as two million remodelling sites may be active at any given time, and it is estimated that nearly one quarter of all trabecular bone

is remodelled each year (Rosen, 2000). In general, resorption takes only 10-13 days, while formation is much slower and can take up to three months. Under ideal circumstances the amount of bone resorbed equals the amount reformed, however in the case of osteoporosis more bone is resorbed than formed, resulting in a net loss of bone.

Previous studies have shown that bone turnover has a direct influence on fracture risk (Riggs and Melton, 2002). Increased bone turnover accelerates osteoclast resorption i.e. removal of old or damaged bone. In trabecular bone, increased osteoclastic resorption on the surface of the trabeculae can reduce their resistance to buckling and increase the risk of failure. It has been shown that a 50% reduction in bone turnover can result in a 4-fold reduction in trabecular perforation (Parfitt, 2002). In compact bone, accelerated turnover affects bone quality in a number of ways. Firstly, highly mineralised bone is removed and replaced with younger bone which contains less mineral, and so reduces the material stiffness. Secondly, the presence of more resorption sites creates more potential stress concentrations that predispose bone to microdamage. Thirdly, increased remodelling impairs isomerisation and maturation of collagen, which increases the fragility of bone (Garnero, 2002; Seeman and Delmas, 2006).

There are still aspects of bone turnover which are not well understood. For example, it is not known how bone strength changes in relation to the rate of bone turnover, or how high bone turnover affects microdamage behaviour. In summary, the biomechanical link into the bone turnover paradigm is still unclear.

1.6.2.2 Microarchitecture

The microarchitecture of bone tissue also has a substantial impact on the quality of bone, and thus its strength. Trabecular bone that is more ‘plate-like’, with thicker and

more trabeculae, enhances strength. Trabecular architecture that is more isotropic i.e. having similar mechanical properties in all directions, may lower fracture risk further (Burr, 2004). Similarly, in cortical bone when porosity in the cortex is increased via longitudinal tunnelling of osteoclasts, the structural integrity is compromised (Hirano, 1999; Burr et al, 2001). Clinical studies have shown that postmenopausal osteoporosis is characterised by loss of trabecular bone mass and connectivity as well as thinning of the cortical bone (Mosekilde, 1989).

Trabecular bone strength and stiffness are related to the connectivity and orientation of the trabeculae (Goulet, 1994). An equivalent amount of bone distributed as widely separated, disconnected thick trabeculae is biomechanically less competent than when arranged as more numerous, better connected, thinner trabeculae. Increased connectivity reduces the unsupported length of trabecular struts (Carter and Hayes, 1977). Euler's theorem states that, in general terms, the strength of a vertical trabeculum is inversely proportional to the square of its effective length. In a study of the effect of mass changes on trabecular bone, it was found that bone loss due to reduced trabecular number had a substantially larger impact on strength than an equal mass loss due to trabecular thinning (Guo, 2002). Therefore, for preventative therapies to be most effective they should not only possess attributes that will preserve bone mass, but also preserve trabecular connectivity.

In cortical bone, the primary structural feature which affects bone strength is the porosity. Small increases in porosity lead to disproportionately large reductions in bone strength (Turner, 2002). The distribution of pores is also an important factor in determining the effect on strength. In long bones, pores in the endocortex have less of an impact on strength than pores near the outer surface due to the higher stresses,

particularly in bending, which can be present at the periosteal surface. In humans younger than 60 years, pore number and size were observed to increase with age, whereas in people over the age of 60 there continues to be an increase in pore size but a decrease in pore number as the pores begin to coalesce this is the case in osteoporosis.

In a study carried out by Waarsing et al (2004), micro computed tomography (μ -CT) technology was used to monitor spatial and temporal bone loss due to ageing and ovariectomy (OVX) in the tibiae of rats. During the first year post-OVX, the tibiae of the animals were scanned at various time points using an *in vivo* μ -CT scanner. Volume fraction (BV/TV), direct trabecular thickness (Tb.Th), structural model index (SMI) and connectivity density (CD) were measured in an attempt to assess the effect of OVX on microarchitecture and bone quality. After 14 weeks BV/TV had decreased by 53% in OVX animals. Trabecular number was also reduced as a result of OVX, however, the remaining trabeculae increased in thickness from 139 to 153 μ m and in some cases complete new trabecular structures were formed. Thus, it is clear that assessing the microarchitecture of bone is an important consideration in terms of the strength of the structure.

1.6.2.3 Microdamage

Microdamage accumulation reduces bone strength, stiffness and toughness (Burr, 1997). It has been shown that microdamage accumulates in athletes and military recruits who experience increased rates and magnitudes of loading (Meurman and Elfving, 1980). The balance between damage and repair is an important one and can be upset by increased damage creation or deficient repair. An imbalance in remodelling may cause microdamage to accumulate in the elderly (Schaffler et al, 1995; Norman and Wang, 1997; Zioupos, 2001) and could contribute to osteoporotic fractures. Microcracks have

been observed in bone *in vitro* due to fatigue loading. They can be classified as either individual cracks which are approximately 100µm in length, or diffuse damage which consists of a collection of small cracks which are between 2-10 µm long and are oriented roughly along the loading direction (O'Brien, 2003). It has been shown in many studies that the majority of microcracks are found in the interstitial bone (Frost, 1960, Burr and Stafford 1990, Lee et al, 1998). Interstitial bone tends to have a higher microdamage burden because it is comparatively older than the surrounding bone. Also, the degree of mineralisation in interstitial bone is normally relatively high, which allows microcracks to propagate easily. Histological measurements of microcracks have shown that when viewed along the longitudinal axis of the bone, cracks are significantly longer than when they are viewed transversely in the bone. This is intuitively correct as the cracks in any material will preferentially travel along the path of least resistance with the 'grain' of the material (O'Brien et al, 2005).

Dai et al (2004) investigated microdamage in rats and attempted to evaluate the potential of microcracks as a measure of bone quality. Ninety rats were ovariectomised and drug treated with 17β-estradiol (EST) at 10µm/kg per day, or sham operated (sham). Compressive mechanical tests were performed on the L5 vertebral body and the maximum load required for failure (ML) and the elastic modulus of the specimens (EM) were determined. Microcrack density (Cr.Dn; which is the number of cracks found per area measured), and microcrack surface density (Cr.S.Dn; which is the total crack length per area measured) of the adjacent L4 vertebra were determined from histological analyses. At week 21 post-OVX the OVX rats showed greater Cr.Dn and Cr.S.Dn and lower ML and EM values than both EST and sham rats. Cr.Dn values in sham, EST and OVX rats were 0.55 ± 0.10 , 0.69 ± 0.11 and 1.32 ± 0.27 (#/mm²), while Cr.S.Dn values

were 26.55 ± 4.7 , 33.69 ± 5.7 and 61.28 ± 11.73 ($\mu\text{m}/\text{mm}^2$), respectively. Their findings showed a positive correlation between microcrack accumulation and reduction in elastic modulus and bone strength.

Theoretical and experimental evidence has shown that the microdamage caused by repetitive stresses can stimulate bone remodelling (Martin and Burr, 1982; Martin, 2000; Lee et al, 2002). The exact mechanism by which microcracks could influence remodelling is still unknown; however, as far back as 1973 Frost proposed that the disruption of canalicular connections by microcracks crossing them may provide the stimulus to initiate remodelling. In more recent times, there is evidence to suggest that microcrack growth may lead to osteocyte apoptosis and that this is one of the targeting mechanisms for remodelling (Noble et al, 1997; Verborgt et al; 2000, Hazenberg et al, 2007).

Noble et al (1997) were among the first to show that osteocyte apoptosis could occur due to mechanical stresses and they also proposed that it may be involved in bone remodelling. Although experimental observations have been made of cell apoptosis near microdamage, a direct link between cracks and cell death has not been found to date (Schaffler et al, 1995; Verborgt et al, 2000). Two popular hypotheses that exist are that cracks may cause apoptosis by the rupturing the cell processes (Hazenberg et al, 2007) or that they may serve to shield cells from local strain (Prendergast and Huiskes, 1996), limiting the exchange of nutrients and waste thus affecting cell homeostasis.

Considering the above discussion it can be said that microcracks, in addition to the other factors discussed in this chapter, are a useful and important parameter for assessing bone quality in osteoporosis. However, there is still much that remains unknown about microdamage such as how its behaviour changes in areas of high bone turnover and also

how microcracks behave in bone which has undergone long term treatment with anti-resorptive drugs.

1.6.2.4 Mineralisation

Increased levels of mineral in bone will increase stiffness but will decrease the flexibility and both of these factors play a role in fracture resistance. The amount of energy that can be absorbed by a bone before fracture is reduced by increasing the mineralisation of the bone tissue (Currey et al, 1996). Suppression of osteoclastic activity, which is the mechanism of action of bisphosphonates in the treatment of osteoporosis, has the effect of increasing tissue mineralisation by lengthening the period of time over which secondary mineralisation can occur (Meunier, 1997; Nuzzo, 2002). This has two effects; firstly, it may increase the tendency for microcracks to initiate by making the material more brittle. Secondly, it increases the homogeneity of the tissue and this may make crack propagation easier. When bone turnover is high, mineralisation is lower due to the reduced mineralisation period and this also has an adverse effect on bone strength as discussed earlier in this chapter.

1.6.2.5 Other factors

The organic matrix of bone has not been widely considered in terms of its contribution to bone strength and quality. Silva et al (2004) studied the demineralised bone matrix from SAMP6 mice, which is a strain of mouse widely used as a model of osteoporosis. They found that, compared with control mice, bone samples from the SAMP6 mice had normal protein content but displayed a reduced fraction of hydroxyproline per total protein, this may lead to differences in collagen fibre orientation and cross-linking

leading to a reduction in bone strength. Anti-resorptive treatments are thought to increase the amount of cross linking, but whether this is a positive or a negative change is not clear at present (Burr, 2004).

1.6.3 Bisphosphonates

A wide range of pharmaceuticals are available for the treatment of osteoporosis including estrogen, selective estrogen receptor modulators (SERMS), calcitonin and parathyroid hormone. However, the most popular drugs for the treatment for osteoporosis are the bisphosphonates.

Bisphosphonates inhibit resorption of bone which occurs as part of the remodelling process. This action counters the loss of bone mass which is the major feature of osteoporosis. 'First generation' bisphosphonates such as etidronate were shown to increase BMD in the spine, hip and other clinically relevant sites but were found to adversely effect bone mineralisation and cause osteomalacia over time (Sparidans et al, 1998; Inui and Takaoka, 2003). 'Second generation' bisphosphonates such as alendronate are approximately 1000 times more potent than etidronate and were also found to increase BMD at all sites studied and reduce clinical fractures by 36% in women with baseline osteoporosis at the femoral neck (Cummings, 1995).

Zolendronic acid is a 'third generation' bisphosphonate and is the most potent bisphosphonate studied in clinical trials to date (Reid et al, 2002). It has been shown to be more than four orders of magnitude more potent than earlier bisphosphonates such as clodronate or etidronate (Green et al, 2002). Zolendronic acid has the added advantage of its efficacy being dependent on total cumulative dose, rather than the dosage

schedule. In a study by Reid et al (2002), 351 postmenopausal women with low BMD were treated with zoledronic acid on five different dosing regimens, 0.25mg, 0.5mg or 1mg at three month intervals, a total annual dose of 4mg as a single dose and two doses of 2mg each, six months apart. There were similar increases of approximately 5% in BMD in all the zoledronic acid groups showing that the determining factor of the efficacy of this drug is the total cumulative dose. This effect was found even over relatively large dosing intervals of up to one year.

However, these results may not be as positive as they initially seem. Bisphosphonates inhibit resorption of bone which occurs as part of the remodelling process. The purpose of this action is to prevent bone loss and bisphosphonates are generally very effective in this regard. However, by inhibiting the process of remodelling it is possible that damage which would otherwise have been repaired is allowed to accumulate.

Studies of etidronate, alendronate and risedronate have shown that they cause no increase in microdamage when administered at the recommended clinical dosage; however, at supra-clinical dosages all showed microdamage accumulation (Forwood et al, 1995; Mashiba et al, 2001a, b). In a study by Forwood et al (1995), 24 adult female beagle dogs were examined for microdamage following two years of treatment with five times the clinical dose of risedronate. Initially the analysis showed no significant differences among groups in Cr.Dn and it was reported that the hypothesis that microdamage accumulation increases following the use of anti-resorptive drugs was not supported. At the time, suggested explanations for this result were that 1) microdamage does not accumulate following treatment 2) transient increases in microdamage at the beginning of the study period had been repaired or 3) the canine femoral neck does not reflect weight-bearing conditions of clinical relevance to humans for assessment of

microdamage. A further explanation was offered later which was that in the original study, cracks which were formed as a result of lamellar debonding were not included in the Cr.Dn measurement.

Hirano et al (2000) investigated the effect of high dose etidronate on the mechanical properties of bone and microdamage accumulation. Skeletally mature beagles were injected with a saline vehicle or etidronate at 0.5 mg/kg/day or 5.0 mg/kg/day for one year. After sacrifice bones were removed for analysis and fractures of ribs and/or thoracic spinous processes were found in 10 of 11 animals treated with the higher dose etidronate. One fracture of a spinous process was found in the low dose and none in the control group. Biomechanical testing showed reduced strength in the ribs and lumbar vertebrae in the high dose group, while histomorphometric analysis showed a significant reduction in bone turnover in the high and low treatment groups. In the high dose group the activation frequency was reduced to zero in both compact and trabecular bone. Interestingly, Cr.Dn increased significantly in the high dose group in the lumbar vertebrae but not in the ribs or spinous processes where fractures occurred. This was most likely the result of excessive amounts of unmineralised bone, and this may explain the occurrence of spontaneous fracture and the absence of microdamage.

A study by Mashiba et al (2001a) demonstrated increased microdamage accumulation following 12 months treatment with oral bisphosphonates. Thirty-six female beagles, 1-2 years old, were divided into three groups. The control group was treated with a saline vehicle and the remaining two groups were treated daily with either risedronate (0.5 mg/kg/day) or alendronate (1.0mg/kg/day). The doses of bisphosphonates were six times the clinical doses approved for treatment of osteoporosis in humans. The L2 vertebral body and right ilium were assigned to histomorphometry, while the L3

vertebra and the T2 spinous process, the right femoral neck and the left ilium were used for microdamage analysis. The L4 vertebrae and T1 spinous process were mechanically tested to failure in compression and shear respectively. One year of treatment with bisphosphonates significantly suppressed trabecular remodelling in vertebrae (90% risedronate, 95% alendronate) and the ilium (76% risedronate, 90% alendronate) and significantly increased microdamage accumulation in all skeletal sites measured (Table 1.2).

Table 1.2: Microdamage analysis of the 3rd lumbar vertebra, left ilium, 2nd thoracic spinous process, and right femoral neck (Mashiba et al, 2001a).

Region	Parameters	Group		
		CNT	RIS	ALN
L3 Vertebra	Cr,Le (µm)	40.5 ± 6.2	49.4 ± 8.1	45.7 ± 2.3
	Cr,Dn (#/mm ²)	0.34 ± 0.09	0.80 ± 0.18 ^a	1.19 ± 0.14 ^c
	Cr,S,Dn (µm/mm ²)	12.7 ± 3.4	39.8 ± 9.1 ^b	53.0 ± 6.0 ^d
Left Ilium	Cr,Le (µm)	53.5 ± 6.1	53.3 ± 3.5	51.9 ± 3.3
	Cr,Dn (#/mm ²)	0.41 ± 0.10	0.74 ± 0.09 ^a	0.72 ± 0.10 ^a
	Cr,S,Dn (µm/mm ²)	22.2 ± 5.9	39.3 ± 6.0	39.0 ± 6.6
Th2 Spinous Process	Cr,Le (µm)	60.1 ± 11.9	62.9 ± 7.6	55.7 ± 3.2
	Cr,Dn (#/mm ²)	0.22 ± 0.05	0.34 ± 0.08	0.44 ± 0.05 ^b
	Cr,S,Dn (µm/mm ²)	12.0 ± 2.9	20.5 ± 4.5	24.3 ± 3.0 ^a
Right Femoral Neck	Cr,Le (µm)	48.7 ± 5.3	49.4 ± 3.2	60.3 ± 4.5
	Cr,Dn (#/mm ²)	0.24 ± 0.06	0.35 ± 0.07	0.43 ± 0.07 ^a
	Cr,S,Dn (µm/mm ²)	13.4 ± 4.6	17.2 ± 2.9	25.7 ± 4.5 ^a

Trabecular bone volume and vertebral strength increased following 12 months of treatment with bisphosphonates, however, it was demonstrated that the normalised toughness was reduced by 21% in both bisphosphonate treated groups. This showed that suppression of bone turnover by high doses of bisphosphonates is associated with significantly increased microdamage accumulation and a reduction in the toughness of the vertebrae.

1.6.4 Experimental animal models of osteoporosis

The use of an animal model is necessary in order to model human biological events in a controlled fashion. Often it is the case that these events cannot be satisfactorily

recreated in any other way. Animal models for osteoporosis research that have been used in the past include rats, mice, non-human primates, dogs, cats, rabbits, guinea pigs, mini-pigs and sheep, all of which have certain advantages and disadvantages. There are many things to be considered when choosing a possible animal model for osteoporosis such as compatibility with the human condition, knowledge of biological properties, cost and availability, adaptability to experimental manipulation, ethical and societal implications (Davidson et al, 1987).

Since 1994, the US Food and Drug Administration (FDA) require data from both the rat and a well validated large animal model for pre-clinical evaluation of new experimental drug therapies at both clinical and supra-clinical doses. The high cost and long time frame of clinical testing are other reasons why animal models play a crucial role in osteoporosis research. A review of the most common animals that have been used as a model for osteoporosis is presented here.

Rat model

Rats are the most commonly used animal model in osteoporosis related research (Lalla et al, 1998; Yoshitake et al, 1999; Schultheis et al, 2000; Bauss et al, 2002). The majority of studies use the ovariectomised rat to simulate postmenopausal osteoporosis. The aims of these studies ranged from observing the effect of bisphosphonates on bone metabolism, to studying the mechanisms of disuse osteoporosis by conducting hind-limb suspension experiments. There is extensive literature relating to the ovariectomised rat including studies which investigate histomorphometric changes, biochemical markers, methodology for bone densitometry and evaluation of bone fragility (Wronski, 1986; Kalu, 1991; Frost, 1992). While the rat is easy to handle, house and is cost effective there are significant differences between it and the human skeleton which

include the bone metabolism, presence of lamellar bone and the capacity for remodelling (Newman et al, 1995). It may also be said that the rat is a poor animal model to study the effect of ovariectomy on cortical bone because of the lack of Haversian systems, while another limitation is the absence of impaired osteoblast function during the late stages of estrogen deficiency (Wronski, 1991).

Non-human primate model

The non-human primate is also a viable option as a model for postmenopausal osteoporosis and as such has been used in many experiments (Hodgen et al, 1977; Smith et al, 2003; Gunji et al, 2003; Cerroni et al, 2003). The primate has many advantages over other animal models of osteoporosis. Firstly, their organ systems closely resemble those in the human i.e. the gastrointestinal tract, endocrine system and bone metabolism (Newman et al, 1995). Also, female macaque monkeys are polyestrous and have hormonal patterns similar to those of humans (Hodgen, 1977). Postmenopausal osteoporosis is hormone related, so the striking similarity in hormonal activity between the primate and the human is a notable advantage of this model. However, the female primate must be sufficiently aged to act as a model for postmenopausal women. The extent of osteoporosis depends not only on the rate of bone loss, but also on the peak bone mass achieved (Rigotti et al, 1991). It has been shown that peak bone mass is not reached in cynomolgus monkeys until nine years of age, however, most studies have used ovariectomised monkeys aged 4-7 years (Jerome et al, 1994). Furthermore, although the non-human primate provides an excellent model on theoretical grounds, in practical terms the acquisition of aged female primates is difficult and very costly.

Mini-pig model

In recent years mini-pigs have been proposed as a large animal model of postmenopausal osteoporosis (Mosekilde et al, 1993; Borha et al, 2002). Prior to this the size of the pig was a limiting factor on their use as a model for research, however the average weight of the mini-pig at maturity is 60kg. The reproductive cycle of the pig is similar to that of the human in duration (18-21 days) and like the human it is continuous (Newman et al, 1995). Another similarity which is important in certain areas of study is the anatomy of the gastrointestinal tract and also the omnivorous diet of the pig. Other useful attributes of the mini-pig are that their level of bone loss may be efficiently monitored *in vivo* by quantitative computed tomography (QCT), and also they suffer from glucocorticoid induced bone loss which has been found to be successfully treatable with bisphosphonates (Borha et al, 2002). However, it has been shown that pigs have a thicker cortical bone and higher BMD in trabecular bone compared with humans (Mosekilde et al, 1993). Moreover, the cost of the mini-pig as well as its rarity in certain areas can cause logistical problems.

Dog model

The dog has been frequently used as an animal model for osteoporosis, specifically the beagle dog due to the lack of genetic variation between animals (Hirano et al, 2000). The most obvious advantage of dogs in the study of osteoporosis is that they exhibit internal bone remodelling of cortical and trabecular bone similar to that found in humans (Boyce et al, 1990). Another of this model is that dogs are monogastric like humans; this would apply particularly to studies using oral bisphosphonates. However, studies on ovariectomised dogs have shown that changes in cancellous bone remodelling were transient phenomena, and the duration of these changes did not appear to be sufficient to create a sizeable reduction in bone volume (Boyce et al, 1990). Also,

unlike humans who are polyestrous, dogs are diestrous, with ovulation occurring twice a year (Newman et al, 1995). The lack of appreciable responses in this model may limit the usefulness of histomorphometry, bone mass and biochemical measurements of dog models for the study of osteoporosis (Shen et al, 1992).

Sheep model

The sheep has been used by many laboratories around the world as an animal model for studying different aspects of osteoporosis (Pastoureau et al, 1989; Chavassieux, 1990; Chavassieux et al, 1991; Geusens, 1992; Turner and Villanueva, 1994; Hornby et al, 1995; Newman et al, 1995; Turner et al, 1995; Turner, 2002; Lill et al, 2002, 2003; Schorlemmer et al, 2003).

The ovine animal model is a good choice for the study of postmenopausal osteoporosis for a number of reasons. It has been reported that there are striking similarities between the hormone profiles of ewes and women (Goodman et al, 2002). A resemblance between the dynamic behaviour of bone from the iliac crest of the sheep and the human has also been reported (Pastoureau et al, 1989; Turner and Villanueva, 1994). However, the most important similarity between ewes and women with regards to this research is the similarities in the bone remodelling cycles, which are both between 2 and 3 months (Turner and Villanueva, 1994; Turner et al, 1995; Lee et al, 2002).

One potential drawback of using the sheep to model osteoporosis is its different gastrointestinal system compared to humans; this is particularly relevant in studies where oral absorption of a bisphosphonate is required. Sheep bone is predominantly plexiform, as is the case with most domestic large animals. However, studies have

shown that Haversian bone can be found at a variety of anatomical sites in aged sheep which have reached full skeletal maturity (Turner, 2001).

Other useful attributes of the ovine animal model are that they are easy to handle and house, they are inexpensive compared to other large animals, they are readily available in this country and they are accepted in society as a research animal. Sheep are a flock animal and therefore suffer the least stress when housed in groups of two or more. They are available in large numbers meaning large scale experiments are possible (Newman et al, 1995). In 1994 the FDA produced draft guidelines on the treatment and prevention of osteoporosis, in these guidelines the sheep was identified and accepted as an animal model for osteoporosis research.

The sheep model has been used to study various orthopaedic conditions including hip replacements, fracture repair, vertebroplasty and osteoporosis. Turner and Villanueva (1994) studied the effect of OVX on aged ewes and showed a significant decline in BV/TV at the iliac crest; significant differences in the proximal femur were also reported between OVX sheep and controls. Subsequent studies by the same group demonstrated bone loss, as measured by DEXA, in the lumbar vertebrae 18 months post-OVX (Turner et al, 1995).

Schorlemmer et al (2003) used steroid-treated OVX sheep as a model for osteoporotic bone, and investigated the effects on trabecular bone density, microarchitecture, biomechanical properties and the formation of new bone. Six months post-treatment BMD was shown to be reduced by 19% while mechanical competence was reduced by 45%. Trabecular bone volume (BV/TV) and trabecular thickness (Tb.Th) were reduced by 21% and 20% respectively. After 12 months, BMD and mechanical competence had

fallen further by 33% and 55% respectively. The differences between the groups were most pronounced in the tibia and femur.

Augat et al (2003) also studied the effects of OVX and steroid treatment on ovine trabecular bone. Biopsies of bone from the proximal tibia were taken at 6 and 12 months post-OVX. The biopsies were scanned using μ CT and three-dimensional reconstructions were created, the samples were then mechanically tested. The BMD of trabecular bone had markedly reduced by 27% after 6 months and 33% after 12 months and elastic modulus had fallen by 36% after 6 months and 62% after 12 months (Augat et al, 2003). For the reasons discussed above, we decided to use ovariectomised sheep as a model for postmenopausal osteoporosis in our study.

1.7 Objectives of this research

This research ultimately seeks to learn more about the relationship that exists between BMD, bone quality and bone strength. Specifically, four individual studies were carried out to investigate how these parameters are related to osteoporosis and bone failure.

Principal objectives

- (1) To design and carry out an experiment to investigate the effect of increased bone turnover on bone quality using the ovariectomised sheep as an animal model.
- (2) To investigate the effects of OVX on bone turnover and microarchitecture in ovine compact bone 12 months post-OVX, and to determine the implications of these changes on bone strength.
- (3) To measure the fatigue life of OVX and control compact bone samples and to quantify resultant microdamage in terms of location and interaction with the surrounding microstructure.
- (4) To analyse the effect of OVX at the whole bone level, specifically to measure bone turnover and microarchitecture in whole lumbar vertebrae and then to assess the effect on the biomechanical properties of the structure 12 months post-OVX.

Chapter 2

Experimental Design, Ovariectomy and Fluorochrome Bone Labels

2.1	Introduction.....	41
2.2	Materials and Methods.....	42
2.2.1	Power analysis and sample size calculations	42
2.2.2	Sheep.....	43
2.2.3	Ovariectomy.....	46
2.2.4	Fluorochrome dye administration	49
2.2.5	Hormone Assays	53
2.2.6	Sacrifice	54
2.3	Results.....	56
2.3.1	Animal weights	56
2.3.2	Hormone analysis.....	57
2.3.3	Mortality.....	58
2.4	Discussion	59

2.1 *Introduction*

This chapter describes the materials and methods for an experiment which used an ovariectomised sheep model to simulate post-menopausal osteoporosis. The methods used to prepare, test and analyse individual bone samples for specific studies are described in Chapters 3, 4 and 5. As discussed in the previous chapter, the ovariectomised sheep is one of a number of research animals which are often used to model post-menopausal osteoporosis.

The sheep has a number of advantages over other animal models of osteoporosis, in particular the commensurate bone remodelling cycles between humans and sheep which are both approximately 3 months (Turner and Villanueva, 1994; Turner et al, 1995; Lee et al, 2002). This has particular relevance to our study because one of the primary parameters of bone quality we wish to investigate is bone turnover. Other advantages of the sheep model are the strong similarity between the general hormone profiles of ewes and women (Goodman, 2002) and the resemblance between the dynamic behaviour of bone from the sheep and the human which has been studied by other authors using double tetracycline labelling techniques (Pastoureau et al, 1989; Turner and Villanueva, 1994).

2.2 *Materials and Methods*

Experiments involving animal models must be designed and conducted so that any adverse effects on the animal are minimised and weighed against the benefits that are likely to accrue. We wished to design an experiment whereby ovariectomised (OVX) sheep would be used to simulate post-menopausal osteoporosis. We required two groups of sheep, each having a predetermined number of OVX and control animals, Group 1 would be sacrificed at 12 months and Group 2 at 30 months post-OVX. This would provide the opportunity to study osteoporosis at different stages in disease progression. It was an important part of our experimental design to calculate the experimental sample size for this study.

2.2.1 *Power analysis and sample size calculations*

Sample size calculations are normally carried out based on three considerations:

- Allowance for Type I error (α) this is the minimum error level that is set for rejecting the null hypothesis.
- Allowance for Type II error (β): this is the minimum error level that one sets for accepting the null hypothesis.
- Estimate of effect size (δ): a measure of difference in distribution characteristics of one or more study variables between two or more groups.

Change in bone mineral density (BMD) is the effect which is normally studied in osteoporosis research, and thus sample size calculations for experimentation are usually based on it. However, in this study, bone quality is of primary interest. Microdamage is

considered to be one of the major determinants of bone quality, thus the effect which we proposed to study was microcrack density (Cr.Dn), rather than BMD. SigmaStat 3.0 statistical package (SYSTAT Software Inc, Chicago, IL 60606) calculated the number of animals required per group, to achieve power $(1-\beta) > 0.90$ where $\alpha=0.05$, to be 19 in order to detect a change in Cr.Dn of $2.0 \text{ [}/\text{mm}^2\text{]}$ between the control and OVX animals in Group 1.

Our working hypothesis was that Group 2 (which had an experimental duration of 30 months post-OVX) would accumulate more microdamage during that time, thus the effect would be greater. Therefore the calculated sample size required for Group 2 was smaller because a greater difference between control and OVX would be expected. However, higher mortality is expected in aged sheep over 30 months and on that basis, it was proposed that extra animals be included in Group 2 and so the sample size for this group was increased from 11 to 19.

2.2.2 Sheep

Seventy-six skeletally mature, aged female mixed-breed sheep were purchased at market in Co. Wicklow in August 2003. The precise age of the animals was not known but the range was between 5-9 years. The sheep were housed at the University College Dublin (UCD) Veterinary Research Facility at Lyons Estate, Co. Kildare. All animals were examined by a veterinarian and their suitability for inclusion in our study was determined. Minor ailments such as mild foot-rot were identified and treated where necessary. Prior to commencing the live animal phase of this project, an experimental license was applied for and granted under the Cruelty to Animals Act, 1876 by the Department of Health (license number: B100/2443). All proposed work was also

approved by the University College Dublin (UCD) Ethics Committee. Each animal was tagged with 2 ear-tags for identification purposes. However, ear-tags may easily be lost or damaged over the course of 1-2 years outdoor grazing, so each sheep was also micro-chipped. Each sheep could then be identified by reading the microchip with an electronic hand held scanner in the event of both ear tags being lost.

Thirty-eight sheep were randomly assigned to undergo ovariectomy to simulate post-menopausal osteoporosis; the remainder served as controls. Animals were then divided into two groups. Group 1 (OVX; n=19, control; n=19) would be sacrificed at 12 months post-OVX and Group 2 (OVX; n=19, control; n=19) would be sacrificed 30 months post-OVX. Group 2 also included a sub-group of 5 OVX sheep which would receive a supra-clinical dose (X5) of a bisphosphonate called zoledronic acid. This drug would be administered to the sub-group at a time-point approximately 24 months post-OVX. This PhD thesis deals only with analyses carried out on sheep from Group 1. Details of analyses carried out on Group 2 animals are discussed in a related study (Brennan et al, 2007). Animal number, ear-tag number and microchip details for control and OVX animals from the 1 year study are shown in Table 2.1.

Table 2.1: Animal groups, ear-tag numbers and microchip numbers.

CONTROL			OVX		
<i>TCD/RCSI Number[^]</i>	<i>Ear-tag Number</i>	<i>Chip Number</i>	<i>TCD/RCSI Number[^]</i>	<i>Ear-tag Number</i>	<i>Chip Number</i>
1	4369/1154	4775	4	4329/1436	5012
2	175/-	8435	8	4365/1327	0394
3	4457/-	3390	9	4337/974	4476
5	4355/4318	4469	10	4383/J137	0865
6	4377/1268	7952	11	4294/1563	5012
7	4315/1282	8721	14	4342/1440	0667
12	4463/156	9595	15	4346/1334	8098
13	4366/1368	6098	18	4479/-	7947
16	4317/1329	1822	19	4354/1422	3437
17	4474/-	1486	21	4374/1173	1535
20	4344/1151	4563	23	4318/1370	8251
22	4312/1232	2520	24	4483/J186	1055
27	4384/R35	5694	25	4372/1441	0194
28	4297/457	5631	26	4350/1035	4904
29	4361/1363	5408	32	4363/1292	8063
30	4478/181	9270	33	4358/1036	5597
31	4332/1144	4234	*	4327/-	-
34	4349/1321	7586	*	119/-	7801
*	4336/1074	2093	*	4325/-	-

[^] TCD/RCSI number was assigned at the time of sacrifice for easier 'in-house' identification.

* These animals died during the course of the experiment and thus were not assigned a TCD/RCSI number. See Section 2.3.3 for details.

2.2.3 Ovariectomy

Ovariectomy was performed through a ventral midline laparotomy under general anaesthesia in the veterinary operating theatre on the Lyons Research Estate, UCD Newcastle, Co. Kildare in November 2003. All procedures were carried out by a veterinary surgeon under Irish Government license number B100/2443. Over the course of 4 days, 38 animals were ovariectomised.

2.2.3.1 Anaesthesia

All animals assigned for surgery were grouped together in a standard animal pen. After weighing each sheep, the region of the left external jugular vein was clipped and an intravenous injection of sodium thiopentone was administered to induce anaesthesia. The sheep were then placed in dorsal recumbency on the operating table and intubated using either a size 7 or 8 rubber cuffed endotracheal tube. The cuff was inflated, tied to the mandible and anaesthesia maintained on 3-4% halothane (Halothane, Merial Animal Health, Harlow, UK) in oxygen. The hind limbs were secured to the operating table using ropes and the sheep maintained in dorsal recumbency for the duration of the surgical procedure.

2.2.3.2 Surgical preparation

The ventral abdomen was close-clipped, shaved with a disposable razor and a standard aseptic surgical preparation performed using chlorhexidine and alcohol. The table was tilted so that the animal was in the Trendelenberg position which allows cranial displacement of the rumen to ease identification of the uterus and ovaries.

2.2.3.3 Surgery

A sterile disposable paper drape was fenestrated isolating the surgical site and secured to the ventral abdomen using 4 towel clips. A ventral midline incision was made commencing just caudal to the umbilicus and extending approximately 10cm caudally. The subcutaneous fat and fascia were bluntly dissected, being careful to protect the milk vein and where necessary ligating branches of it. The linea alba was incised using a scalpel and scissors. The uterus was identified in the caudal abdominal cavity, exteriorised and the ovaries traced. The ovarian vessels were identified and ligated using a simple ligature of 3 metric polydioxanone (PDS, Ethicon, Johnson & Johnson, Brussels, Belgium). The ovary was then removed and each ligated pedicle carefully checked for haemorrhage (Figure 2.1). When satisfied that no haemorrhage was evident the pedicle was returned to the abdomen. The contra-lateral ovary was then removed in a similar manner.

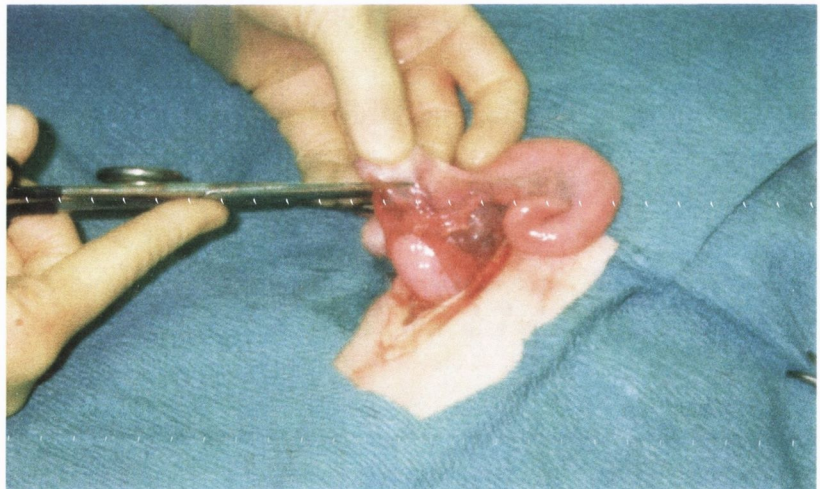


Figure 2.1: Surgically removing sheep ovaries through a midline ventral laparotomy.

Prior to abdominal closure, benzyl penicillin sodium (10mg/kg, Crystapen, Shering-Plough Animal Health, Ireland) was administered intraperitoneally as an additional prophylactic measure against peritonitis. The linea alba was closed using a simple

continuous suture of 5 metric polydioxanone (PDS, Ethicon, Novartis, USA). The subcutaneous layer was apposed using a simple continuous suture of 3 metric polydioxanone (PDS, Ethicon, Novartis, USA). Skin closure was achieved with a simple continuous suture and the surgical wound sprayed with an aluminium powder based wound spray (Alluspray, Vetoquinol Ireland Ltd, Dublin). A long-acting injection of amoxicillin antibiotic was administered intramuscularly (15mg/kg, Betamox LA, Norbrook Laboratories Ltd, Ireland). An analgesic, flunixin meglumine, was also administered by intramuscular injection (2.2 mg/kg, Flunixin Inj, Norbrook Laboratories Ltd, Ireland). Oxytetracycline (50mg/kg, Terramycin LA, Norbrook Laboratories Ltd, Ireland) was administered by slow intravenous injection into the jugular vein prior to anaesthetic recovery. The sheep were observed carefully for the return of a swallow reflex and were extubated once this reflex had returned. They remained indoors under observation until completely recovered from anaesthesia and capable of normal ambulation. Most sheep were ambulatory within 20 minutes of completion of ovariectomy.

2.2.3.4 Post-operative care

The sheep were observed closely over 48-hours post-operatively. At 24 hours post-operatively a second analgesic injection of flunixin meglumine was administered if deemed necessary based on clinical evaluation. At 48 hours all surgical wounds were re-inspected for signs of swelling, infection or wound breakdown. Wounds were inspected again at 10 days post-operatively and skin sutures removed at this time. No wound infection was identified in any sheep. One sheep, at 10 days, was found to have a small incisional hernia which was repaired surgically under anaesthesia. Wound healing occurred uneventfully.

2.2.4 Fluorochrome dye administration

Fluorochromes are substances that can absorb energy in the form of light of a short wavelength and release light of a longer wavelength. This action is known as the Stokes shift, named after George Stokes the Irish physicist. When a molecule or atom absorbs light, it enters an excited electronic state. The Stokes shift occurs because the molecule loses a small amount of the absorbed energy before re-releasing the rest of the energy as luminescence or fluorescence (the so-called Stokes fluorescence). Ultraviolet light can be shone on a fluorochrome to achieve this effect, oxytetracycline, for example, fluoresces yellow. The fluorochromes that were used in this study were chosen because of their ability to bind to exposed calcium phosphate through stable covalent bonds (Parkesh et al, 2007). In bone, this is only possible in two situations, when bone is being mineralised during formation or demineralised during resorption, but the latter is transient as the labelled bone is removed. However, during formation the fluorochrome becomes locked in by the ossification process and permanently marks any bone which was in the process of formation when it was administered. Rahn (1977) developed a labelling system that balances toxic effects of these agents and their luminescence. An adapted version of that protocol was used in this study. Other studies have successfully used the same fluorochromes and similar labelling sequences as those chosen for this work (Lanyon et al, 1979; Goodship et al, 1979; Lee and Taylor, 2003, Hardiman et al, 2005).

In one such study by Lee and Taylor (2003), mechanical loading in the sheep proximal radius was increased by ulnar osteotomy (Group O), decreased by Steinmann pinning (Group P) and unaltered in sham operated controls (Group C). A series of intravenous fluorochromes (alizarin complexone, calcein, oxytetracycline, xylenol orange and

calcein blue) were given to label bone formation and the adaptive response in each group was measured at intervals up to 24 weeks. They found that surface strains were reduced in Group P and increased in Group O. The adaptive action responsible for the reduction in surface strain was measured using the fluorochrome labels. This study concluded that the adaptation process following surgery was targeted, as opposed to stochastic, and accurate in that the response did not overshoot. In another study, carried out by Hardiman et al (2006), an established rat disuse osteoporosis model, hindlimb-suspension, was used to relate morphological change and gene expression to altered mechanical load in the under-loaded femora and the ostensibly normally loaded humeri of the suspended rats (39 days old at onset; 1, 3, 7 and 14 days suspension). Morphological changes were measured by labelling new bone formation with fluorochrome dyes (oxytetracycline and calcein blue) during the experimental period and subsequent histological analysis of bone sections post-sacrifice. Bone formation rate was reduced at the mid-diaphysis of the unloaded femora while no significant effect was found in the loaded humeri. Gene expression patterns of two candidate genes (c-fos and osteocalcin) were assessed in periosteal tissue. Altered gene expression patterns were identified and tracked over the suspension period. The altered levels of both genes were found to be consistent with the changes observed in the histological analysis

All of the fluorochromes used in this study (with the exception of oxytetracycline, which is commercially available as 'Terramycin/LA Injectable Solution') were purchased in powder form and added to sterile veterinary water on a magnetic stirrer to achieve the required concentration. The pH was measured and adjusted to between 7.2-7.4 using NaOH or HCL solution. The concentrations and dosages for each of the fluorochromes are shown in Table 2.2.

Table 2.2: List of fluorochrome dyes, solution concentrations and dosages.

Fluorochrome Agent	Solution Concentration	Dosage
Oxytetracycline (Pfizer Animal Health, Dublin)	200 g/l	50mg/kg ^{IV}
Alizarin complexone (Lennox Laboratory Supplies, Dublin)	30 g/l	25 mg/kg ^{IV}
Calcein (Sigma Aldrich, Dublin)	5 g/l	10 mg/kg ^{*IV}
Xylenol orange (Sigma Aldrich, Dublin)	90g/l	90mg/kg ^{*IV}
Calcein blue (Sigma Aldrich, Dublin)	30 g/l	30mg/kg ^{*IV}

[^] From Lanyon et al (1982); ^{*}from Rahn, (1977)

To achieve a sterile solution a 'Millipore' filter system (Millipore, Bedford, MA, USA) was initially used. However, this proved to be very time consuming and was superseded by the VacuCap® 90 PF sterile vacuum filtration device (Pall Gelman Laboratory, Co. Meath) and a vacuum pump. This system operates by drawing the solution from the preparation flask by vacuum, through a 0.22 mm disposable filter and into a sterile flask (Figure 2.2). The solutions were then tightly sealed. All glassware was sterilised using a standard autoclave.

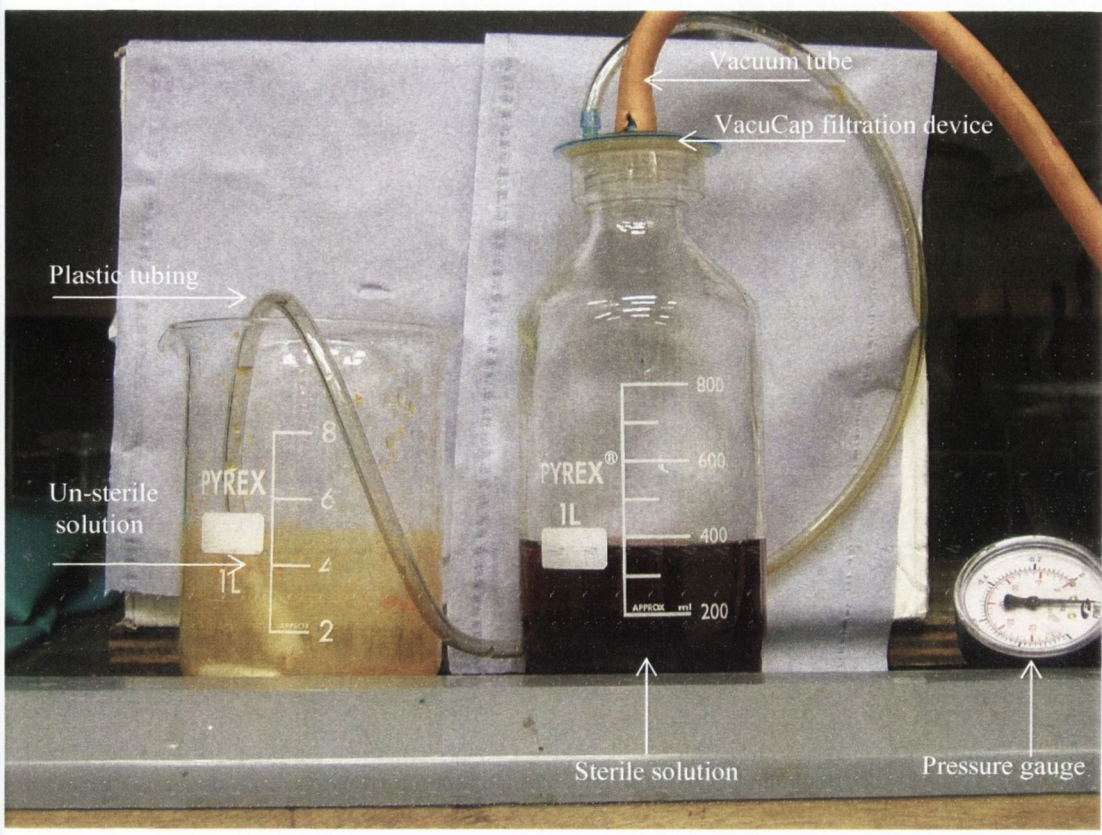


Figure 2.2: Apparatus for sterilising fluorochrome dyes using a VacuCap ® filtration device.

The fluorochromes were administered intravenously according to the schedule shown in Table 2.3. With the sheep manually restrained, the fleece was clipped from the lateral side of the neck and the jugular vein identified. The vein was distended by digital pressure and each fluorochrome administered by slow intravenous injection via a 16 gauge hypodermic needle. When the volumes for injection were large (>50ml), an extension tube was attached to the needle to minimise injury to the vein while changing syringes. This reduced the need for repeated venipuncture. The interval between fluorochrome administrations in Group 1 was chosen to be 3 months because this coincides with the remodelling cycle of the animal. In Group 2 however, the schedule for administrations was different due the longer experimental duration of that group.

Table 2.3: Timetable of events and fluorochrome administrations during year 1.

Month	Year 1 Control (n=19)	Year 1 OVX (n=19)
0	Oxytetracycline	OVX + Oxytetracycline
3	Alizarin Complexone	Alizarin Complexone
6	Calcein	Calcein
9	Xylenol Orange	Xylenol Orange
12	Calcein Blue <i>Sacrifice</i>	Calcein Blue <i>Sacrifice</i>

2.2.5 Hormone Assays

Between the 1st and the 15th of November 2004, which was approximately 12 months post-OVX and three weeks prior to sacrifice, seven blood samples were taken from each animal. The ovine oestrous cycle necessitates sampling over approximately 14 days to achieve accurate measurements. Specific hormone assays were run on all of the samples to measure the level of progesterone and estradiol. Approximately 238 blood samples were centrifuged to isolate the blood serum. One sample of serum was taken to measure progesterone (P4) and one for estradiol (E2). All samples were then labelled and frozen. Specific hormone assays were run to measure the level of P4 (AutoDELFIA, Wallac Oy, Finland) and E2 (MAIA, Adaltis, Italy) in each sample. This analysis was carried out to verify that the ovariectomy procedure had been functionally successful and that the oestrogen level was reduced in the OVX animals.

2.2.6 *Sacrifice*

Animals in Group 1 were sacrificed 12 months post-OVX. On the day of sacrifice sheep were gathered in an animal pen, counted and weighed. The region of the left metatarsal and left metacarpal bones were marked with sheep marker spray (Raidex Animal Spray, Stuttgart, Germany) in order to distinguish the left and right limbs upon removal. All animals were then loaded into a large animal transport vehicle. A transport permit for these animals was obtained from the local district veterinary office. The sheep were taken to Irish Country Meats Animal Processing Facility (ICM) in Navan, Co. Meath. Upon arrival animals were transferred to an onsite holding pen. On the processing line, a station was set up at the point where the heads, metacarpals and metatarsals would be removed. A box with pre-labelled bags (in ascending order from 1-34) was positioned there to ensure that when each specimen was collected, it was identified and stored correctly.

Before each sheep entered the processing line, its number was checked and entered into the on-site computer system, the number was also hand-written as a back-up. Animals were humanely slaughtered using a captive bolt according to the Department of Agriculture protocol. The head, metatarsal and metacarpal bones were removed and placed in pre-labelled polyethylene bags and made ready for storage. The remaining carcasses were left to chill for 24 hours. The following day, a large polyethylene bag was attached to each of the 34 carcasses with a cable-tie. Each bag contained 9 smaller bags, which had been carefully labelled using an indelible marker and an adhesive label as a secondary measure. Each label displayed the name of the bone or set of bones which the bag would hold. The skeleton was divided up and stored according to Table 2.4.

Table 2.4: Details of labelling system used to store all of the bones from each sheep.

BAG LABEL	CONTENTS
Left Front Limb (LFL)	Scapula, Humerus, Radius/Ulna
Right Front Limb (RFL)	Scapula, Humerus, Radius/Ulna
Left Hind Limb (LHL)	Femur, Tibia
Right Hind Limb (RHL)	Femur, Tibia
Pelvis	Pelvis
CV	Cervical Vertebrae (C1-C5)
TV	Thoracic Vertebrae (T1-T12)
LV	Lumbar Vertebrae (L1-L6/7)
Ribs	Rib cage (split at sternum)

The following day, a team of RCSI/UCD researchers along with trained butchers from ICM harvested all of the bones from each animal. In total approximately 1500 bones were harvested from Group 1. Nine freezers had been purchased and installed in the RCSI laboratory area specifically for this project and all of the Group 1 bones were stored there at -20°C.

2.3 Results

An experiment to simulate post-menopausal osteoporosis in a group of aged ewes was successfully designed, developed and implemented. The surgical procedure was functionally successful in reducing the level of estradiol and progesterone in the OVX group. Fluorochrome dyes were prepared and administered in order to label bone turnover at 5 time-points during the 12 months post-OVX. Following sacrifice, all bones from each animal were harvested, labelled and frozen at -20°C.

2.3.1 Animal weights

The average weights of control and OVX animals at each time-point are shown using a box-plot in Figure 2.3. Animals were also weighed at the time of sacrifice, however, because this was only 2 weeks after the 5th time-point the data was virtually identical and thus is not included in Figure 2.3. In general, the average group weight tended to increase as a function of time over 12 months post-OVX. However, there was no significant difference between control and OVX at any time-point ($p > 0.05$).

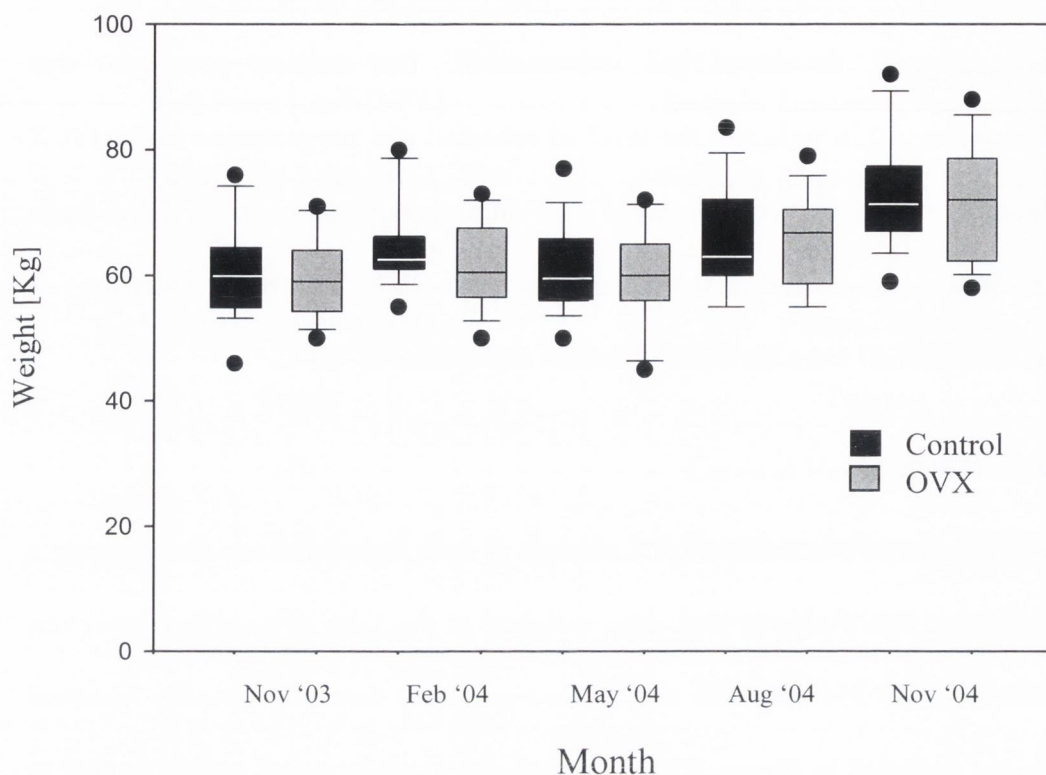


Figure 2.3: Box plot of the weights of control and OVX animals at the time of each fluorochrome administration.

2.3.2 Hormone analysis

The mean, minimum and maximum levels of progesterone and estradiol analyses, as measured by specific immunoassays in both groups are shown in Table 2.5. The average progesterone level was 3.18 and 0.596 (ng/ml) in control and OVX animals, respectively. The average level of estradiol was 0.772 and 0.326 (pg/ml) in control and OVX groups, respectively. These data show a significant reduction in both hormones in the OVX animals compared to controls ($p<0.001$)

Table 2.5: Mean, minimum and maximum levels of P4 and E2 from control and OVX groups.

	Progesterone (P4) (ng/ml)			Estradiol (E2) (pg/ml)		
	Mean	Min	Max	Mean	Min	Max
Control	3.18	1.183	11.428	0.772	0.588	1.350
OVX	0.596	0.159	1.152	0.316	0.0314	0.760

2.3.3 Mortality

Four sheep, numbered 119/-, 4325/-, 4327/- and 4336/1074, died during the course of this study. Sheep number 4327/- was recumbent and weak 48 hours following ovariectomy so it was euthanized on humane grounds and excluded from the study. Post mortem examination revealed poorly clotted blood in the abdominal cavity and evidence of liver damage (most likely from a previous liver fluke infection) which may have compromised normal clotting mechanisms. Euthanasia was achieved via an intravenous injection of sodium pentobarbitone into the jugular vein. Sheep number (119/-) died unexpectedly 10 months post-OVX, operative notes showed that this animal underwent a second operative procedure to repair an incisional hernia approximately one month after the OVX operation (10/12/03). There were no post-operative complications and the animal’s recovery was uneventful. Two other animals (4325/-, 4336/1074) also died unexpectedly, but had no events of note in their histories which could have contributed to their death. The post-mortem analyses were performed by a veterinary pathologist in UCD, in all cases the report determined that death was not related to our intervention.

2.4 Discussion

The surgical procedure of removing the ovaries was straightforward and was carried out within the anticipated timeframe without undue stress on the animals involved. In most cases, wound healing occurred uneventfully and all animals were fully mobile shortly after surgery. All sheep increased in weight during the experimental period and there was considerable individual variation among the animals. However, on average, the changes in weight over 12 months did not differ between the OVX animals compared with controls. One explanation for the weight increase in these sheep could be that prior to their involvement in this experiment, these were cull-animals which were due for slaughter. Once they were included in our study, they became valuable experimental animals and their husbandry, maintenance and feeding was closely monitored by an experienced animal handler. Thus they were healthy, better fed animals after 12 months in this study.

The use of fluorochrome dyes made up a substantial part of this project in terms of the time spent on their preparation and administration, and also in terms of scientific importance as they enabled us to measure bone turnover at specific skeletal sites. All of the intravenous dye administrations were completed successfully. All animals tolerated the injections well, it was noted that the urine was coloured by the injected solution briefly, otherwise no detrimental effects were observed. The fluorochrome dyes were also successful in their intended purpose of labelling sites of bone turnover. This was evident from epifluorescence microscopy analyses which were carried out on harvested bone samples after sacrifice. These analyses are discussed in more detail in Chapters 3, 4 and 5.

Sheep are a polyestrous species and as such experience an oestrous cycle several times each year. Even within species the duration of the cycle may vary, however, standard practice in hormone measurement of sheep dictates that samples should be taken over approximately 14 days. During this period, estradiol which is one of the main naturally occurring estrogens in sheep, was measured. Progesterone, another sex hormone which is involved in the regulation of estradiol, was also measured in both groups prior to sacrifice. Results show that the average level of both hormones in was significantly lower in the OVX group compared to the controls. Our data compares well to other findings in the literature. Lill et al (2002) found plasma progesterone levels in normal sheep to be between 0.3 and 5.8 ng/ml. Johnson et al (2002) found a significant reduction in serum estradiol levels (approximately 5-fold) between control and OVX sheep 12 months after surgery. Newton et al (2004) also measured serum estradiol concentrations in sheep 12 months post-ovariectomy and found a reduction of 11% in the OVX animals.

In conclusion, the design, development and implementation of an experiment to simulate osteoporosis using OVX sheep was successfully achieved. As with any study there are limitations associated with this experiment. Firstly, we used mixed breeds of sheep with unknown lambing histories. This was necessary because purpose bred sheep are very difficult to source. This may introduce variability in to our study in terms of the baseline hormone levels, duration and frequency of oestrous cycles and response to ovariectomy. Secondly, while all animals were skeletally mature (5-9 years) we did not know their exact age. Again, this was necessary because sourcing aged sheep, of any breed, is quite difficult. This may affect baseline bone mechanical properties, particularly porosity. However, one major advantage of this study was that osteoporosis was induced using OVX alone. Other methods of simulating osteoporosis combine

OVX with dietary or steroid regimens to achieve greater BMD loss. This introduces another variable to the system and could, potentially, have other unknown side-effects. In this study we have an opportunity to examine bone response to reduced hormone levels alone.

Chapter 3

The Effect of OVX on Bone Turnover and Microarchitecture in Compact Bone

3.1	Introduction.....	63
3.2	Materials and methods	68
3.2.1	Bone histomorphometry.....	68
3.2.2	MicroCT analysis.....	69
3.2.3	Biomechanical testing.....	70
3.2.4	Statistical analysis.....	71
3.3	Results.....	72
3.3.1	Histomorphometric measurements	72
3.3.2	Porosity measured by microCT.....	77
3.3.3	Biomechanical testing.....	79
3.4	Discussion	81
3.5	Conclusions.....	86

3.1 Introduction

Bone quality describes specific aspects of the tissue composition and structure that contribute to strength independently of bone mineral density (BMD). As one of the primary contributors to bone strength, bone quality is also of relevance to fracture risk prediction. One of the main parameters of bone quality is bone turnover; it has been shown that it has a direct influence on fracture risk (Riggs and Melton, 2002). Understanding the concept of bone turnover is important in the diagnosis and treatment of osteoporosis. The message can be summarised as follows: If bone turnover is high, then for any given BMD, the fracture risk is greater than if bone turnover is low (Compston, 2004). This chapter describes an experiment which was designed to investigate the effects of bone turnover and microarchitecture on strength in control and OVX bone.

Recently, Meier et al (2005) in a study of 151 elderly men, followed prospectively over 6.3 years, demonstrated that accelerated bone resorption was associated with an increased incidence of osteoporotic fractures, independent of BMD. Bone turnover was assessed by measuring serum carboxyterminal crosslinked telopeptide of type-I collagen (S-ICTP), a biochemical bone resorption marker. Combining measurements of BMD and bone resorption improved the fracture predictions further (Figure 3.1). There are various theories to explain why bone turnover negatively affects bone strength. One of the most popular was proposed by Parfitt (1996). He proposed that, high bone turnover constitutes a mechanical threat to bone strength as horizontal trabeculae are removed which withdraws lateral support from the remaining vertical ones which bear compressive loads. The resistance to buckling decreases as the square of the increase in unsupported length. Each episode of

bone remodelling that occurs on an unsupported vertical trabecula acts as a stress concentrator and represents a focal weakness. Consequently, when turnover increases, the risk of buckling will increase within only a few weeks, as the number of resorption sites increases (Parfitt, 2002).

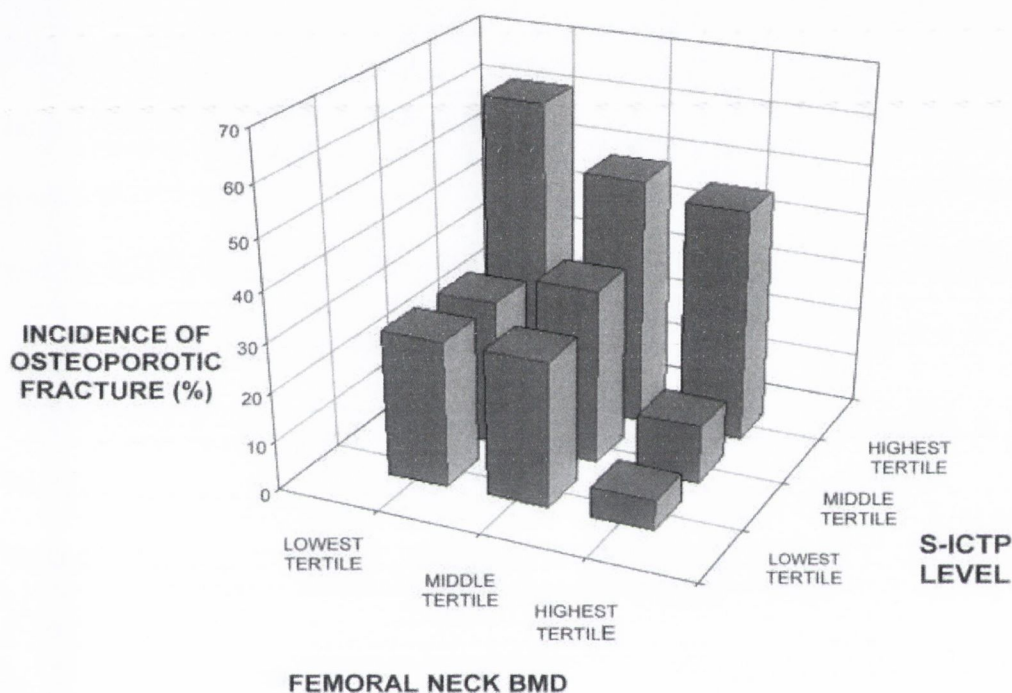


Figure 3.1: Graph of incidence of osteoporotic fracture according to serum carboxyterminal crosslinked telopeptide of type I collagen (S-ICTP) levels and femoral neck BMD. Case-cohort control study of 151 older men from the Dubbo Epidemiological Study (DOES) followed prospectively over 6.3 years (Meier et al, 2005).

The microarchitecture of bone is an important structural property and it also has a major impact on bone quality. Microarchitecture can be understood in terms of the trabecular microstructure, which encompasses the orientation, thickness and spacing of the trabeculae as well as the extent to which they are interconnected. Cortical bone microstructure is complex and hierarchical and encompasses porosity, distribution of porosity and cortical

thickness among other factors. An illustration of the cortical bone hierarchical structure is shown in Figure 3.2.

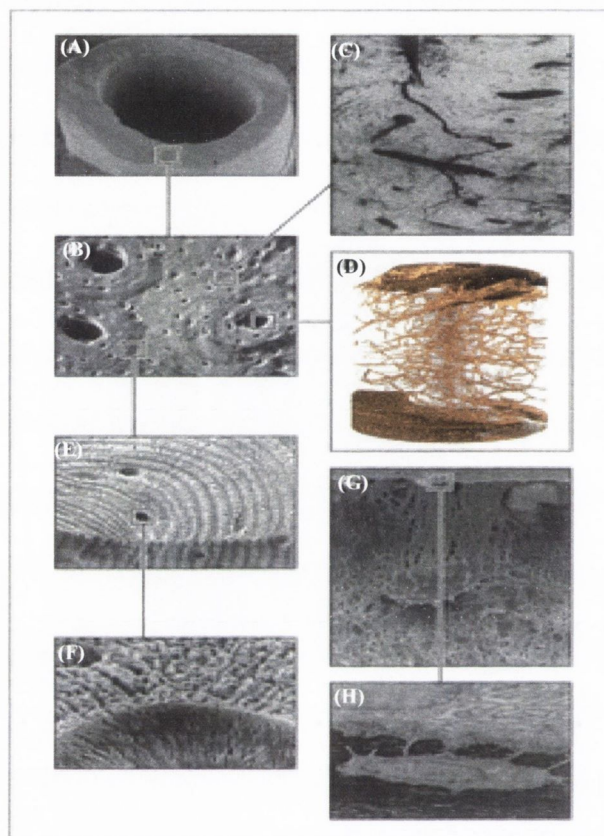


Figure 3.2: Within a cortical bone shaft, shown in cross-section (A) are osteons surrounded by interstitial bone and osteocytic lacunae distributed around the central Haversian canal (B). Panel C shows a microcrack that is largely confined to interstitial bone. Panel D shows the Haversian canal network in cortical bone. In Panel E, alternating high-density and low-density concentric lamellae of an osteon produce a composite structure. Panel F depicts an osteocyte lacuna at a high resolution showing collagen fibres. In Panel G, osteocytes connect with lining cells and with one another through a network of canaliculi. Panel H shows the detail of a bone lining cell connected to an osteocyte (Seeman and Delmas, 2006).

The majority of studies that investigate osteoporotic bone quality tend to focus on trabecular bone tissue. This is because of the prevailing belief that the rate of bone turnover is higher in areas of trabecular bone; thus most of the deterioration in bone quantity and quality, including microarchitecture, will be found in these areas. Neither of these suppositions is necessarily true. Parfitt (2002) noted that ‘it has often been asserted, without

qualification, that cancellous bone has higher turnover than cortical bone.’ He went on to comment that there are circumstances in which this is indeed true, but there are also circumstances in which it is not. Bell et al (2000) investigated the relationship between remodelling and bone loss and osteonal diameter in the femoral neck of patients with hip fracture and compared findings with age- and gender- matched healthy controls. Composite osteonal systems, defined as clusters of remodelling osteons which resulted in particularly large Haversian canals, were found to be nearly twice as prevalent in patients with fractures. This suggests an important relationship between compact bone microarchitecture and fracture risk in osteoporosis.

In this study, we used the OVX sheep model to study the development of osteoporosis, and its effect on bone quality in compact bone. The sheep has been used by many laboratories around the world as an animal model for studying different aspects of osteoporosis (Chavassieux, 1990; Chavassieux et al, 1991; Pastoureau, 1989; Newman, 1995; Turner, 1995; Lill et al, 2002; Schorlemmer, 2003). The ovine animal model is a good choice for the study of postmenopausal osteoporosis for a number of reasons. It has been reported that there are striking similarities between the hormonal profiles of ewes and women (Goodman, 2002). The metabolic rate of sheep, based on O₂ consumption per gram of body weight, is 0.22 which is closer to that of humans (0.21) than to that of other animal models such as rat (0.87) or dog (0.33) (Schmidt and Nelson, 1977). However, the most important similarity between ewes and women with regards to this research is the similarity in their remodelling cycles, which are both between 2 and 3 months (Turner et al, 1995; Lee et al, 2002).

The main objective of this study was to investigate the effects of OVX on bone quality in compact bone using an OVX sheep model. Bone turnover and microarchitecture are the two main parameters of bone quality which were assessed to achieve this objective. Specific aims of the study were:

- (1) To assess bone turnover at five time-points during the 12 month experimental period by measuring the number of fluorochrome labelled osteons.
- (2) To measure the resorption levels and porosity at 12 months post-OVX using histomorphometry and microCT (μ CT), respectively.
- (3) To assess the effects of these parameters on bone strength in compression.

3.2 *Materials and methods*

As described in Chapter 2, animals from both groups were sacrificed 12 months post-OVX.

In this study we used a sample of bone from the mid-shaft of the left metatarsal (Figure 3.3). This area was chosen because it consists entirely of compact bone and *in vivo* it is loaded predominantly in compression.

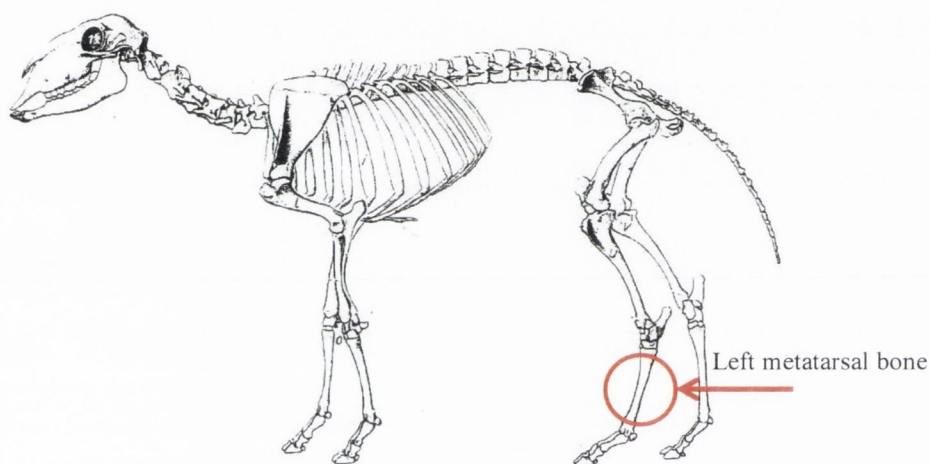


Figure 3.3: Illustration of a full sheep skeleton with the left metatarsal bone highlighted.

3.2.1 *Bone histomorphometry*

A cross-sectional sample, 11mm in thickness was removed from the mid-diaphysis of the left metatarsal of each animal using a slow speed diamond saw (Struers, Accutom 50, Ballerup, Denmark). For analysis of bone histomorphometry, a 1mm histological slice was taken from the proximal end of this sample using the same instrument. This slice was then split to make two histological sections. Each section was ground down to 100 μ m and mounted on a glass slide. Each slide was examined using brightfield microscopy (Olympus IX51, Hamburg, Germany) at X1 magnification. The cortical area and the average cortical

thickness were measured using a digital image analysis system (analySIS; Soft Imaging Systems, Munster, Germany). Each slide was then examined using a combination of ultra-violet (UV) ($\lambda=365\text{nm}$), blue ($\lambda=470\text{nm}$) and green ($\lambda=546\text{nm}$) epifluorescence microscopy at X10 magnification. The number of fluorochrome labelled secondary osteons was measured (N.On/B.Ar) and intracortical bone turnover at each time-point was calculated at 0, 3, 6, 9 and 12 months. Any secondary osteons which contained no fluorochrome labels, i.e. were formed prior to the experimental period, were not included in this measurement. The number of resorption spaces per unit area was then measured. Resorption spaces were identified by their scalloped edges which lacked a cement line or any fluorochrome labels.

3.2.2 *MicroCT analysis*

The remainder of the metatarsal sample (10mm in thickness) was then scanned using a μCT scanner (Scanco, μCT -40, Bassersdorf, Switzerland). Samples were placed in a cylindrical specimen holder and fixed into the scanner. During the scanning process, X-rays are directed towards the sample and, after passing through the sample, they are detected by a 2048 x 256 element CCD array which is controlled by a dedicated workstation. A specific measurement protocol (control file) was created before scanning began so that all parameters, such as source energy, scan time and resolution, were identical for every sample in the study. Source energy was 70 kV, scan time for each sample was less than 30 minutes and the scan resolution was $8\mu\text{m}$ (Laib, 2000; Bagi, 2006). Samples were wrapped in moist gauze for the duration of scanning. When a full 3D reconstruction of the sample had been created, Image Processing Language (IPL, Scanco, Bassersdorf, Switzerland) was used to manipulate the bone image so that, using a 'negative' of the image, the intracortical

porosity could also be reconstructed. This image was then combined with the original so that the distribution of the porosity throughout the cortex could be visualised. Porosity was calculated using a program which counted the number of voxels in the pores within the cortex and divided that number by the bone volume.

3.2.3 Biomechanical testing

After the samples had been scanned using the μ CT, they were wrapped in moist gauze and frozen at -20°C until testing. The proximal and distal cross-sectional areas were measured using an optical microscope and the mean area was calculated. The surface of each specimen was polished and compression tests were performed between steel platens on a servo-hydraulic materials testing machine (Instron, 8501, Bucks, UK). The specimen was placed on the bottom platen, and a ball joint allowed the top platen to rest flat on the specimen as the actuator was lowered onto the test piece. Each sample was cycled five times in the load range 100 - 300N in order to reduce the viscoelastic effects of the bone and to allow proper seating between the platens and the surfaces of the sample. The specimens were then loaded at a rate of 0.01 mm/sec until failure while simultaneously recording all relevant load and displacement data using a data-logging system (Labview, National Instruments, Austin, USA). The maximum load (F_{max}) required to compress the sample was determined from the load displacement curve. The compressive strength was calculated by dividing F_{max} by the average cross-sectional area of the sample.

3.2.4 Statistical analysis

Data are presented as mean \pm standard deviation (SD). For statistical analyses, groups were assessed for normal distribution and then compared using a t-test. For those variables failing the normality test, a nonparametric Mann-Whitney rank sum test was used. SigmaStat 3.0 statistical package (SYSTAT Software Inc, Chicago, IL 60606) and R-project statistical software (Free Software Foundation, Boston, MA 1307) were used for statistical analyses. A p value of <0.05 was considered to be significant.

3.3 Results

3.3.1 Histomorphometric measurements

The mean cortical area (Ct.Ar) of the transverse section of the metatarsal was 122.87 ± 10.80 and $125.50 \pm 9.98 \text{ mm}^2$ in control and OVX groups respectively, the difference was not statistically significant. Mean cortical thickness (Ct.Th) was 2.91 ± 0.30 and $2.99 \pm 0.34 \text{ mm}^2$ in control and OVX, respectively, and again the difference was not significant. However, the number of resorption cavities per unit area was significantly greater in the OVX group compared with controls ($p < 0.01$) (Table 3.1).

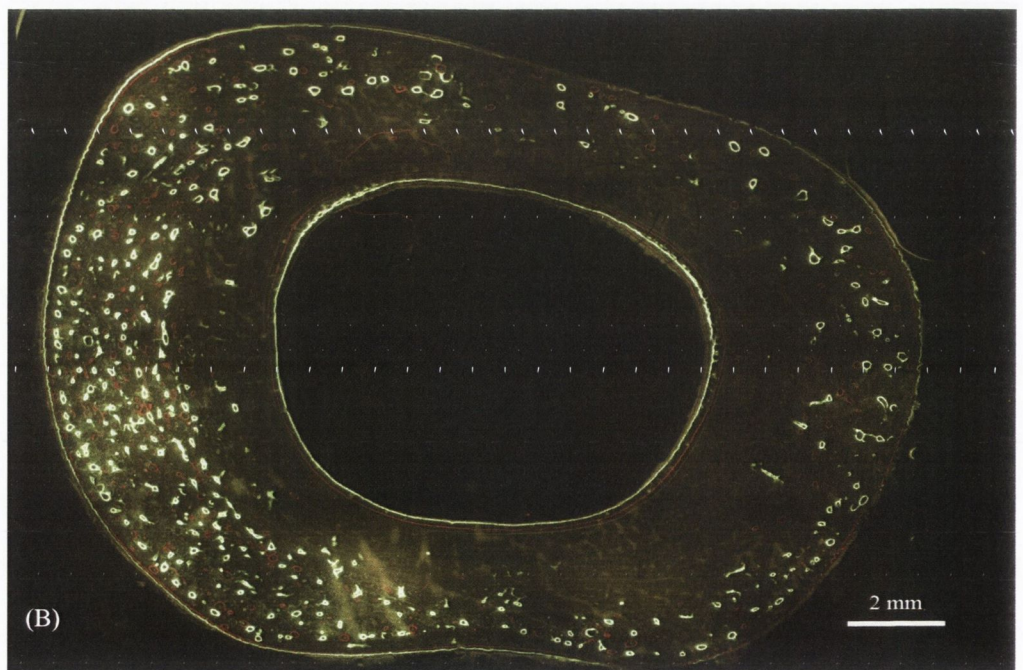
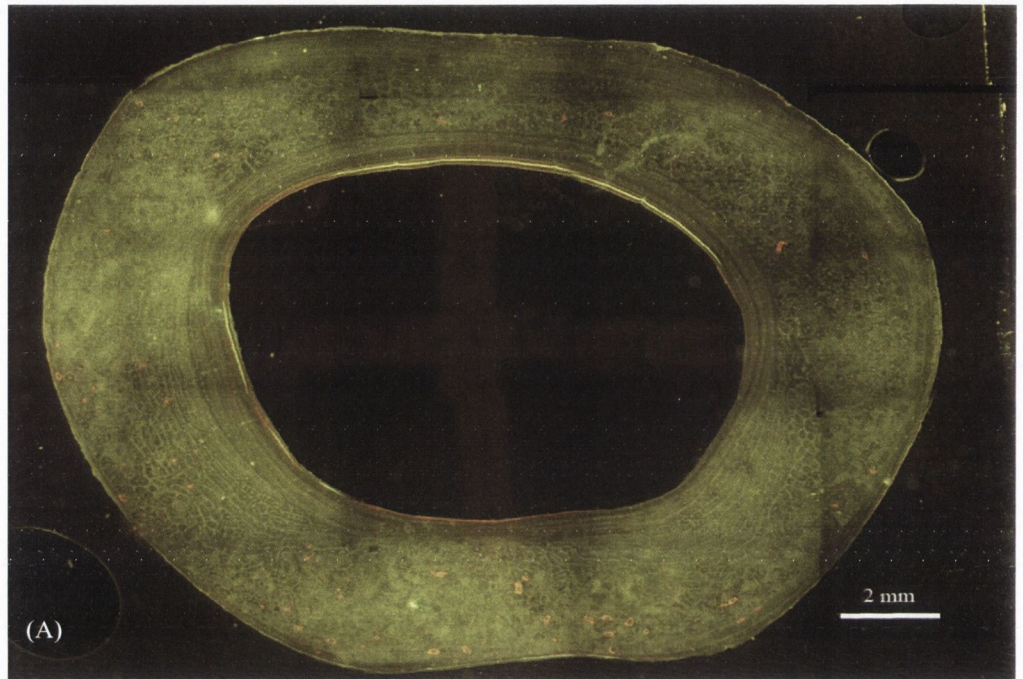
Table 3.1: Bone dimensions and resorption cavity number in control and OVX groups.

	Control (n = 18)	OVX (n = 16)	<i>p</i>
Ct.Ar (mm²)	122.87±10.80	125.50±9.98	NS
Ct.Th (mm²)	2.91±0.303	2.99±0.34	NS
No. Resorption Cavities (#/mm²)	0.016±0.009	0.046±0.026	<0.01

Ct.Ar, cortical area; Ct.Th, cortical thickness; NS, not significant.

Figure 3.4 shows typically labelled bone turnover sites found in control and OVX cortical bone. This image illustrates the small number of labelled osteons throughout the control bone cortex compared with the OVX bone (Figure 3.4 A,B). Higher magnification images (X10) of the control and OVX bone sections are also shown (Figure 3.4 C,D). In the image from the control bone two osteons labelled with xylenol orange can be seen. High numbers of osteons labelled with calcein, which was administered at month 6, are present in the

OVX bone. This image also shows an example of an osteon labelled with alizarin complexone, which was administered at month 3, and various osteons labelled with xylenol orange, administered at month 9.



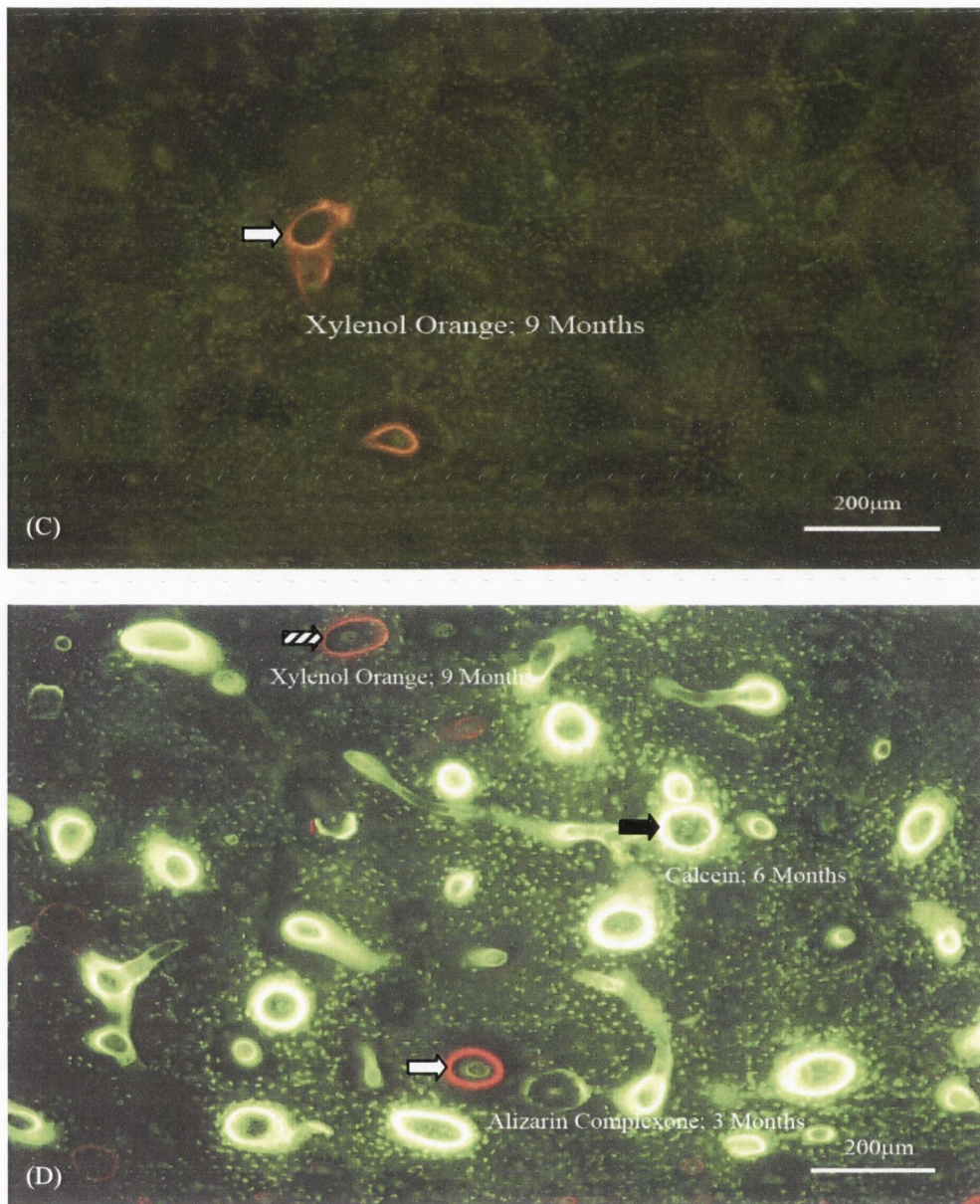


Figure 3.4: Intracortical bone turnover sites labelled with different fluorochrome dyes at X4 magnification from (A) control and (B) OVX bone. The same samples at X10 magnification are shown in (C) control and (D) OVX. Images were taken using blue epifluorescence ($\lambda=470\text{nm}$).

The bone turnover data from control and OVX bone samples are summarised in Table 3.2. The level of intracortical bone turnover is expressed as the number of labelled osteons per cortical bone area (N.On/Ct.Ar) for each time-point. At 0 months post-surgery (the day of ovariectomy), bone turnover was greater in the control group, but this difference was not statistically significant ($p=0.156$) and was a random occurrence due to the sheep selected. At 3 months post-OVX, bone turnover was higher, but not significantly so, in the OVX animals indicating accelerated bone turnover. At 6 months, bone turnover was significantly higher in OVX animals versus controls ($p < 0.05$). Similarly at 9 and 12 months bone turnover was significantly higher in the OVX animals versus controls ($p < 0.01$).

Table 3.2: Labelled osteon densities in control and OVX groups at 0,3,6,9 and 12 months post-OVX.

	Control (n = 18)	OVX (n = 16)	<i>p</i>
N.On/Ct.Ar at 0 months (#/mm²)	0.043±0.017	0.030±0.055	NS
N.On/Ct.Ar at 3 months (#/mm²)	0.016±0.027	0.066±0.112	NS
N.On/Ct.Ar at 6 months (#/mm²)	0.091±0.144	0.316±0.677	<0.05
N.On/Ct.Ar at 9 months (#/mm²)	0.267±0.149	0.930±0.829	<0.01
N.On/Ct.Ar at 12 months (#/mm²)	0.0553±0.035	0.142±0.088	<0.01

N.On/Ct.Ar, number of labelled osteons per unit area; NS, not significant.

Labelled osteon density in the control animals varied during the 12 month period. This demonstrates the seasonal effect on bone turnover in normal sheep (Figure 3.5A). A similar pattern was found in bone turnover of OVX animals but was more pronounced (Figure 3.5B). Our data shows that turnover increased from 0 - 9 months, and then decreased at 12 months although the absolute values in the control group were lower than OVX at all time-points (except at month 0, which was prior to our intervention).

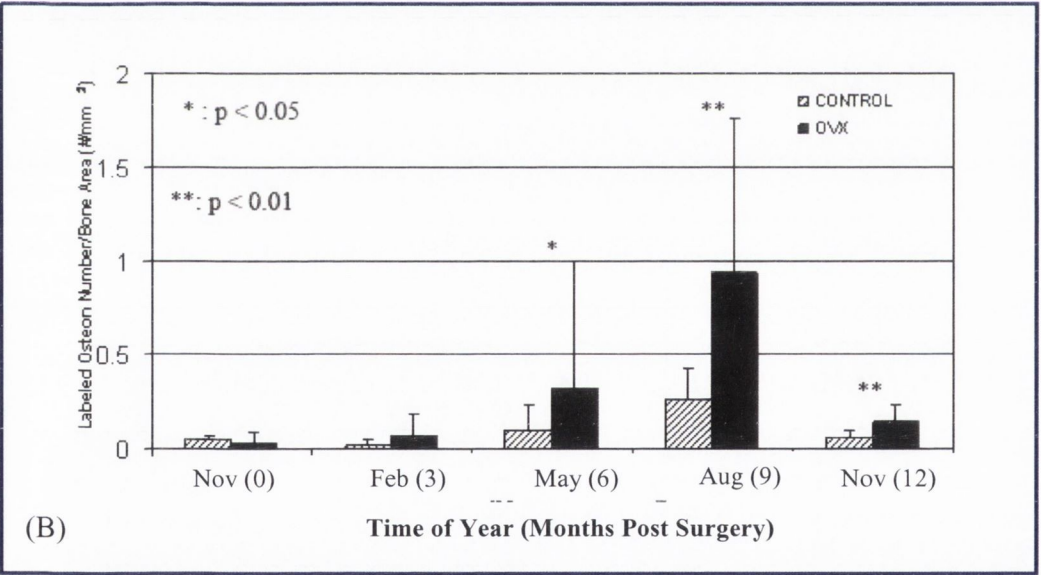
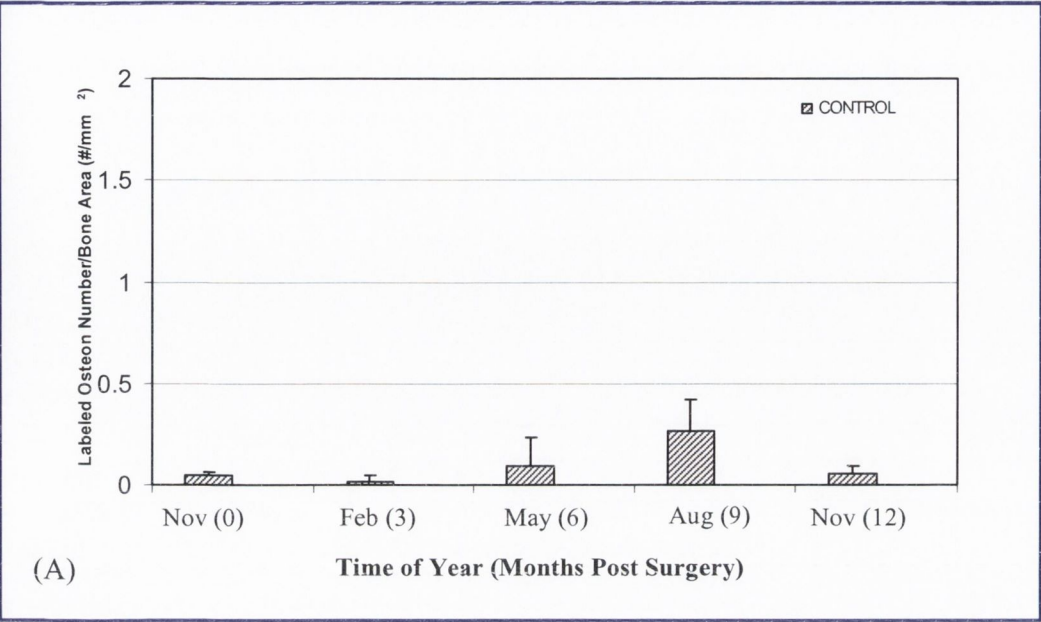
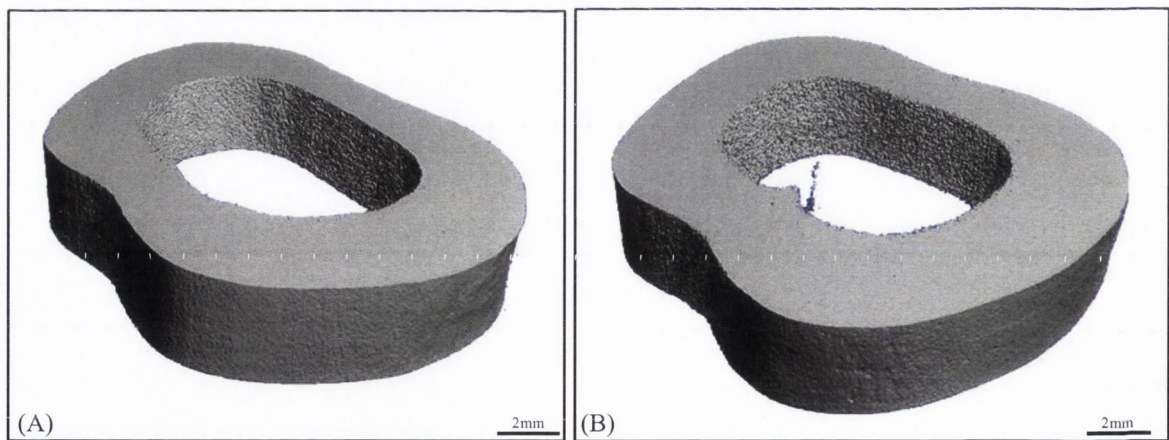


Figure 3.5: The number of intracortical labelled osteons in (A) control and (B) control and OVX bone samples at 0, 3, 6, 9, 12 months post-OVX.

3.3.2 Porosity measured by microCT

μ CT scanning allowed us to create a 3-D image of a portion of the left metatarsal which was directly adjacent to the site from which a histological section was removed. This image was then processed so that the pores within the cortex could be visualised. Because this is a non-destructive technique, this sample could later be used for mechanical testing. Figure 3.6 shows typical μ CT images of the original bone scan, the inverted image which visualises the pores and also the final concatenated image of the pore distribution within the cortex. The resolution used to evaluate porosity ($8\mu\text{m}$) was high enough to give an accurate representation of Haversian canals, which have a typical diameter of $20\text{-}80\mu\text{m}$ and resorption cavities which have a larger diameter ($100\text{-}200\mu\text{m}$). Figure 3.7 shows quantitatively that porosity was greater in the OVX group compared with controls ($p < 0.01$). The measurement of porosity was carried out *in vitro* and thus these data cannot be directly compared to the individual histological time-points.



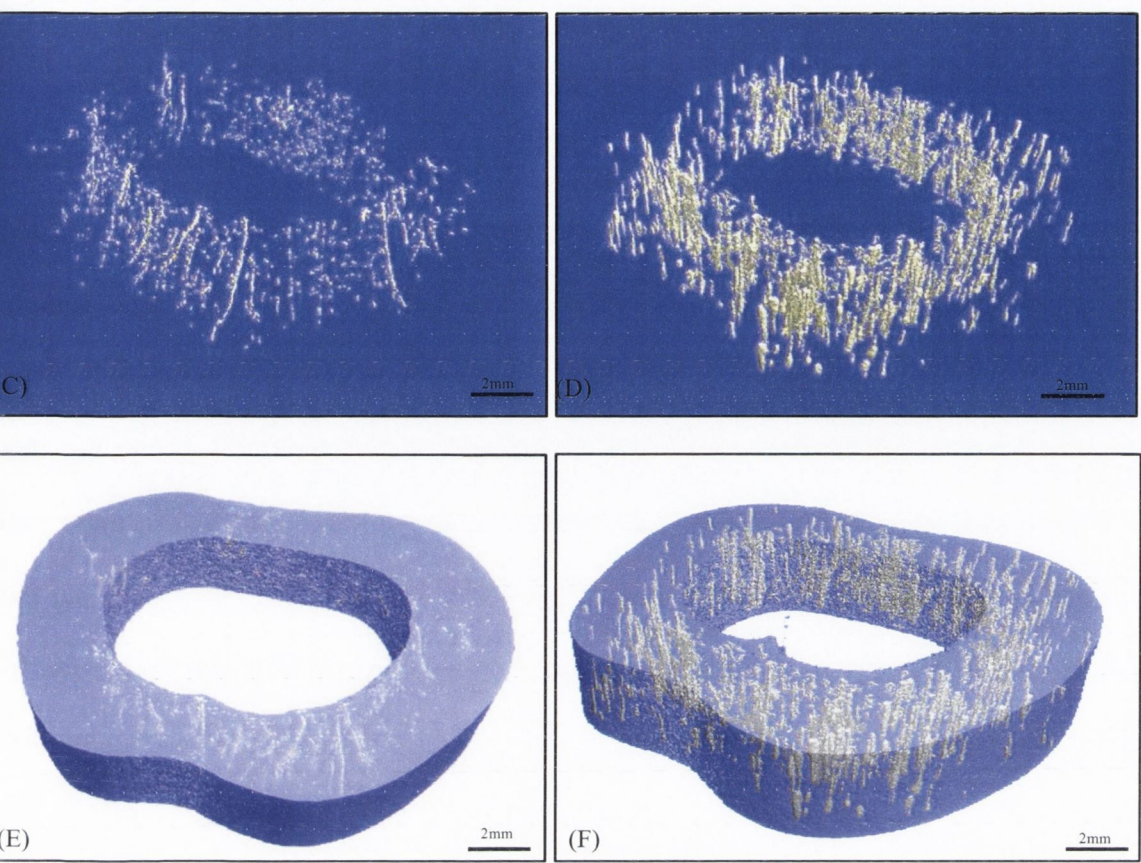


Figure 3.6: μ CT reconstruction of a portion of ovine compact bone from the mid-diaphysis of the left metatarsal. (A) Shows a standard scan of a sample from the control group and (B) is a sample from the OVX group. (C) Shows the pores within the control sample isolated from the main structure. (D) Shows the internal pores of the OVX sample. Images A-D were then processed so that the distribution of the pores throughout the cortex could be visualised in (E) control and (F) OVX bones.

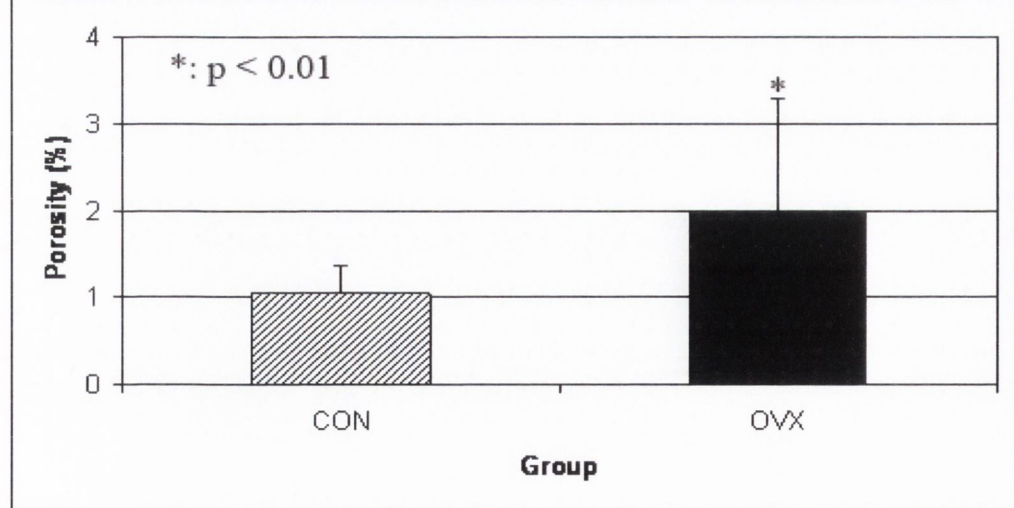
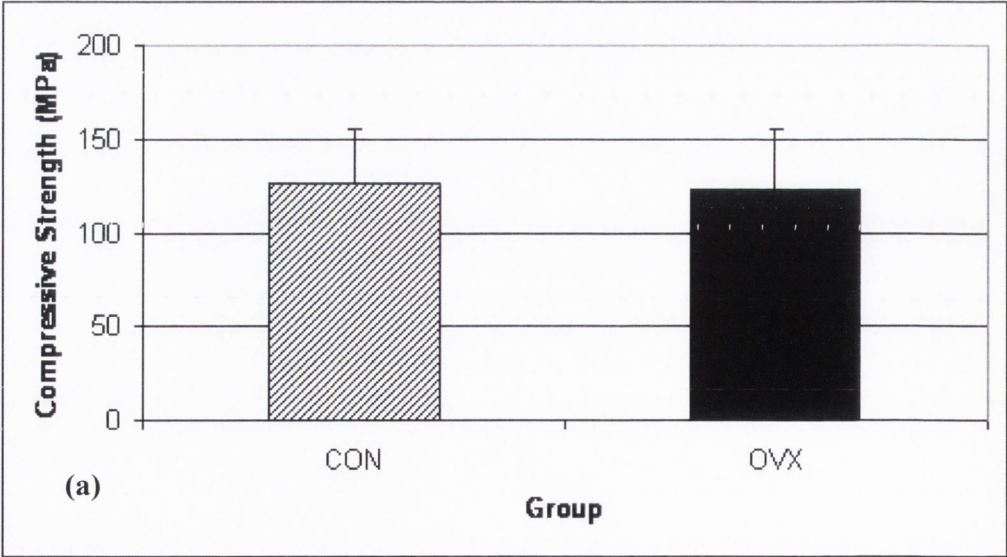


Figure 3.7: The intracortical porosity of control and OVX compact bone samples, calculated using μ CT techniques.

3.3.3 Biomechanical testing

Figure 3.8 shows the ultimate compressive strength, Young’s modulus and work to fracture of bone samples from the control and OVX groups after 12 months. The tests were carried out on the same samples which were analysed using the μ CT scanner. The Young’s modulus was significantly reduced in the OVX group compared with the controls. The ultimate strength and work to fracture were also reduced in the OVX group, but this difference was not significant. However, the comparative differences between these two parameters could be described as marginally significant ($p<0.06-0.09$). We found that the average area of a labelled osteon was 0.25mm^2 . By multiplying this figure by the number of all labelled osteons present and comparing the two groups, the amount of new bone that was formed during the 12 month experimental period was increased from 2.49% in the control group to 10.16% in the OVX group. The presence of a larger amount of recently formed bone, and the increased porosity, in the OVX group may explain some of the reduction in biomechanical properties.



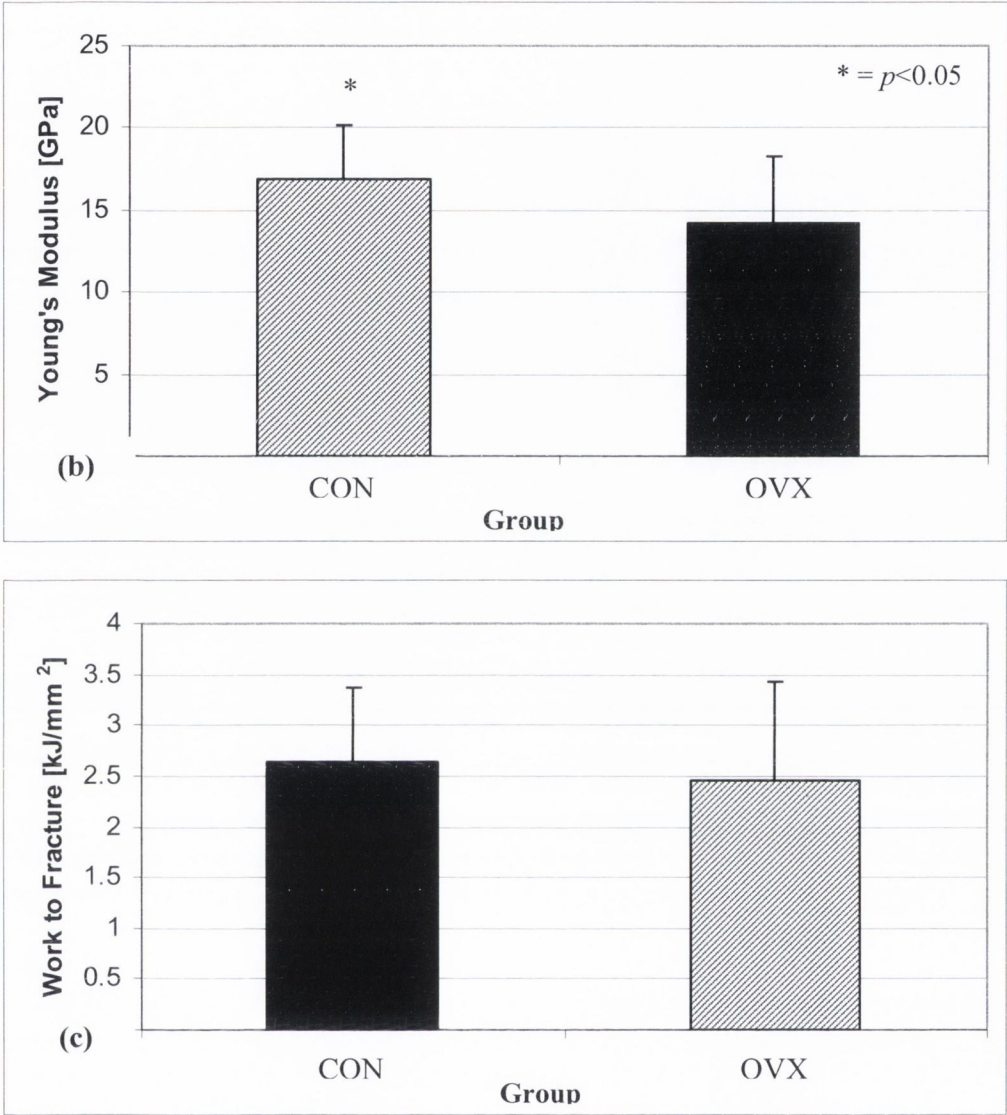


Figure 3.8: (a) The ultimate compressive strength (b) Young's modulus and (c) work to fracture of control and OVX compact bone samples.

3.4 Discussion

Bone quality is a term that describes characteristics which influence bone strength, but are not related to BMD. These characteristics fall into two main categories; material properties and structural properties. The material properties of bone include mineral/collagen content and composition, and the amount of microdamage present. These material properties are directly affected by the rate of bone turnover. The structural properties of bone include its size, shape and microarchitecture - trabecular and cortical (Cheng, 1997; Follet, 2004). The aim of this study was to investigate bone quality in osteoporotic compact bone and to assess how these parameters influence bone strength.

The effect of increased turnover on bone strength remains poorly understood, particularly with respect to compact bone tissue. This is partly because, due to lower surface area, compact bone turnover sometimes occurs relatively slowly when compared with trabecular bone. Clinically, information on bone turnover is obtained by means of biochemical bone markers such as bone specific alkaline phosphatase in the case of bone formation and C-terminal telopeptide in bone resorption. While these markers are undoubtedly useful, they give a systemic measure of skeletal activity rather than a localised measure. A specific local measurement of bone turnover may prove more useful in assessing its effect on bone quality and, ultimately, bone strength and fracture risk.

We used five fluorochrome dyes, each of which fluoresces a different colour under UV incident light, to obtain information on the effect of ovariectomy on compact bone turnover. Multiple fluorochrome labelling techniques have previously been used to assess

various aspects of bone physiology in a number of animal models (Frost, 1969; Lindsay, 1990; Lee et al, 2002). To our knowledge, this is the first study in which five different fluorochrome bone labelling dyes have been used to study the progression of osteoporosis in ovine compact bone. Each fluorochrome was administered intravenously to all animals at three monthly intervals during the year beginning on the day of surgery and finishing four weeks prior to sacrifice. The three month interval coincides approximately with ovine and human remodelling cycles (Turner et al, 1995; Lee et al, 2002).

Our results indicate that, at the time of surgery, the number of labelled osteons was slightly higher, but not significantly so, in the control group. This was a result of natural variation and was not related to our intervention. After three months, there were more labelled osteons in the OVX than the control group; again the difference was not significant, however, after 6 months there was a significant increase in the OVX group ($p < 0.05$). Similarly, at 9 and 12 months the number of labelled osteons in the OVX group was significantly greater relative to the controls ($p < 0.01$). These data suggest that ovariectomy begins to increase bone turnover in ovine compact bone around 3 months post-OVX. The effect continues with time and becomes significant at 6, 9 and 12 months. These findings are in support of work carried out by Turner et al (1995), who used bone biochemical markers to show accelerated remodelling in sheep 3 months post-OVX. The same group carried out work which showed that marginal osteopenia occurred at some sites between 6 and 12 months post-OVX. In our study, the level of bone turnover in both experimental groups increased in months 3, 6 and 9 post-OVX. Both groups then displayed a marked decrease at 12 months (Figure 3.4), this was due to seasonal variation. Sheep have a regular estrous cycle during the autumn and winter months but show anestrus cycles during the

longer days of the summer (Malpaux and Karsch, 1990). This agrees with the increase in labelled osteons found in our study at 6 and 9 months which occurred in May and August respectively. It is also worth noting that the scatter in the data is greater at 6 and 9 months compared to the other time-points. Other workers have also reported similar findings; Jerome et al (1995) observed that the increase in remodelling is less consistent in sheep than in postmenopausal women, monkeys and rats. Other factors which may have had some effect on this outcome are calcium intake, breed and lambing history (Chavassieux et al, 2001).

High bone turnover in the OVX relative to the control group also contributed to increased levels of porosity within the cortices of the OVX bone. This was due to the presence of more resorption cavities and Haversian systems. We quantified this effect using a μ CT technique in which the porosity was accurately measured and also visualised with greater ease than the standard histomorphometric methods. Also, this method is non-destructive and provides actual quantitative data as opposed to representative 3-D data which is extrapolated from 2-D observations. Intracortical porosity was 1.04 ± 0.29 and 2.07 ± 1.28 (%) in control and OVX groups, respectively. Again, there is more variation in the data from the OVX group. Our porosity data compared favourably with work carried out by Chavassieux et al (2001) who used standard histomorphometry to measure cortical porosity of iliac crest bone biopsies taken from sham and OVX sheep. They found that porosity was 0.97 ± 0.32 and 2.77 ± 0.78 (%) 6 months post-OVX in sham and OVX respectively. Burr et al (2001) found similar results in a study which used sham and OVX cynomolgus monkeys to assess the effect of human parathyroid hormone on bone turnover and strength. They

measured intracortical porosity at 18 months post-surgery to be approximately 1.30 and 2.60 (%) in sham and OVX groups, respectively.

The data from the biomechanical testing in this study showed that the Young's modulus was significantly different between the OVX and control groups, but ultimate strength and work to fracture were not. The latter two parameters showed differences that were marginally significant ($p < 0.06-0.09$). This may be due to a statistical power problem, or alternatively due to the fact that the data support the null hypothesis. Our data show the same trend for each of the parameters measured, which was that OVX bone displayed reduced biomechanical properties in comparison to controls. This is consistent with our stated hypothesis, and would suggest that the reason for marginal significance of two measured parameters was due to statistical power rather than data that support the null hypothesis. It is also worth noting that while it is recognized that a power relationship exists between porosity and compressive strength, the increase in porosity in our case was relatively small, in absolute terms. This, combined with the scatter which is inherent in the testing of any biological material, may explain the marginal significance between the two experimental groups.

Based on bone turnover it was estimated that the OVX group contained about 7% more new bone per area than controls. This can be thought of as a 7% reduction in bone area that is able to support mechanical load. Similarly, as a result of the higher number of resorption spaces and Haversian systems in the OVX bone cortex, the overall porosity doubled from approximately 1% in the control bone to 2% in the OVX bone. Again, this would mean that less bone was present which could support load. Based on the linear relationship between

stress, force and area in compression, our estimation would be that compressive strength would be decreased by approximately 8% in the OVX group compared with controls. This corresponds to a difference in strength between the groups of approximately 10 MPa. *In vitro*, the mean ultimate compressive strength was 126.00 ± 23.44 and 123.13 ± 15.27 (MPa) in the control and OVX groups respectively, a difference in strength of 2.87MPa, given the amount of scatter in the experimental data, this compares reasonably well with our estimation.

The most important result from this study was that significant changes in the material and structural properties of OVX bone were observed 12 months post-OVX and that these changes resulted in a slightly reduced macroscale mechanical strength in the OVX group. An explanation why these changes did not have a significant effect on the mechanical strength may be that the increases in intracortical bone turnover and porosity take place at the microscopic level and thus require longer than 12 months to exert a detectable effect at the macroscale level. However, this finding may be useful in clinical settings. If the onset of osteoporosis can be detected by increased bone turnover and intracortical porosity before it affects mechanical strength, then preventative measures could be taken before fracture occurs.

3.5 *Conclusions*

- (1) Ovariectomy significantly increased intracortical bone turnover in OVX sheep at 6, 9 and 12 months post-OVX compared with controls, as measured by labelled osteon density.
- (2) Resorption cavity number was increased in the OVX group at 12 months but no changes in cortical area or cortical thickness were observed. Intracortical porosity was also increased in OVX animals compared with controls at 12 months.
- (3) The changes in these parameters did not translate into a significant reduction of compressive strength at the macroscale after 12 months; however, the slight reduction in strength which was observed in the OVX group was consistent with our estimations which were based on the porosity and turnover changes.

Chapter 4

Fatigue Induced Microdamage in Control and OVX Compact Bone

4.1	Introduction	88
4.2	Materials and methods	94
4.2.1	Sample preparation.....	94
4.2.2	Fatigue testing	95
4.2.3	Histological analysis	96
4.2.4	Statistical analysis	98
4.3	Results	99
4.3.1	Fatigue testing	99
4.3.2	Crack density and crack surface density	100
4.3.3	Crack interaction with osteons	103
4.4	Discussion	108
4.5	Conclusions	116

4.1 Introduction

As discussed in the previous chapters, bone quality is a combination of parameters which contribute to bone strength, independently of BMD. One of the primary contributors to bone quality is the accumulation of microdamage and its subsequent behaviour under load. This chapter describes an experiment which was designed to investigate how increased bone turnover affects the behaviour of fatigue-induced microdamage in compact bone.

The ability of any material to withstand fatigue loading is a function of its resistance to crack initiation and propagation. These two factors are in turn highly dependent on the microstructural characteristics of the material. Osteonal bone is often compared to a fibre composite material where osteons serve as large fibres and collagen fibrils as small ones. It is not known precisely how cracks initiate in bone tissue but natural discontinuities, such as fibres, laminae and voids, may provide stress concentration sites for crack initiation. However, these same features may also serve as barriers to crack growth which slow down and sometimes halt crack propagation completely.

The manner in which composite materials keep cracks small and running in harmless directions gives rise to a characteristic three-phase damage accumulation history as they are cyclically loaded to failure (Figure 4.1). In phase I, a rapid but limited loss of stiffness occurs due to the initiation of microdamage. The type and amount of microdamage is determined by the properties of the composite. Phase I normally ends within approximately 25% of the fatigue life of the material and is characterised by the stabilisation of the rates of stiffness loss and damage accumulation. The reason for this is that crack tips are arrested at

the lamellar interface so their propagation is halted. Damage accumulation in phase II then shifts to interlamellar debonding whereby cracks travel parallel to the lamellar interfaces which are normally aligned with the principal stress directions. Thus, they do not tend to cause catastrophic failure nor do they reduce the elastic modulus appreciably. Despite this, these cracks play an important role in the fatigue life of the material. The surface area of these cracks is very large which serves as an energy-sink and prevents the growth of a single, large and more dangerous crack.

Failure occurs in phase III of the composite material's fatigue life. It is preceded by a rapid series of events where stiffness reduction, lamellar debonding and matrix degeneration all occur. This results in the remaining undamaged regions of material being subjected to increased stresses, and they begin to fracture. Unlike the damage in phase I which is self-limiting, the damage in phase III is self-progressing because as the load-aligned fibres break they increase the stress in the remaining elements. This phase normally constitutes the final 10% of the total fatigue life of the material and ends in the ultimate failure of the structure.

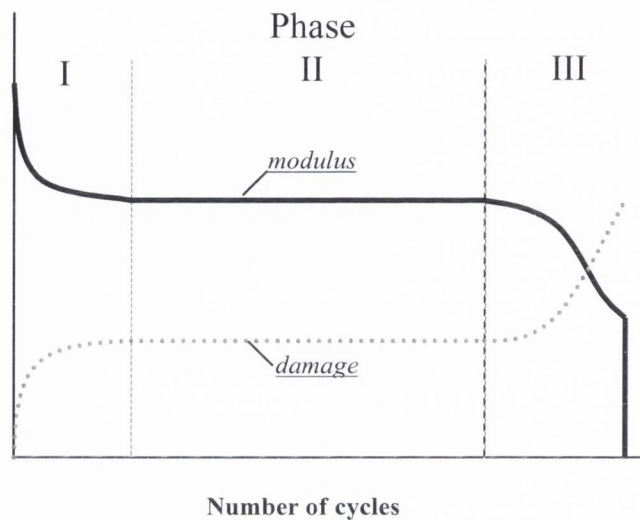


Figure 4.1: Typical three-phase damage accumulation history as a result of fatigue loading in a composite material. In phase I the modulus declines as damage begins under initial loading. In phase II the rate of change of damage and modulus are small and constant. In phase III damage builds up quickly until failure and modulus reduces accordingly (Adapted from Martin and Burr, 1998).

It is known that everyday loading of human bone *in vivo* creates small microcracks in the matrix which are typically 100µm long in the transverse direction (Frost, 1960; Burr and Stafford, 1990; Lee et al, 1998; Donahue et al, 2000). Microdamage is the focus of many researchers in the field of skeletal biomechanics for two main reasons. Firstly, it has been shown that cracks are detected and repaired by the body through the process of remodelling (Frost, 1969; Martin et al, 1998; Lee et al, 2002); this was discussed in detail in Chapter 1. If repair is not possible, or cannot be completed quickly enough, cracks can grow to macroscopic lengths, causing stress and fragility fractures (Burr, 1997; Sanderlin and Raspa, 2003).

The second reason is related to the first insofar as it addresses the underlying mechanism behind the relationship between cracks and remodelling. While we know that cracks are detected and then removed by the remodelling process, the precise series of events between when a crack occurs and when it is removed via remodelling remain unknown. It has been shown that a good correlation exists between the fatigue life of cortical bone and the rate at which it is replaced by remodelling. Martin et al (1998) estimated that if the fatigue life of a given human femur is around 30 million cycles, based on extrapolation from various *in vitro* experiments (Schaffler et al, 1995; Pattin et al, 1996), and a person's daily activity is roughly equivalent to 1.5 million load cycles/year, then approximately 20 years would be required to accumulate 30 million cycles. The turnover rate for the cortex of a bone like the femur is about 3% per year in adults (Parfitt, 1983), but this rate would be higher in the elderly. So, if we assume an average value for turnover of 5%, then in approximately 20 years all the bone in a given region would be replaced. Thus, a rough relationship between the two exists.

There have been many suggestions regarding the relationship between microcracks and remodelling. One of the early suggestions was that the action of stopping a crack propagating at osteonal cement-lines initiates a remodelling cycle. This could happen because debonding of the osteon during crack trapping produces a local disuse state, which activates a new BMU (Martin and Burr, 1982). However, an experiment by Bentolila et al (1998) demonstrated that remodelling can be activated in association with fatigue damage in a bone that ordinarily lacks osteons, and therefore has no cement-lines. This suggested that cement-line debonding is not necessarily associated with the activation of remodelling. However, the same experiment supported the other commonly held theory for the

relationship between microcracks and remodelling which was first described by Frost (1973). He postulated that damage acts directly on osteocytes by triggering a response through disruption of the canalicular network. There is evidence that stress can provoke responses in osteocytes (Weinbaum et al, 1994; Cowin, 1995; Owan et al, 1997). More recently, there is evidence to suggest that microcrack growth may lead to osteocyte apoptosis and that this is one of the targeting mechanisms for remodelling (Noble et al, 1997; Verborgt et al, 2000; Hazenberg et al, 2007).

There are various studies in the literature which investigate the process of damage accumulation during a bone's life. The earliest studies analysed fatigue induced microdamage by stopping the tests prior to failure to allow histological analysis of damage which occurred before fracture (Forwood and Parker, 1989; Burr, 1995; Boyce et al, 1995). Akkus and Rimnac (2001) developed on these findings to look at the process of initiation and propagation of individual microcracks. They found that microcracks initiated, propagated and generally arrested within 10,000 cycles at a stress range of 80MPa. Their results are in keeping with the theory for the 'phase I' behaviour of cracks in a composite material as discussed earlier in this section. O'Brien et al (2005) applied fluorescent chelating agents at specific intervals during the fatigue testing of bone specimens to sequentially label fatigue induced microdamage. They found that microcracks shorter than 100µm tended to stop at cement-lines and those greater than 100µm tended to be deflected around the osteon. Only those greater than 300µm were able to penetrate through the cement-line into the osteon. These data supported the hypothesis that secondary osteons act as barriers to crack propagation in compact bone (O'Brien et al, 2005; Mohsin et al, 2006).

There is still much that remains unknown about microdamage in compact bone such as how its behaviour changes in areas of high bone turnover and whether or not the age of the osteons encountered by cracks during propagation affect their behaviour. Both of these are features of osteoporosis. Also, microcrack behaviour in bone which has undergone long term treatment with anti-resorptive drugs, such as bisphosphonates, remains an area of much interest but one in which little work has been carried out. The specific aim of this study was to investigate the effects of osteoporosis on bone quality by:

- 1) Measuring the fatigue life of control and OVX compact bone samples
- 2) Quantifying the resultant microdamage in terms of location and interaction with the surrounding microstructure.

4.2 *Materials and methods*

4.2.1 *Sample preparation*

Samples of cortical bone were removed from the diaphysis of 18 control and 16 OVX right ovine metatarsals using a band-saw (Figure 4.2). Rectangular beams were removed from the anterior quadrant of each sample using a diamond saw (Accutom-50, Struers, Ballerup, Denmark). Initially, beams were approximately 40mm in length and had irregular cross sections. The final dimensions (2x2x36mm) were obtained using a slow speed grinding wheel (DP10, Struers, Ballerup, Denmark) and a custom-made gripping device. All machining was carried out under wet conditions and the specimens were not allowed to dry out. Visual inspection of the final specimens showed no obvious machining defects and a good surface finish. The thickness and height were measured at three points across the mid-span of each specimen (Figure 4.2) using a micrometer and the average value was calculated. All specimens were stored at -20°C prior to testing.

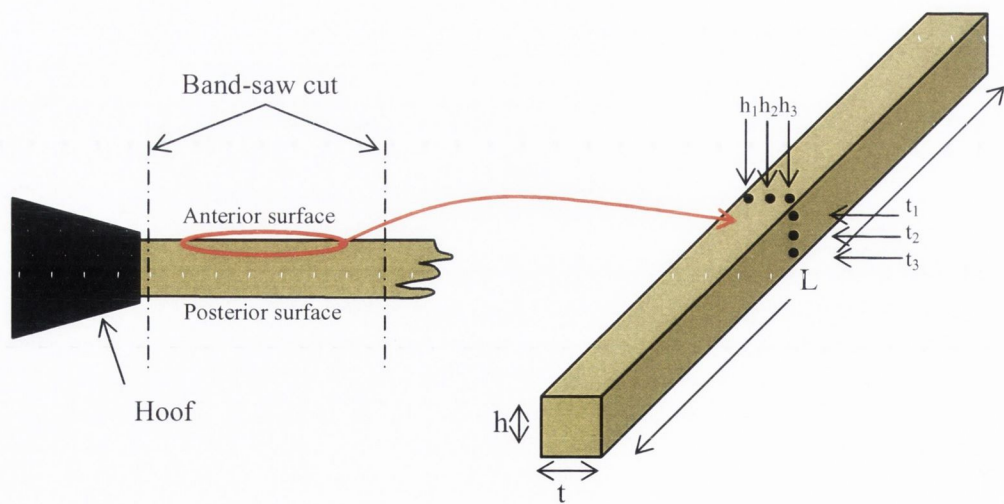


Figure 4.2: Schematic drawing of the location and dimensions of the beam specimens of cortical bone from the right metatarsal.

4.2.2 *Fatigue testing*

A horizontally configured, low-force materials testing machine (MTS 250, Tytron, USA) was used in conjunction with a custom-made rig (Figure 4.3) which loaded specimens in 3-point bending fatigue until failure occurred. The testing rig had a span of 30mm giving a span/depth ratio for our specimens of 15, which complies with American Society for Testing and Materials (ASTM) standards for this mode of testing. Load was applied to specimens such that compression would be induced towards the endosteal surface and tension towards the periosteal surface. All tests were carried out at a frequency of 3 Hz, with a stress range of 110 MPa and a stress ratio of 0.1, which is defined as the ratio of minimum to maximum stress. Specimens were continually hydrated with saline solution during the tests, which were carried out until outright failure occurred. Dedicated MTS Tytron computer software was used to log the relevant data from all tests. Bending modulus was calculated as the average slope of the stress-strain curve from the first 10 cycles.

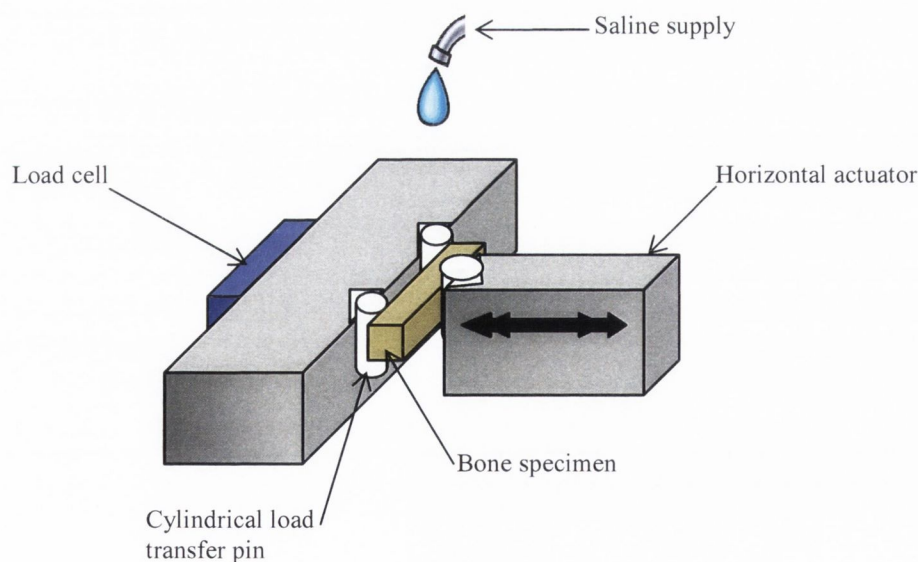


Figure 4.3: Schematic of apparatus used to fatigue-load cortical bone specimens in 3-point bending.

4.2.3 Histological analysis

Following failure, specimens were stained *en bloc* with basic fuchsin to label microdamage which had accumulated during the fatigue test. An established protocol was used to do this (Lee et al, 2002) (Table 4.1).

Table 4.1: Protocol for *en bloc* staining of compact bone with basic fuchsin.

Prepare 1% solutions of basic fuchsin in 70%, 80%, 90% and 100% ethanol. Fix each specimen overnight in 70% ethanol and then bulk stain in 4mls of the following solutions in a vacuum desiccator at -20psi vacuum:
1. 1% basic fuchsin in 70% ethanol for 2 hours Change solution
2. 1% basic fuchsin in 80% ethanol for 2 hours Change solution
3. 1% basic fuchsin in 90% ethanol for 2 hours Change solution
4. 1% basic fuchsin in 100% ethanol for 2 hours Change solution
5. 1% basic fuchsin in 100% ethanol for 2 hours
Rinse in 100% ethanol for 1 hour. Re-hydrate in distilled water for 24 hours.

The protocol in Table 4.2 was used to obtain sections of suitable thickness and quality for histological examination (Adapted from Frost, 1958).

Table 4.2: Protocol for the preparation of ground sections of bone for histological analysis.

-
- | | |
|----|--|
| 1. | Clamp each specimen in the diamond saw and make an initial cut adjacent to the failure surface. Cut a section of approximately 200µm thickness. |
| 2. | Place a sheet of No. 400 silicon carbide paper on a flat surface under running water and place the section in the centre. Wrap another piece of paper around a glass slide and grind the section down manually between the two pieces of paper in a circular fashion using light pressure. |
| 3. | Continue grinding until the required thickness (100 -120µm) is obtained. |
| 4. | Agitate specimens in 0.01% detergent in a beaker and place in a Coors porcelain funnel with fixed perforated plate and wash in distilled water. |
| 5. | Leave specimens to air dry and then mount using standard mounting medium and a coverslip. |
-

Sections were examined at X4 magnification to measure bone area (Olympus IX51, Hamburg, Germany) and then were examined using epifluorescence microscopy at X10 magnification to identify microdamage. Linear microcracks were identified using standard criteria which are described in Table 4.3.

Table 4.3 : Criteria for identifying microcracks in bone (Lee et al, 1998).

-
- | | |
|----|---|
| 1. | Intermediate in size, larger than canaliculi but smaller than vascular canals. |
| | <i>Method:</i> Fluorescence, green incident light (546nm), X125 magnification. |
| 2. | Sharp borders with a halo of basic fuchsin staining around them. |
| | <i>Method:</i> Fluorescence, green incident light (546nm), X125 magnification. |
| 3. | Stained through the depth of section. |
| | <i>Method:</i> Fluorescence, UV incident light (365nm), X125 magnification. |
| 4. | When the depth of focus is changed, the edge of the crack is observed to be more deeply stained than the intervening space. |
| | <i>Method:</i> Transmitted light microscopy, X 250 magnification. |
-

The measurement area was divided at the midpoint into two regions; compressive and tensile. Microdamage was classified in terms of region, location (interstitial Vs osteonal) and interaction between microdamage and microstructural features, specifically fluorochrome labelled osteons. Crack density (Cr.Dn) was calculated by dividing the number of cracks by the measured area. Similarly, crack surface density (Cr.S.Dn) was calculated by dividing the total length of all cracks by the measured area.

4.2.4 Statistical analysis

Variables were expressed as mean ± standard deviation (SD). For statistical analyses, groups were assessed for normal distribution and then compared using a t-test. For those variables failing the normality test, a nonparametric Mann-Whitney rank sum test was used. SigmaStat 3.0 statistical package (SYSTAT Software Inc, Chicago, IL 60606) was used for all statistical analyses. A *p* value of <0.05 was considered to be significant.

4.3 Results

4.3.1 Fatigue testing

The average number of cycles to failure was $169,557 \pm 121,613$ and $158,172 \pm 119,256$ in control and OVX groups, respectively. These data are represented graphically in Figure 4.4. These results represent a 7% reduction in fatigue life of the OVX group compared to the controls. This difference was not significant due to the relatively large amount of scatter present. This graph also shows best fit curves which were drawn according to the Weibull equation: $\text{Probability}(x) = 1 - \exp(-(x/\lambda)^k)$, where λ and k are constants >0 .

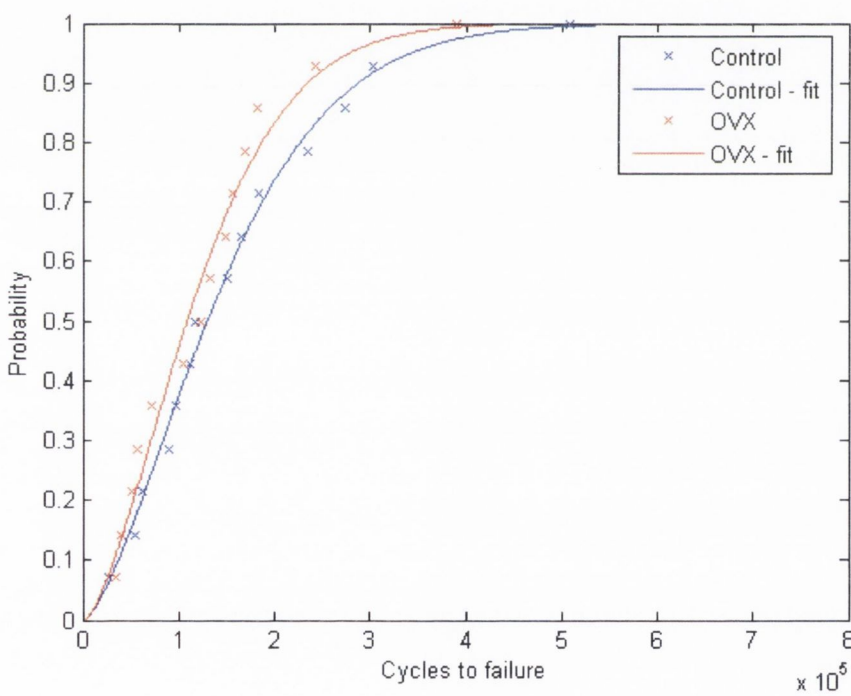


Figure 4.4: Probability of failure as a function of the number of cycles to failure from fatigue tests of control and OVX bone samples at a stress range of 110MPa. The lines on this graph are Weibull best-fit lines.

The bending modulus was also reduced in the OVX group compared with controls, 17.65 ± 2.11 and 20.37 ± 7.93 (GPa), respectively.

4.3.2 Crack density and crack surface density

Following fatigue testing Cr.Dn was increased in the OVX group compared to controls; this difference was not significant however, owing to the high level of scatter in the fatigue data (Figure 4.5).

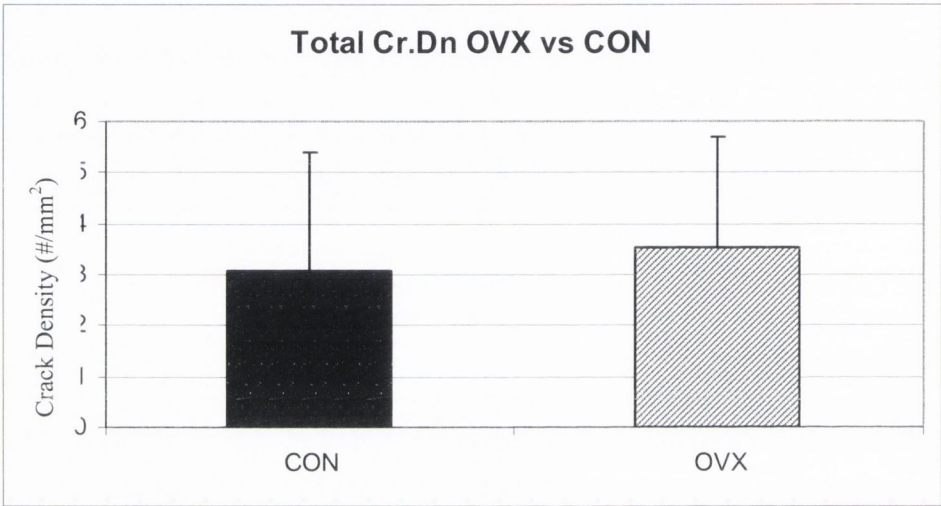


Figure 4.5: Graph of total Cr.Dn in control and OVX bone samples.

When region (compressive Vs tensile) was considered, Cr.Dn was significantly higher (3.5 and 2.5 times greater) in compressive compared to tensile areas in OVX and controls ($p < 0.05$). These data are illustrated in Figure 4.6.

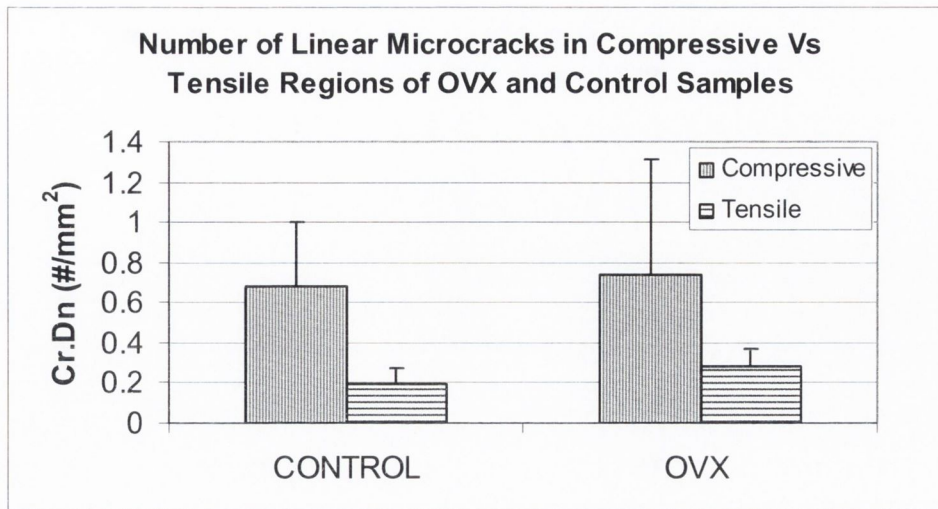


Figure 4.6: Graph of Cr.Dn in compressive and tensile regions of OVX and control bone samples.

A statistically significant difference was found between Cr.S.Dn in the control group compared with the OVX ($p < 0.05$). These data are illustrated in Figure 4.7. Considering that the control group displayed a higher Cr.S.Dn than the OVX group then it follows that they must contain a large proportion of relatively long cracks. In order to quantify this, cracks which were 300 μ m or longer were measured in the control and OVX groups. The controls contained a significantly higher number of long cracks ($>300\mu$ m) compared to the OVX group. These data are illustrated in Figure 4.8.

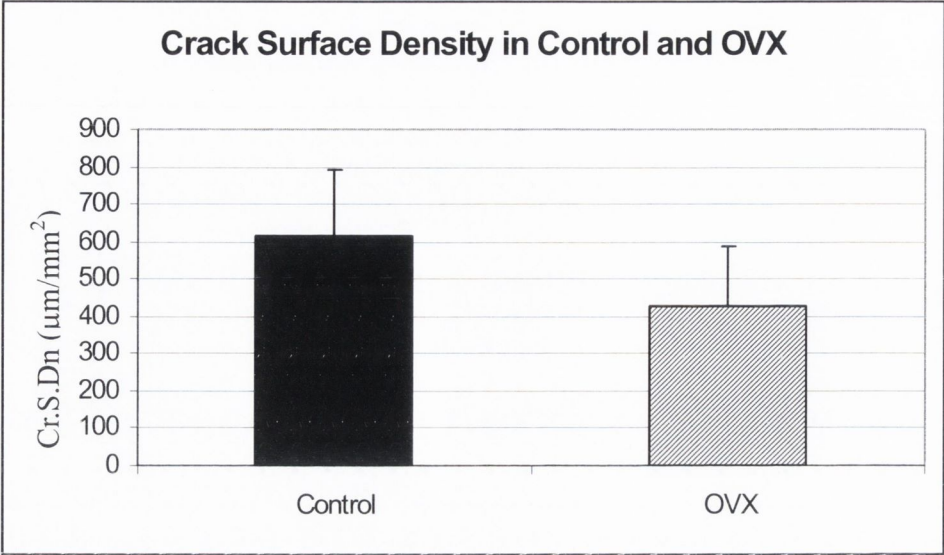


Figure 4.7: Graph of crack surface density in control and OVX bone samples.

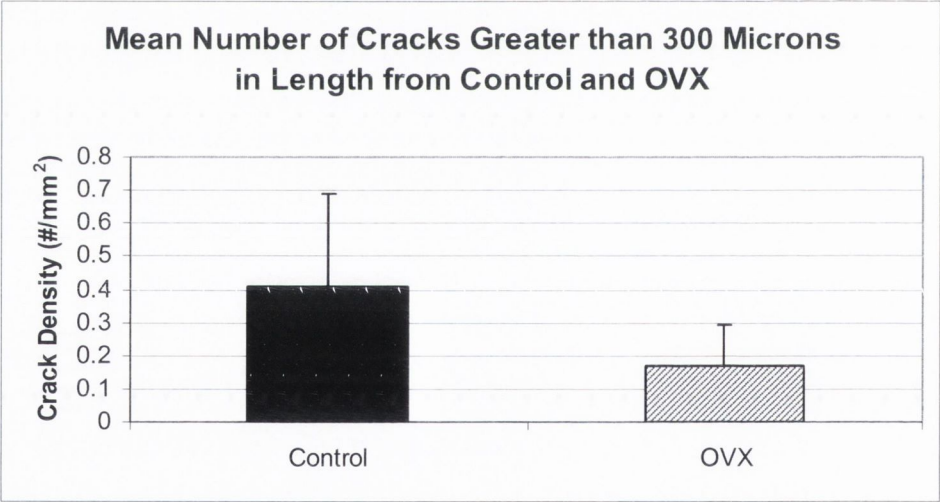


Figure 4.8: Graph of long crack ($>300\mu\text{m}$) density in control and OVX groups.

4.3.3 Crack interaction with osteons

Pooled results from both groups (control and OVX) showed that 91% of microcracks remained in interstitial bone, 8% penetrated through the cement-line of old (unlabelled) osteons and only about 1% penetrated into new (labelled) osteons. An example of each of the crack classifications is shown in Figure 4.9. The data from these analyses are illustrated in Figure 4.10. Interestingly, all cases of new osteon penetration were in control samples.

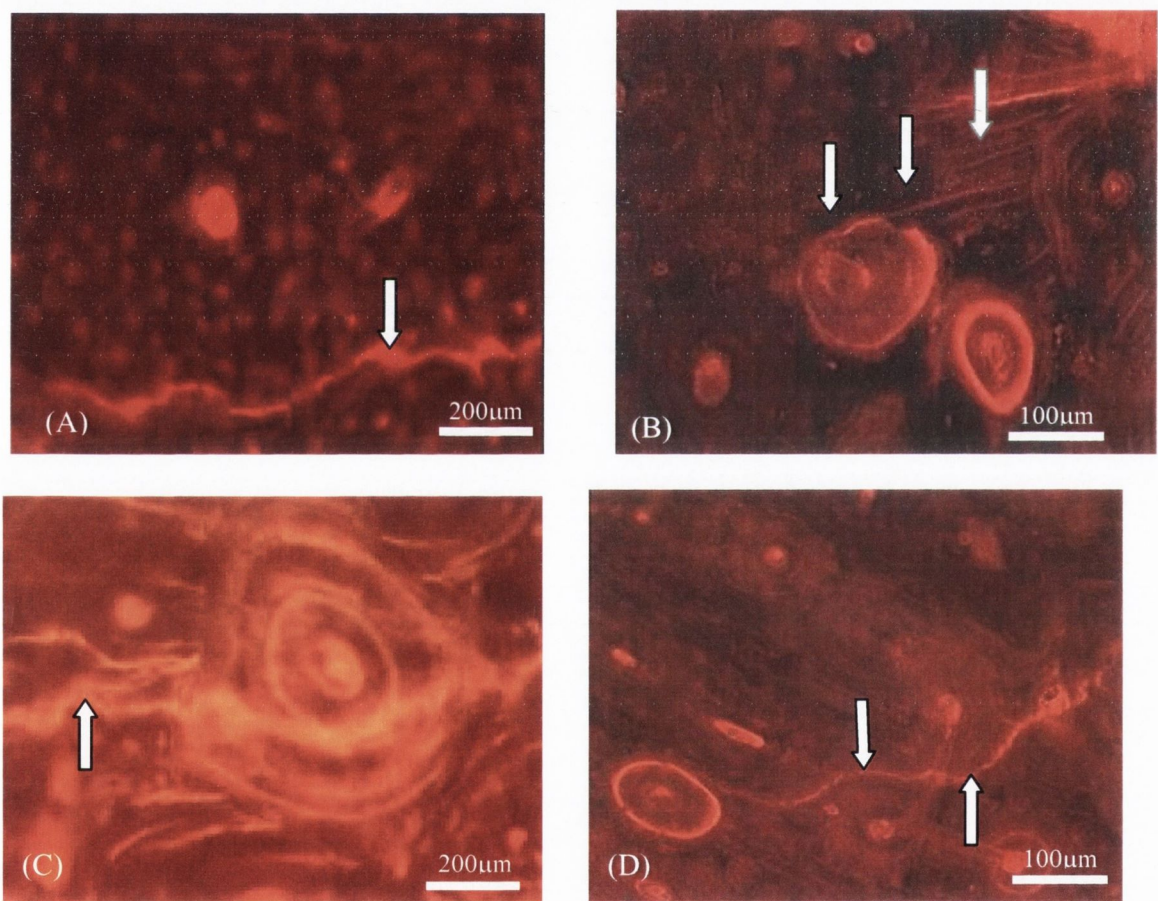


Figure 4.9: Microcracks viewed using green epifluorescence: (A) in interstitial bone and (B) in interstitial bone with the crack tip on the right penetrating into an unlabelled osteon while the one on the left is arrested at a labelled osteon. (C) A long crack penetrating into a labelled osteon from the left and exiting on the right and (D) a long crack being deflected around two unlabelled osteons and halting at a labelled osteon.

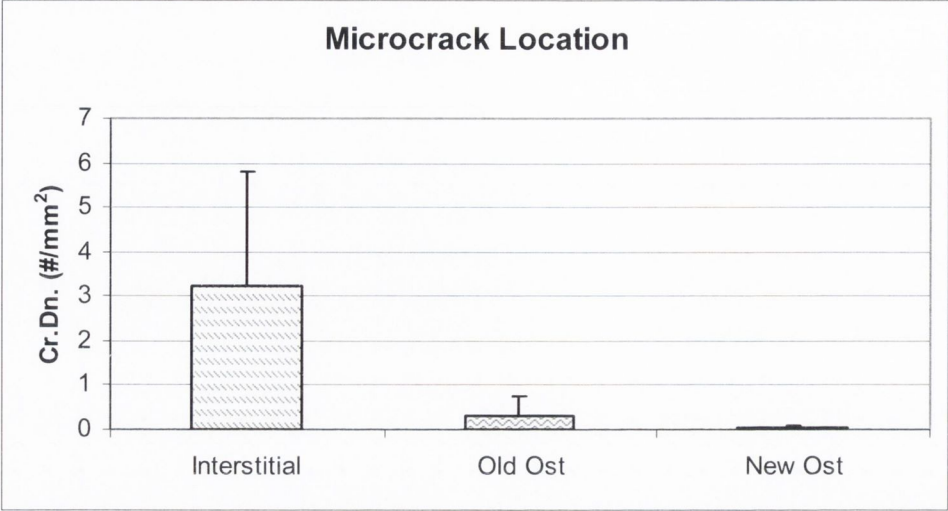


Figure 4.10: Pooled data from OVX and control groups of microcrack location. Cracks were classified as interstitial, penetrating old (unlabelled) osteons or penetrating new (labelled) osteons.

Long cracks ($>300\mu\text{m}$) were observed to deflect around old osteons more often than new ones and to become arrested at the boundary of new osteons more often than old ones. Examples of this effect are shown in Figure 4.11 where long cracks deflecting around an old osteon can be seen in the image on the left and cracks being stopped at the boundary of a new one can be seen on the right.

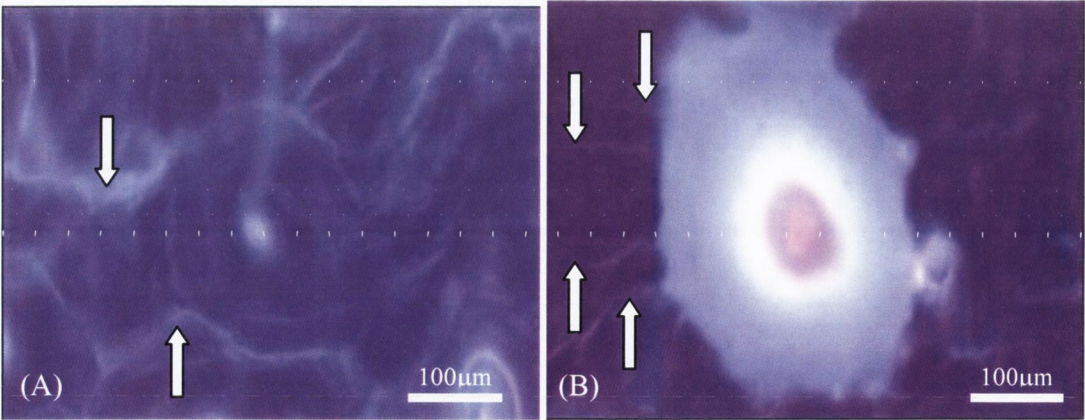


Figure 4.11: Microcracks viewed using UV epifluorescence: (A) in an area of old osteons where cracks are seen to deflect around osteons and (B) in an area of new (labelled) osteons where cracks tend to be attracted towards, and then stopped at, the boundary of the osteon.

A schematic diagram illustrating this idea further is shown in Figure 4.12 where cracks are represented by red arrows and new osteons are shown with green labelled boundaries.

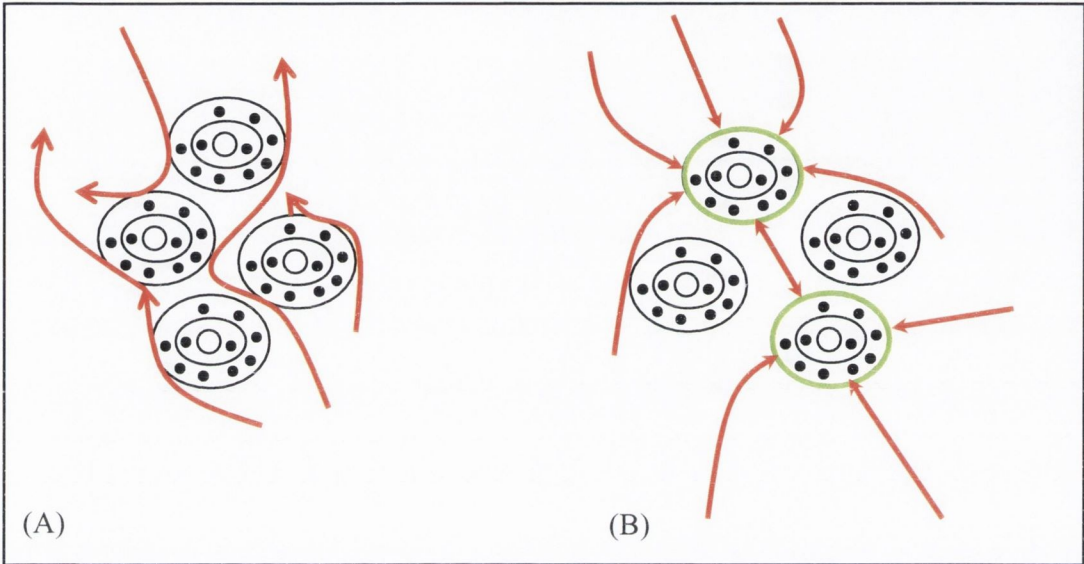


Figure 4.12: Schematic diagram of the behaviour of microcracks (shown here as red arrows) in relation to (A) old (unlabelled) osteons and (B) new (labelled) osteons.

In order to quantify the effect of osteon age on microcrack behaviour the number of crack deflections around old and new osteons was measured. The number of cracks that stopped at new osteons and the number that stopped at old osteons was also measured. Examples of cracks deflecting around old osteons are shown in Figure 4.13 A, C, and E. Examples of cracks stopping at the boundary of new (labelled) osteons are also shown in Figure 4.13 B, D, and F. The number of crack deflections around old osteons was significantly greater compared to new osteons ($p<0.05$) (Figure 4.14). The number of long cracks which were stopped at new osteon boundaries was significantly higher compared with old osteons ($p<0.05$) (Figure 4.15).

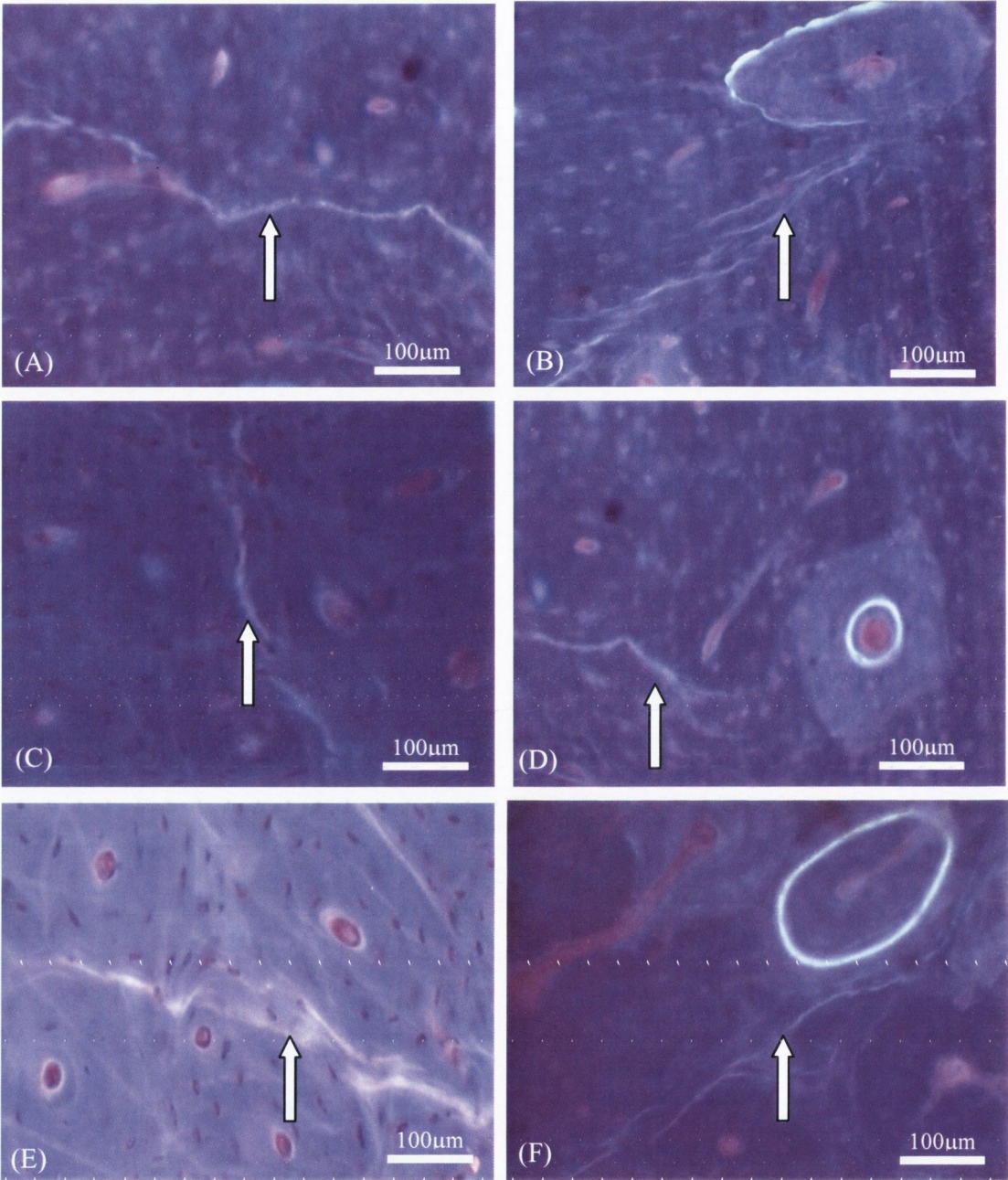


Figure 4.13: Long microcracks viewed using UV epifluorescence: A, C and E show cracks which deflect around old (unlabelled) osteons and B, D, and F show cracks stopping at the border of new (labelled) osteons.

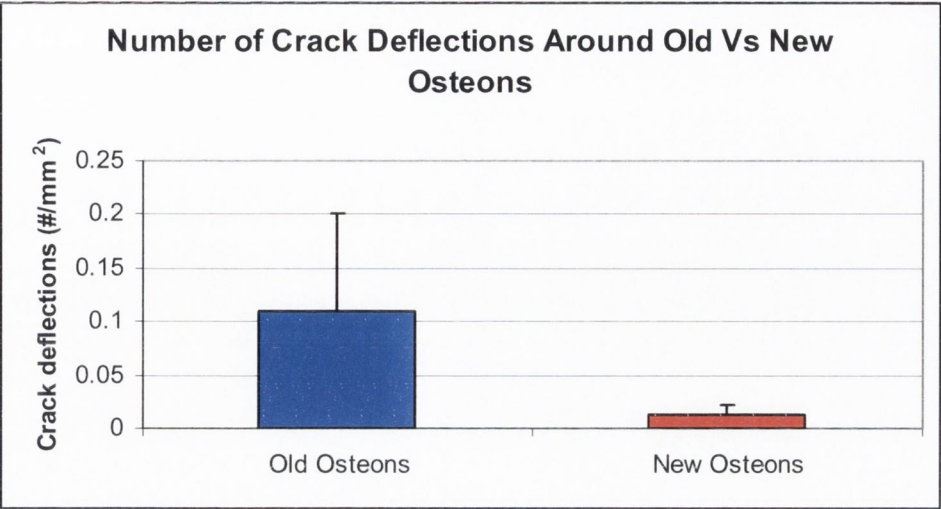


Figure 4.14: Graph of the number of crack deflections around old osteons compared with new osteons.

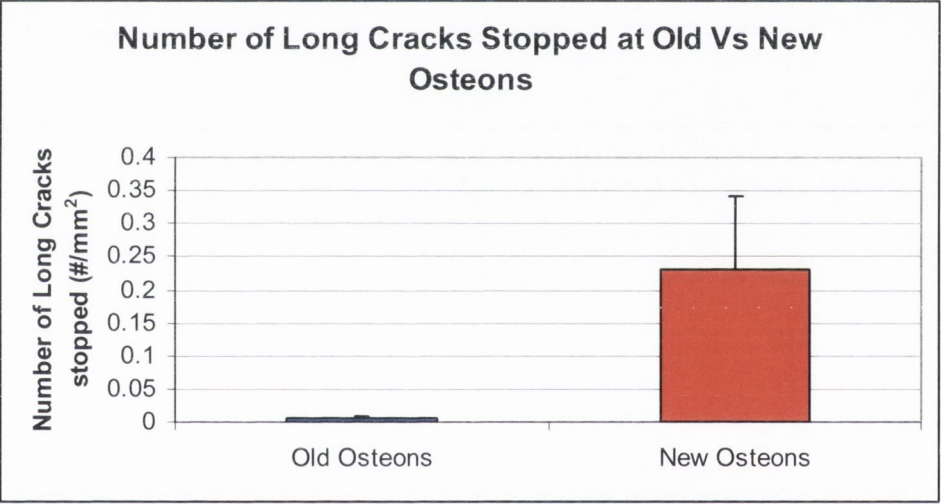


Figure 4.15: Graph of the number of long cracks that stopped old osteons compared with new osteons.

4.4 Discussion

Understanding the etiology and pathophysiology of osteoporosis is becoming increasingly important as the world's elderly population continues to grow. Although bone strength and fracture risk are clinically assessed by measuring BMD, the mechanical properties of bone are determined not only by bone mass but also by bone quality (Burr, 2004). One important parameter of bone quality is microcrack accumulation. The objective of this study was to investigate the effect of osteoporosis on bone quality. Specifically, we measured the fatigue life of control and OVX compact bone samples and quantified resultant microdamage in terms of region, location and interaction with secondary osteons.

While considerable scatter was present in the fatigue data, the mean number of cycles to failure (N_f) was 7% lower in the OVX group compared to controls. This difference was not statistically significant, however, our values compared well with the literature. Other authors have found a similar degree of scatter in N_f from various types of fatigue testing of bone (Carter et al, 1981; Taylor et al, 1999). It is most likely that microstructural differences, such as orientation of the lamellae, porosity and degree of mineralisation are responsible for the large variation from specimen to specimen. The modulus of bending was also lower in the OVX group compared to the control (17.65 ± 2.11 and 20.37 ± 7.93 (GPa), respectively). Once again these values compared well to the literature, Currey (1988) reported an average modulus of bending of 18.9 ± 2.2 GPa from fatigue testing of beam shaped specimens taken from sheep metatarsus. Their beams were of similar dimensions ($2 \times 3.5 \times 30$ mm) to the ones used in the present study ($2 \times 2 \times 30$ mm).

Cr.Dn was higher in the OVX group compared to controls, but the difference was not significant. Cr.S.Dn was significantly higher in the control group compared to the OVX ($p<0.01$). Furthermore, the number of long cracks ($>300\mu\text{m}$) was significantly increased in the control group compared to the OVX. If we assume that our samples behave like fibre-reinforced composites then these data agree with the theory for crack behaviour in that type of material. This theory states that in a composite material with a large number of fibres, cracks will tend to initiate easily but find it difficult to grow. Conversely, in a composite with a small number of fibres, cracks will not initiate as readily, but those ones that do form will tend to find it easier to grow. There are also other factors which can affect crack initiation and growth including material strength and fibre diameter. In general, a reduction in the strength of a material increases the potential for crack initiation but it also increases the resistance to crack growth. A summary of the relationship between crack behaviour and material strength, fibre diameter and fibre spacing is shown in Table 4.4 A.

This theory is relevant to this study as follows: the OVX samples displayed more new osteons and more cracks, which did not propagate far. This agrees with Table 4.4 if we consider that fibre spacing is reduced due to increased osteon numbers. Thus, we would expect increased crack initiation and decreased propagation (Table 4.4 B).

Table 4.4 A: Relationship between material strength, fibre diameter and spacing to crack initiation and propagation. In this table ‘+’ indicates an increase and ‘-’ indicates a decrease. (Adapted from Martin and Burr, 1998).

	Resistance to Crack Initiation	Resistance to Crack Propagation
Increased Material Strength	+	-
Decreased Material Strength	-	+
Increased Fibre Diameter	-	+
Decreased Fibre Diameter	+	-
Increased Fibre Spacing	+	-
Decreased Fibre Spacing	-	+

Table 4.4 B: Relationship between control and OVX bone and crack initiation and propagation. In this table ‘+’ indicates an increase and ‘-’ indicates a decrease.

	Resistance to Crack Initiation	Resistance to Crack Propagation
Control Bone	+	-
OVX Bone	-	+

More linear microcracks were present in the compressive region compared with the tensile region in both groups. This is consistent with other findings in the literature; Diab and Vashishth (2005) carried out a study of the effects of damage morphology on bovine cortical bone fragility. Damage morphology was classified as either linear microcracks or diffuse damage. In their study, beams of cortical bone were tested in fatigue and the resultant microdamage was assessed in terms of its morphology and the sequence in which it formed. More linear microcracks were found on the compressive side of all samples in this study which compares favourably to our findings. Another study by the same group (Diab et al, 2006), examined the role of microdamage accumulation in the age-related increase in human bone fragility. Once again, beam shaped cortical bone samples were tested in fatigue and, following microcrack analyses, more microcracks were observed in the compressive region. Diffuse damage was found to predominate in the tensile region in both of the above studies. Our analysis did not consider areas of diffuse damage because it occurs at the ultrastructural level where the mechanisms of interaction with the microarchitecture are quite different. Thus, comparisons cannot be made with that aspect of their study.

Our Cr.Dn and Cr.S.Dn data are slightly higher than those from the aforementioned studies. There are a number of possible explanations for this. Firstly, different types of bone were used in each of these studies. We used aged ovine bone which has a high osteon density relative to bovine bone. This would provide more crack initiation sites when the bone is cyclically loaded. Secondly, our test specimens were smaller (our cross sectional area was approximately half the size) and thus would be expected to have a longer fatigue life based on the reduced probability of the specimens containing a critical defect (Taylor, 2000).

Thirdly, the studies discussed above used a failure criterion of 50% stiffness reduction, in our study specimens were tested to outright failure. Some of these effects can be addressed using a stressed volume analysis.

Taylor (2000) developed a method for quantifying the effect of stressed volume in fatigue testing of bone samples. This method can also be used to compare fatigue data from different specimens and different animals. It was formulated from a statistical analysis of previous data, the intention being to show that data from various sources, tested in a variety of ways can be compared and from this, new predictions can be made. The data from our fatigue tests fit in well with this theory (Figure 4.16). The stressed volume of our samples during testing was calculated to be 4.8mm^3 and the fatigue strength at 100,000 cycles was 83 MPa.

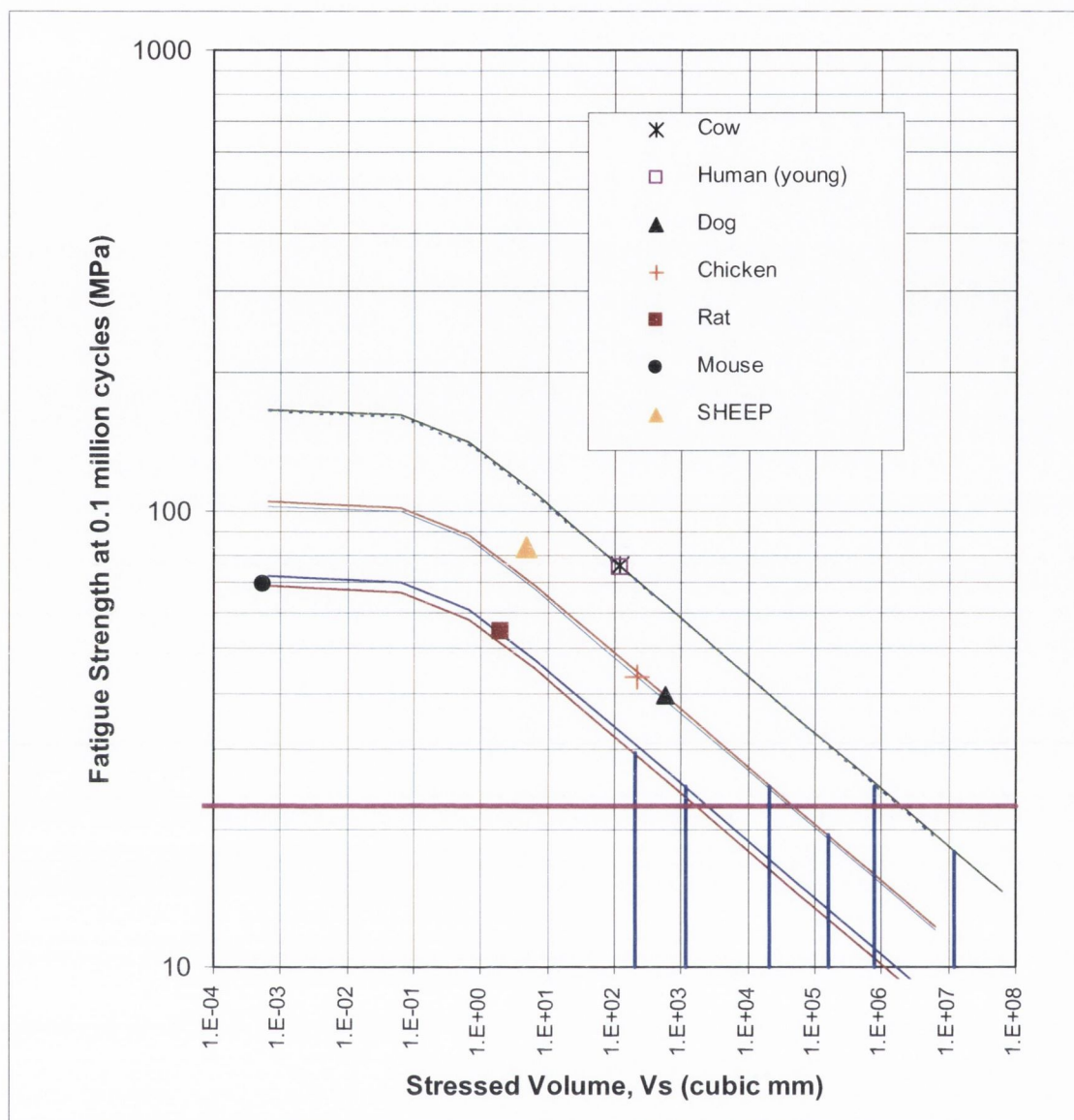


Figure 4.16: Experimental data on the fatigue strength of bone from different animals plotted as a function of the stressed volume of the bone or sample (Taylor, 2000). This graph also shows theoretical predictions. The curved lines show the predicted variation of fatigue strength with volume for each species. The bold vertical lines represent the total stressed bone volume of each species. The bold horizontal line is the average strength value at the intersection points, i.e. the average fatigue strength of whole bones. The results from our study are represented by the 'SHEEP' data point on this graph. This data point lies between the line for 'Dog' and the line for 'Human', which makes intuitive sense as the volume of a sheep bone is intermediate between these two.

It is known that the behaviour of microcracks depends on crack length, in other words, the energy of the crack (O'Brien et al, 2005). In other studies from the same laboratory, a microstructural barrier effect in bone was described whereby short cracks ($\sim 100\mu\text{m}$ in length) tended to stop at osteons, longer cracks (up to $300\mu\text{m}$) tended to deflect around the osteon and cracks over $300\mu\text{m}$ were found to penetrate into the osteon (O'Brien et al, 2005; Mohsin et al, 2006). In our study, most microcracks were found in interstitial bone which is consistent with these studies and others (Schaffler et al, 1995; Norman and Wang, 1997; Boyce et al, 1998; Taylor, 1998). Long cracks ($>300\mu\text{m}$) were observed to penetrate old (unlabelled) osteons, which can be explained because the crack has sufficient energy and the osteon is sufficiently old (and thus mineralised) to result in penetration. However, long cracks ($>300\mu\text{m}$) were observed to behave differently on interaction with old (unlabelled) osteons compared to new (labelled) osteons. This suggests that the status of the osteon contributes to the behaviour of a propagating microcrack. This can be explained by assuming that new osteons, containing relatively undermineralised bone, do not bear much load and so essentially behave like pores in the matrix. These then tend to attract propagating cracks, as normal pores would, and thus serves to blunt them at the point of impingement.

This raises an interesting and important question. When do new osteons cease to act as effective crack stopping interfaces? To answer this question, we must consider our choice of animal model. In the ovine skeleton, Haversian remodelling, in the long bones, begins at around 5 years of age. The animals used in this study were not older than about 9 years. Therefore, what we considered to be 'old' osteons in this study can not have existed for

more than 3 years. This suggests that the change in behaviour of secondary osteons, in relation to propagating cracks, takes place between 1 and 3 years post formation. The literature contains many studies that have examined crack propagation in compact bone. It is well recognized now that osteons, considerably older than the ones in this study, serve as effective crack arrestors. This is at variance with our data, however, this can be explained by noting that the cracks which were considered in this study were relatively large ($>300\text{ }\mu\text{m}$) compared to the one studied in the literature. Larger cracks possess more energy, as they propagate, than smaller cracks. Therefore, different behaviour may be expected for cracks of different length during propagation.

A small number of new (labelled) osteons were penetrated by long microcracks. All of these were found in the control group. This may be explained by noting that Cr.S.Dn in the control group was significantly higher than in OVX. Significantly more long cracks ($>300\text{ }\mu\text{m}$) were also found in the control group compared with OVX. In each of the incidences of labelled osteon penetration, the cracks responsible were very long (some were $>500\text{ }\mu\text{m}$). These cracks can be considered almost macroscopic and thus outside the realm of microdamage. This observation agrees with O'Brien et al (2005) who found that osteons serve to halt crack growth, but only up to a certain point. When cracks become sufficiently long the role of osteons can then reverse, and they begin to serve as points of weakness in the bone.

4.5 *Conclusions*

In conclusion, this study shows that compact bone specimens from the metatarsals of sheep 12 months post-surgery displayed an OVX effect compared with controls as follows:

- 1) Fatigue life was reduced in OVX compared to controls.
- 2) Quantitative analysis of microdamage showed that Cr.Dn was increased in the OVX group; conversely, Cr.S.Dn was found to be higher in the control group compared to OVX.
- 3) More linear microcracks were found in the compressive region compared to the tensile, in both groups.
- 4) Finally, osteon penetration during microcrack propagation was observed to depend on the nature of the osteon as well as the length, and thus energy, of the crack. Therefore, fatigue-induced microcrack behaviour depends not only on the crack properties, but also on the properties of any microstructural features which it may meet during propagation.

Chapter 5

The Effects of Osteoporosis on Bone Quality in Ovine Vertebrae

5.1	Introduction	118
5.2	Materials and methods	123
5.2.1	Sample preparation.....	123
5.2.2	DEXA scanning	123
5.2.3	Histological preparation	125
5.2.4	Histological analysis	127
5.2.5	MicroCT analysis	128
5.2.6	Biomechanical testing	129
5.2.7	Statistical analysis	131
5.3	Results	132
5.3.1	DEXA scanning	132
5.3.2	Histomorphometry	132
5.3.3	MicroCT data	134
5.3.4	Biomechanical testing	140
5.4	Discussion	143
5.5	Conclusions	153

5.1 Introduction

This chapter describes a study which investigates the effects of bone quality on bone strength in the L3 vertebra from control and OVX sheep 12 months post-surgery. While hip, Colles and other types of fractures are commonly seen in osteoporosis; vertebral fractures represent the classic hallmark of the disease (Cummings et al, 1990; Cooper et al, 1992). A group that carried out an epidemiological study in the USA found that approximately 300,000-500,000 men and women are affected each year by osteoporosis (Cooper et al, 1992). The same group carried out a related study which showed that hospital admissions for vertebral and hip fractures increased 10-fold in people aged between 65 and 90 years (Jacobsen et al, 1992). Thus, the cost of managing osteoporotic fractures is very high.

The lumbar vertebrae are particularly susceptible to osteoporotic fractures, therefore there is a need for their structure and behaviour to be accurately characterised in order to predict failure. The most common metric of vertebral body strength in osteoporosis assessment is bone mineral density (BMD), which has been correlated epidemiologically with fracture risk (DuBoeuf et al, 1995; Ito et al, 1997; Legrand et al, 2000; Lang et al, 2002). However, BMD increase correlates poorly with fracture risk reduction in clinical trials of osteoporosis therapies conducted in postmenopausal women (Cefalu, 2004). Although BMD may increase with therapies such as bisphosphonates, the overall increase is too small to account for the timing and magnitude of fracture risk reduction.

The large, rapid reduction in fracture risk with anti-resorptive therapies precedes much of the small overall increase in BMD. Indeed, some postmenopausal women continue to lose BMD during the first year of anti-resorptive therapy, and those with the greatest losses during the first year are most likely to gain BMD with continued treatment (Briggs et al, 2004). Therefore, use of BMD as a surrogate or proxy for anti-fracture efficacy has limited clinical utility by itself. As discussed in previous chapters, bone strength is derived from bone quantity and bone quality, which consists of structure, material properties, and bone turnover amongst other things. Much of the data in the literature concerning vertebral fracture prediction focus on BMD and trabecular architecture. However, data are beginning to accrue suggesting that changes in bone turnover may be an accurate predictor of vertebral fracture risk.

In accelerated bone turnover, resorption exceeds bone formation, producing a general thinning of the trabeculae that can lead to irreversible loss of trabeculae and to reduced connectivity within the matrix, contributing to fracture risk (Parfitt, 1992; Parfitt 2002). It is not possible to assess trabecular connectivity clinically, but high levels of bone turnover markers can predict fracture risk in untreated individuals. Osteocalcin is one such marker for formation and collagen type I telopeptides such as CTX and NTX are markers for resorption. Recent studies of anti-resorptive therapies have focused on the relationship between bone turnover and fracture risk reduction (Delmas, 2000; Delmas et al, 2000; Greenspan et al, 2000). This study attempts to elucidate the link between changes in bone turnover and bone architecture at the L3 lumbar vertebrae of a sheep model of osteoporosis. The sheep spine has often been used to model various conditions of the human spine (McLain et al, 2002; Ebihara et al, 2004). Wilke et al (1997) carried out a detailed

anatomical comparison between sheep and human spines. They measured 21 dimensions of each vertebra including the vertebral body, pedicles, spinal canal, transverse and spinous processes, facets, endplates and discs. The results showed that a fundamental difference between the species is that the human vertebra is characteristically wider than tall, whereas the sheep vertebra is taller than wide. However, for both species, vertebra width is greater than depth. Overall conclusions from this study were that strong similarities exist between the major dimensions of the sheep and human lumbar spinal region, and that this anatomical location in the sheep provides a good model of the human in biomechanical terms.

Mechanical testing at the whole-bone level measures properties of the entire bone as a structure, which incorporates the properties of the materials that compose the whole bone, as well as its internal and external geometry. At this hierarchical level, most specimens include both cortical and trabecular bone, and therefore contain multiple architectures. These specimens can be either entire excised bones, such as a whole femur, or large portions of an entire bone, such as a proximal femur. The mechanical behaviour of whole-bone specimens most closely approximates the behaviour of these structures *in vivo*. In testing whole-bone specimens, it is assumed that the various architectural features are insignificant as individual entities. Hypotheses regarding the mechanical behaviour of an intact bone, as well as how this may be altered due to aging, therapy or genetic mutations may be addressed at the whole-bone level of hierarchy (An and Draughn, 2000).

Mechanical testing of whole vertebral bodies has been used in the past, in conjunction with quantitative computed tomography (QCT) and μ CT in order to understand the mechanism

of localised trabecular failure and ultimately vertebral fracture. This approach is potentially useful for improving prediction of vertebral fracture risk. Cody et al (1991) assessed the significance of regional quantitative computed tomography (rQCT) measurements of BMD with respect to mechanical strength in the human lumbar spine. 58 vertebrae (from 12 males, 10 females) were scanned and then compressed to failure. Data from this study suggested strong correlations between regional BMD (rBMD) measurements from QCT and whole vertebrae failure load. In a similar study, McCubbrey et al (1995) investigated whether a characterisation of the macroscopic architecture within the vertebral centrum would improve predictions of vertebral strength, and also if regions in the centrum where least bone loss with age occurs are more predictive of vertebral strength. They found that vertebral failure properties were better predicted by combinations of vertebral regional cancellous density and they also determined a relationship between rBMD measurements and whole vertebral static and dynamic mechanical properties.

More recently, Thomsen et al (2002) investigated the relationship between static histomorphometry and bone strength of human lumbar vertebral bone. The ability of vertebral histomorphometry to predict vertebral bone strength was compared with that of vertebral densitometry. A strong correlation was found between vertebral bone strength and BV/TV, which is defined as relative bone volume where BV is bone volume and TV is total volume. A strong correlation was also found between strength and Tb.Sp, which is defined as the mean trabecular separation of the sample, an absolute value of $r = 0.86$ was found in both cases. The addition of Tb.Th, defined as mean trabecular thickness, significantly improved the correlation between BV/TV and bone strength. The ability of histomorphometry to predict vertebral bone strength was comparable to that of

densitometry. Bone structure which was assessed by connectivity density did not improve the correlation between static histomorphometric measures and vertebral bone strength. In this study we considered the third lumbar vertebra, with the end-plates removed, to act as a whole-bone structure. Various other studies in the literature have used this approach (Mosekilde, 1989; Ito et al, 2002).

The aim of this study was to investigate the contribution of bone quality to whole bone strength in the lumbar vertebrae in sheep 12 months post-OVX by assessing:

- (1) Bone turnover in the compact and trabecular bone regions of the vertebral body, and then relating it to the biomechanical properties
- (2) The microarchitecture, particularly of trabecular regions, of the vertebral body in control and OVX animals
- (3) The relationship between structural and material bone quality parameters and BMD from the L3 vertebral body of control and OVX animals

5.2 Materials and methods

5.2.1 Sample preparation

The L3 vertebra from control (n=18) and OVX (n=16) animals was removed and frozen at -20°C within 6 hours of being harvested from the sheep carcass. The vertebrae were carefully cleaned of soft connective tissue with a scalpel and scissors. The transverse and spinous processes were removed from each of the vertebrae using a slow speed diamond cutting saw (Accutom, Struers, Ballerup, Denmark). This process was carefully carried out to ensure that the main body of the vertebra was not damaged.

5.2.2 DEXA scanning

A fan-beam X-ray bone densitometer (QDR 4500™ Elite, Hologic, USA) in the Department of Anatomy, Trinity College Dublin was used to measure BMD in each of the L3 vertebral bodies. Bone samples were positioned for scanning within a 40x20x60cm saline-filled Perspex tank (A.C. Taylor Ltd, Dublin) (Figure 5.1).

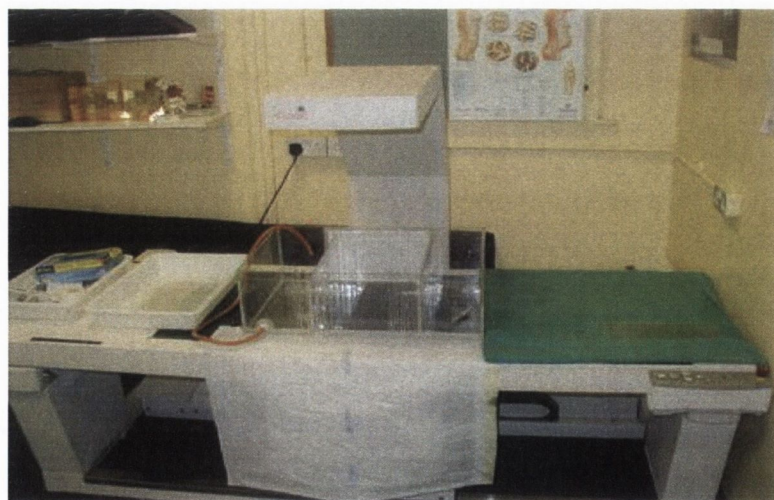


Figure 5.1: Image of the apparatus used to carry out DEXA scanning of the L3 lumbar vertebrae.

The midline of the vertebral body was aligned longitudinally with the machine's laser light system. Rotational alignment was also achieved using the laser light facility. Vertical alignment of each bone was obtained by positioning Perspex holding pins as close to the central axis of the bone as possible. Further visually aided adjustment of anatomical straight edges and landmarks at either end of the bone was performed with a grid on the side wall of the scanning tank (Figure 5.2).

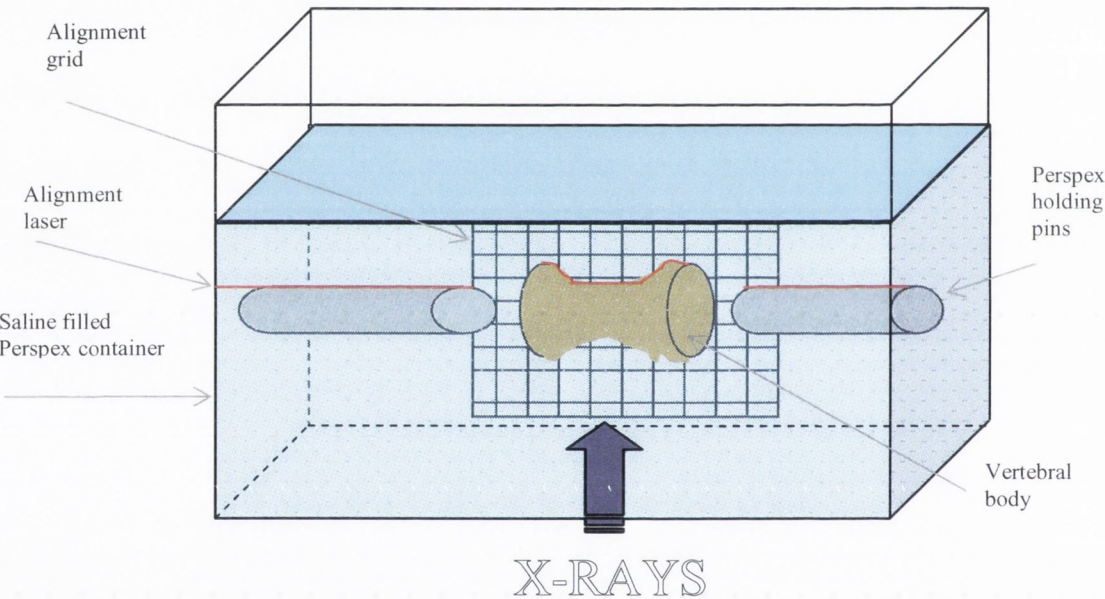


Figure 5.2: Schematic diagram of the apparatus used to align vertebrae prior to scanning.

Two scans were then performed with identical alignment procedures, but with a 180° change in orientation. Projected images then underwent pixel analysis using software for X-ray absorption. Estimated area (EA, cm^2), bone mineral content (BMC, g) and bone mineral density (BMD, g/cm^2) for each of the two tests (T1, T2) was then recorded. As part of a

quality control procedure, repeat scans of samples were performed if there was an $EA > 1 \text{ cm}^2$ difference between the two scans.

5.2.3 Histological preparation

After DEXA scanning, the vertebrae were cut approximately 5mm inside both endplates to obtain specimens with planoparallel ends (Figure 5.3).

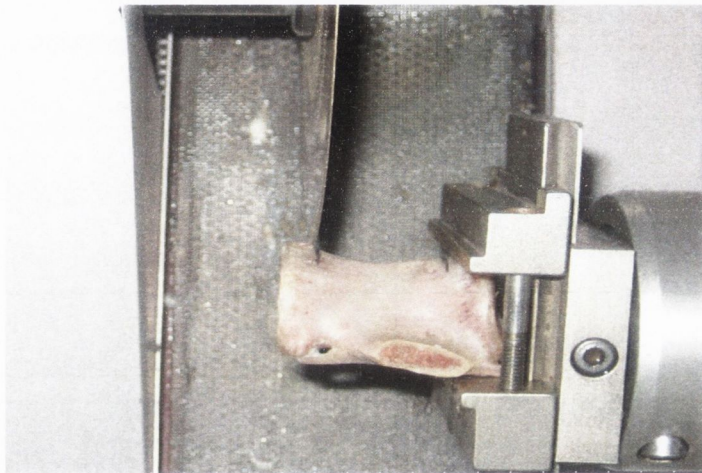


Figure 5.3: Image of an L3 vertebra clamped in a diamond saw with a 5mm portion being removed from the cranial aspect.

A section with a thickness of approximately $400\mu\text{m}$ was then removed from the cranial and caudal aspects of the vertebral body (Figure 5.4) ensuring maintenance of the planoparallel ends for compression testing (Mosekilde and Mosekilde, 1986; Thomsen et al, 2002). The main vertebral body was then wrapped in moist gauze and frozen at -20°C .

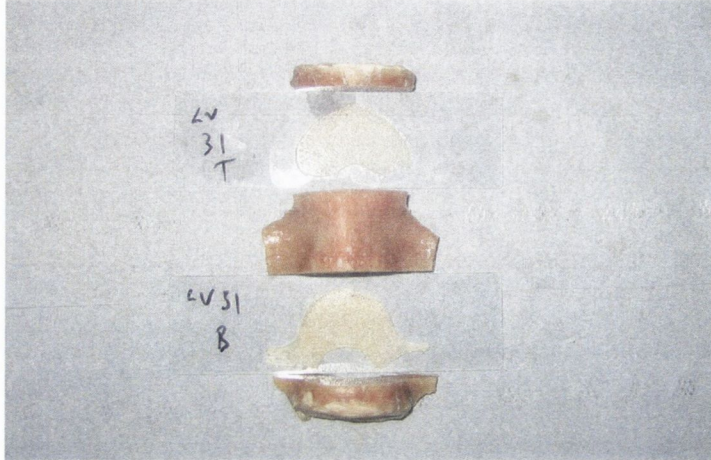


Figure 5.4: An L3 vertebra with histological sections which have been removed cranially and caudally.

Each 400µm thick section was glued to a standard glass slide using an even distribution of Superglue ensuring that sufficient glue was used to attach the entire trabecular bone area to the slide. Sections were then left to air-dry for 24 hours. The following day sections were ground down to approximately 120µm on an automatic rotating grinding plate (DP10, Struers, Ballerup, Denmark) (Figure 5.5). Section thickness was routinely checked during the grinding process using a digital micrometer. All grinding was carried out under running water for cooling and lubrication. Once the required thickness had been obtained, sections were covered using standard mounting medium (DPX, Sigma Aldrich, Ireland) and glass coverslips.

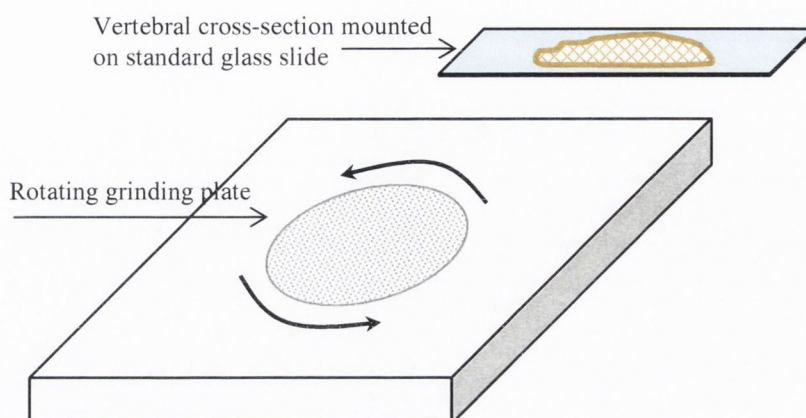


Figure 5.5: Schematic of the automatic grinding plate used to grind sections down to 150 μ m thickness.

5.2.4 *Histological analysis*

Histological analyses of cranial and caudal sections were carried out on an inverted fluorescence microscope (IX51, Olympus, Hamburg, Germany). Sections were initially viewed at X4 magnification using transmitted white light and the total cross sectional area was measured. The areas of the compact and trabecular bone regions were then measured using a digital image analysis system (AnalySIS, Soft Imaging Systems, Munster, Germany). Sections were then viewed using blue epifluorescence microscopy ($\lambda=470\text{nm}$) at X10 magnification. The fluorochrome dye calcein, which was administered at 6 months post-OVX in our study, reaches near maximum excitation under incident light of this wavelength.

Chapter 3 of this thesis showed that there was a statistical difference in bone turnover levels in the metatarsal between control and OVX sheep in this study at 6 months post-OVX. Thus, bone turnover in this study of the L3 vertebra was assessed by measuring the number

of sites of bone turnover labelled with calcein. Bone turnover was assessed in the compact bone region by measuring the number of labelled osteons per measured area. Similarly, in the trabecular bone region bone turnover was assessed by measuring the number of calcein labelled new bone ‘packets’ per measured area (Figure 5.6). These histomorphometric parameters are derived from the American Society for Bone and Mineral Research (ASBMR) nomenclature (Parfitt et al, 1987; Schorlemmer et al, 2005).

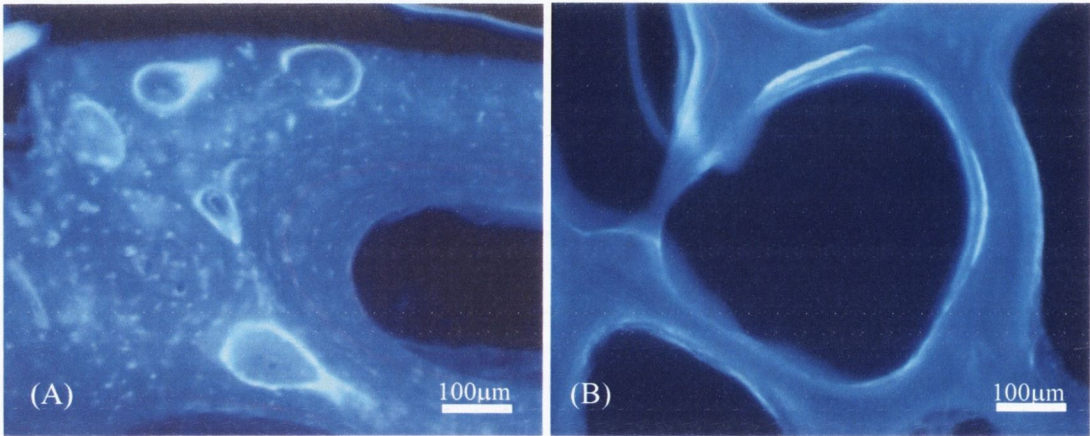


Figure 5.6: Histological images showing (A) labelled osteons in the vertebral cortex and (B) labelled bone ‘packets’ in trabecular bone.

5.2.5 *MicroCT analysis*

Each of the vertebral bodies was thawed out at room temperature for approximately 6 hours prior to scanning. Samples were wrapped in moist gauze and placed in a cylindrical specimen holder (height=80mm, diameter=36mm) and the holder was then fixed into the μ CT scanner (Scanco, μ CT-40, Bassersdorf, Switzerland). Each sample was then scanned using a similar protocol to the one described in Chapter 3 of this thesis. The only differences in this case were that a larger specimen holder was required to hold a whole vertebra and that three separate scans were taken from each vertebral body. The scan areas were divided up into cranial, mid-vertebral and caudal regions (Figure 5.7).



Figure 5.7: Scanned image of a lumbar vertebra divided into 3 regions; cranial, mid-vertebra and caudal.

When a full 3D reconstruction of the sample had been created, various parameters which describe the trabecular architecture of the bone were calculated including BV/TV, Tb.N, Tb.Th, Tb.Sp, which were discussed earlier and also the degree of anisotropy (DA).

5.2.6 Biomechanical testing

To prepare the vertebral bodies for mechanical testing, the planoparallel ends were checked using a standard spirit-level. The height of each sample was also measured using digital Vernier calipers. Compression tests were performed between steel platens on a servo-hydraulic materials testing machine (Instron, 8501, Bucks, UK). The specimen was placed on the bottom platen, and a ball joint allowed the top platen to rest flat on the specimen as the actuator was lowered onto the specimen. Each vertebral body was pre-loaded five times in the load range 100 - 400N and then held for five minutes at 200N. This protocol was used in order to reduce the viscoelastic effects of the bone and to allow proper seating between the platens and the surfaces of the vertebra.

The specimens were then loaded at a rate of 0.15 mm/sec ($\sim 0.5\%$ strain/second) to an end point of 5% strain. Strains were based on the initial height of each specimen as measured with calipers. The specimens were unloaded to 200N and held for 1 minute to minimise viscoelastic creep and to reach a steady-state displacement (Keaveny et al, 1999; Kopperdahl et al, 2000). They were then subjected to a second loading cycle, under the same conditions as the first, to beyond their ultimate point to 10% strain. The 1 minute hold between load cycles was set at 100N rather than 0N to prevent the platens from lifting off the specimen and to reduce the nonlinearity in the load-deflection curve of the second load cycle. To estimate the plastic deformation at 0N after one load cycle, a straight line was fitted to the reload cycle and the intersection of this line with the displacement axis was defined as the residual displacement at 0N. An example of the loading curve produced from this test is shown in Figure 5.8. The loading was applied in this way to highlight the effect of increased remodelling in the OVX group on biomechanical properties of the whole bone.

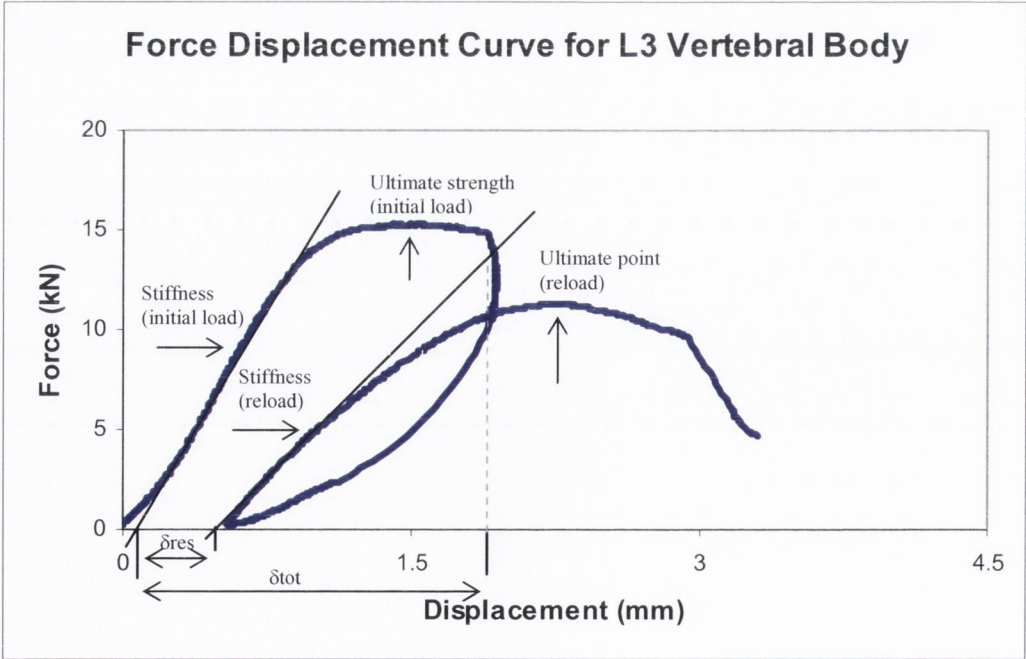


Figure 5.8: Typical load-reload force displacement curves for L3 lumbar vertebrae.

Measured parameters from this test included ultimate strength, proof stress, stiffness from the load-deformation curves of each cycle and also the residual strain. The ultimate strength and proof stress were defined as the stresses at the local maximum point on the initial and reload curves, respectively. To obtain stiffness, the tangent modulus was found at each data point on the load-deformation curve by fitting a straight line to the range of data whose centre point was located on the data point of interest and whose width was equivalent to 0.3% of the original specimen height. The stiffness was then defined as the maximum tangent modulus. The residual strain, or the amount of unrecovered strain prior to reloading, was calculated as the residual deformation at 0N prior to reloading divided by the initial specimen height.

5.2.7 *Statistical analysis*

Variables were expressed as mean \pm standard deviation (SD). For statistical analyses, groups were assessed for normal distribution and then compared using a t-test. For those variables failing the normality test, a nonparametric Mann-Whitney rank sum test was used. SigmaStat 3.0 statistical package (SYSTAT Software Inc, Chicago, IL 60606) was used for all statistical analyses. A p value of <0.05 was considered to be significant.

5.3 Results

5.3.1 DEXA scanning

The DEXA scanning data showed that the mean BMD in the OVX group was lower than in the control group, but the difference was not significant. Values of BMD were 0.799 ± 0.074 and 0.785 ± 0.084 (g/cm²) in the control and OVX groups, respectively. These data are represented in graphical form in Figure 5.9.

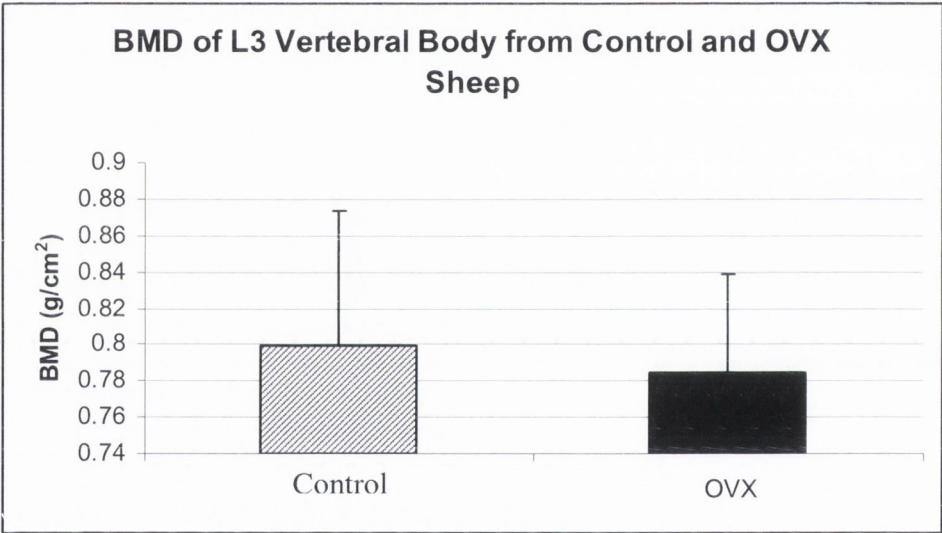


Figure 5.9: Mean BMD data from L3 vertebrae of control and OVX animals as measured by DEXA.

5.3.2 Histomorphometry

The cross-sectional cortical bone area (Ct.Ar) and the trabecular bone area (Tb.Ar) from the L3 vertebra did not differ significantly between the control and OVX groups, the data are shown in Table 5.1. However, bone turnover was significantly increased in the OVX group compared to the controls, both in areas of compact and trabecular bone (Table 5.1)

Table 5.1: Mean cortical and trabecular bone area and turnover for L3 from control and OVX sheep.

	Control	OVX	<i>p</i>
Cortical Bone Area (mm ²)	35.93±5.95	33.40±3.83	NS
Trabecular Bone Area (mm ²)	112.6±15.74	119.6±14.7	NS
Compact Bone Turnover (#/mm ²)	1.13±0.89	3.00±1.11	<0.001
Trabecular Bone Turnover (#/mm ²)	0.92±0.57	1.87±0.97	=0.001

Figure 5.10 shows an image of a cross-section of two L3 vertebrae, one from the control group and one from the OVX group. The images were taken at X4 magnification using blue epifluorescence microscopy ($\lambda=470\text{nm}$). The image from the OVX bone shows a large number of bone turnover sites that have been labelled with calcein, which fluoresces green, at 6 months post-OVX. The image from the control bone shows a relatively small number of these labelled bone turnover sites.

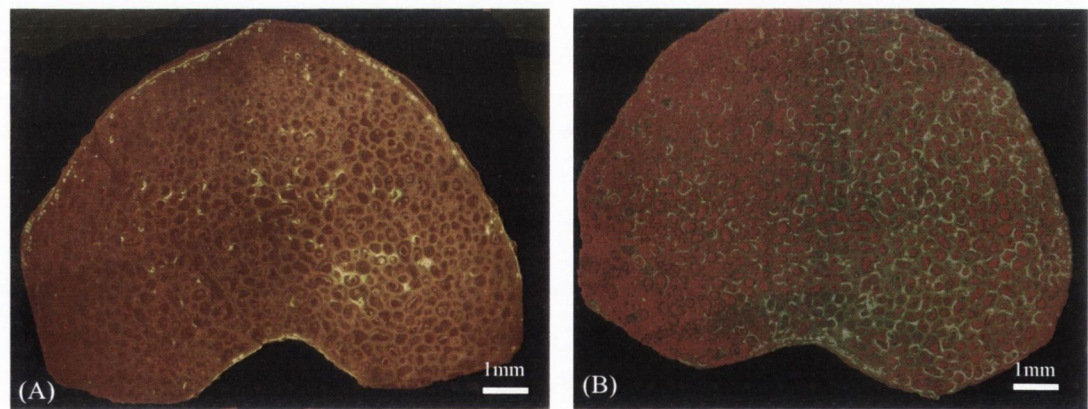


Figure 5.10: Composite image of a cross-section through an L3 vertebra from (A) control and (B) OVX sheep. The majority of the bone structure is trabecular with a thin shell of cortical tissue around the outside. A large number of bone turnover sites labelled with calcein can be seen in the OVX image compared with the control. Images were viewed using blue epifluorescence ($\lambda=470\text{nm}$) at X4 magnification.

Figure 5.11 demonstrates the bone turnover data graphically. Labelled sites of bone turnover, in cortical and trabecular tissue, were increased in OVX animals at 6 months post-surgery.

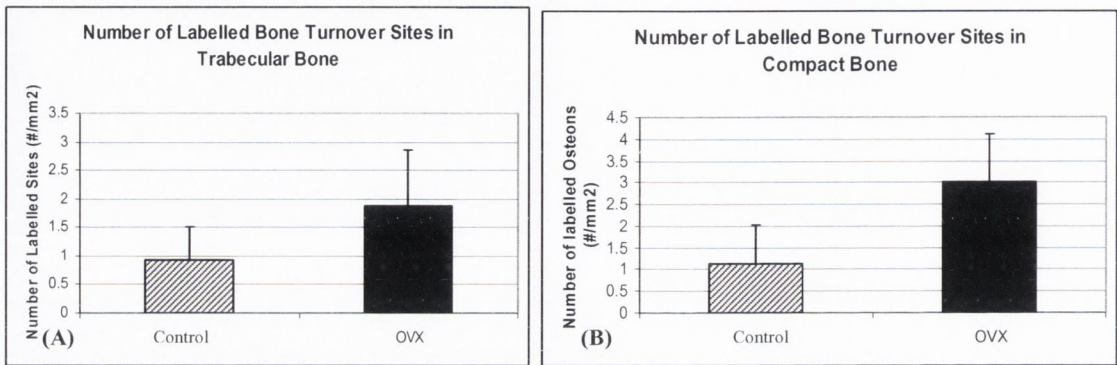


Figure 5.11: Average number of labelled sites of bone turnover in (A) trabecular and (B) cortical bone tissue in control and OVX groups.

5.3.3 *MicroCT data*

MicroCT scans of each L3 vertebra were carried out in three regions; cranial, mid-vertebral and caudal. The average trabecular number (Tb.N) in the three regions, from both groups of vertebrae, are shown in Figure 5.12. Tb.N was significantly higher in the cranial region compared to both mid-vertebral and caudal regions ($p<0.001$). Tb.N was also significantly higher in the caudal region compared with the mid-vertebral ($p<0.01$).

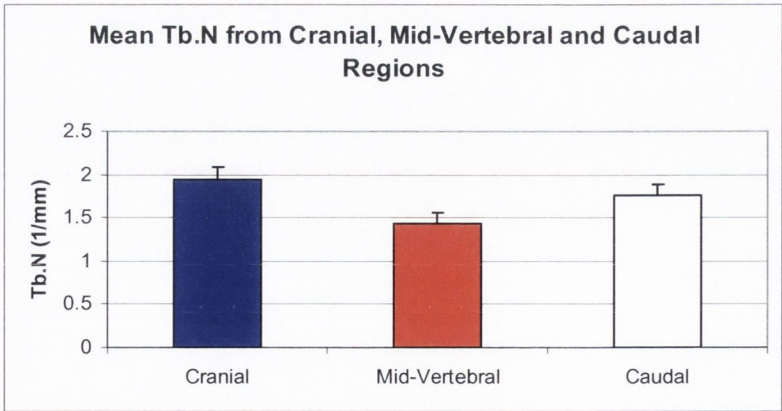


Figure 5.12: Mean Tb.N in three regions of L3, pooled data from both groups.

The same data are shown in Figure 5.13, but the experimental groups are also considered. The same trend as before is evident but no intra-group differences are apparent.

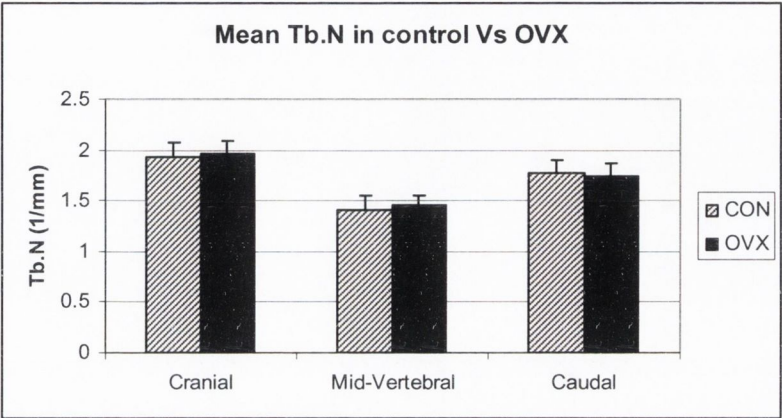


Figure 5.13: Mean Tb.N in three regions of L3, from control and OVX groups.

The average trabecular thickness (Tb.Th) in each region, from both groups of vertebrae, are shown in Figure 5.14. Tb.Th was significantly higher in the mid-vertebral region compared to both cranial and caudal regions ($p<0.001$). Tb.Th was also slightly higher in the cranial region compared with the caudal.

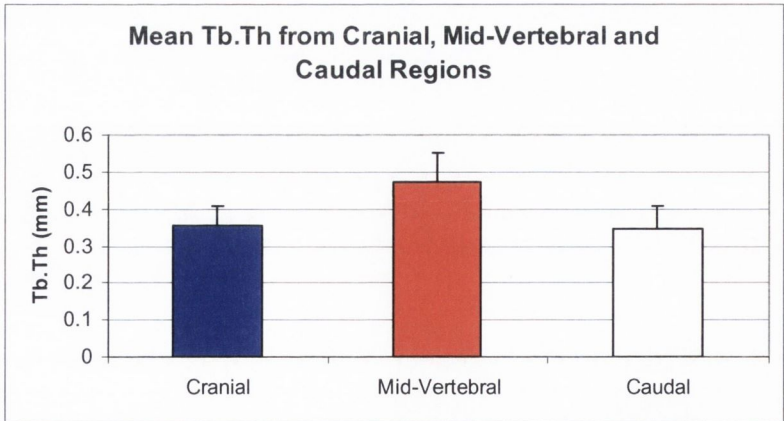


Figure 5.14: Mean Tb.Th in three regions of L3, pooled data from both groups.

The same data are shown in Figure 5.15, but here the experimental groups are also considered. The same trend as before was evident between regions. While no significant inter-group difference was found, a trend showing reduced thickness in the OVX group in the mid-vertebral and caudal regions is evident.

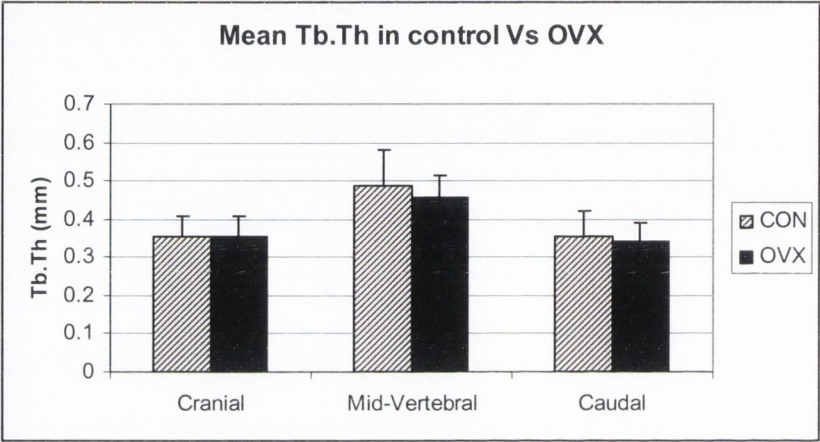


Figure 5.15: Mean Tb.Th in three regions of L3, from control and OVX groups.

The average trabecular separation (Tb.Sp) in the three regions, from both groups of vertebrae, are shown in Figure 5.16. Tb.Sp was significantly higher in the mid-vertebral region compared to both cranial and caudal regions ($p<0.001$). Tb.Sp was also significantly higher in the caudal region compared with the cranial ($p<0.01$).

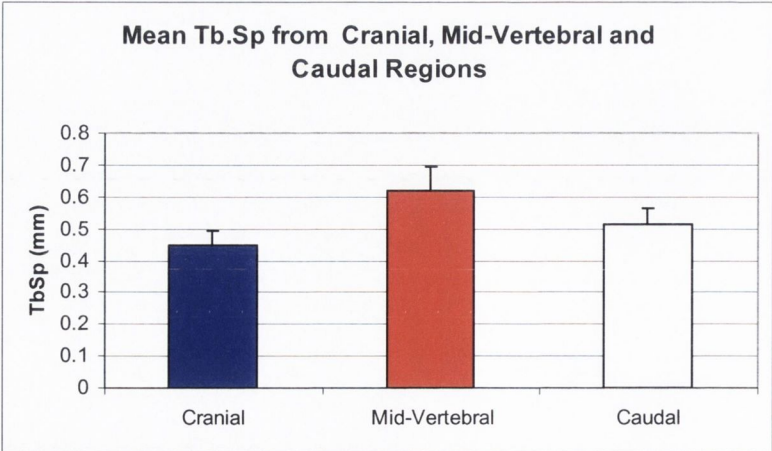


Figure 5.16: Mean Tb.Sp in three regions of L3, pooled data from both groups.

The same data are shown in Figure 5.17, but here the experimental groups are also considered. The same trend as before was evident between regions. No significant inter-group difference was observed at any of the three measurement regions.

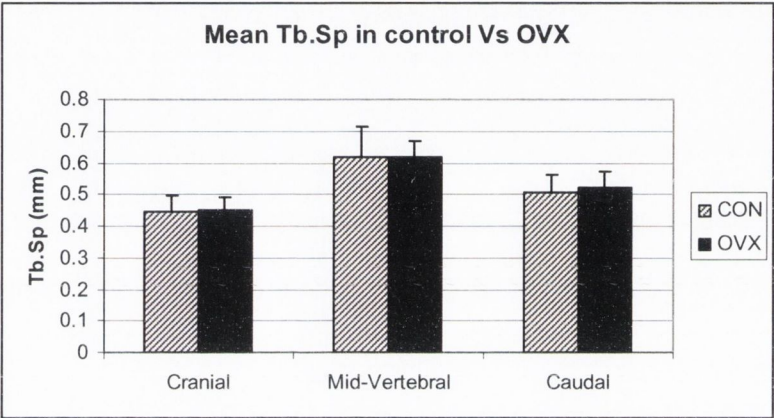


Figure 5.17: Mean Tb.Sp in three regions of L3, from control and OVX groups.

The average degree of anisotropy (DA) for the three regions, from both groups of vertebrae, is shown in Figure 5.18. DA was significantly higher in the cranial region compared to the mid-vertebral region ($p<0.05$). DA was also significantly higher in the caudal region compared with the mid-vertebral ($p<0.05$).

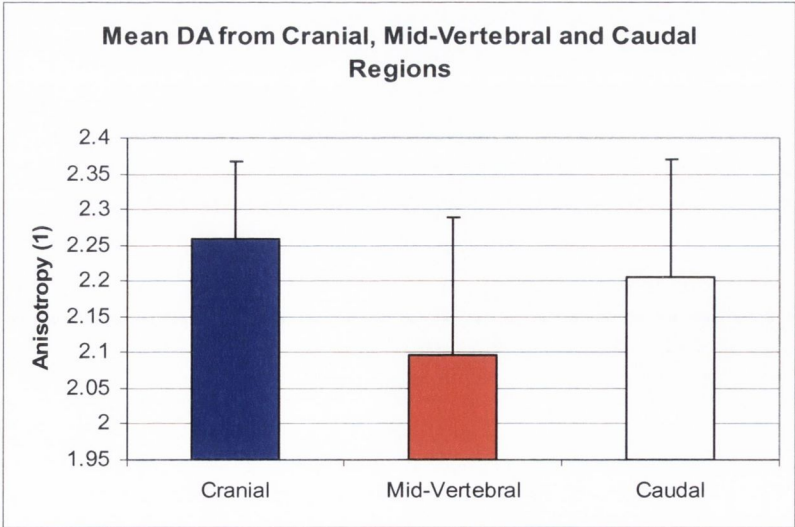


Figure 5.18: Mean DA in three regions of L3, pooled data from both groups.

These data are shown again in Figure 5.19, but here the experimental groups are considered. The same regional trends are apparent and a non-significant trend of increased anisotropy in the OVX group at the mid-vertebral and caudal regions is evident.

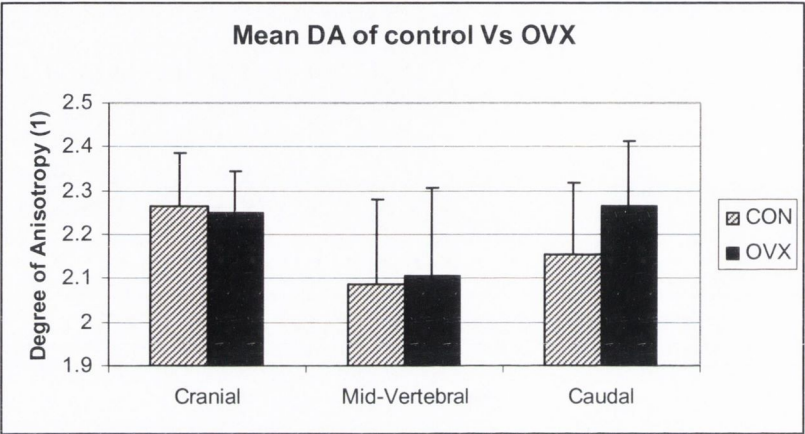


Figure 5.19: Mean DA in three regions of L3, from control and OVX groups.

The average bone volume (BV/TV) for the three regions, from both groups of vertebrae, is shown in Figure 5.20. BV/TV was higher in the cranial region compared to both mid-vertebral and caudal regions. BV/TV was higher in the mid-vertebral region compared with the caudal, however these differences did not reach statistical significance ($p>0.05$)

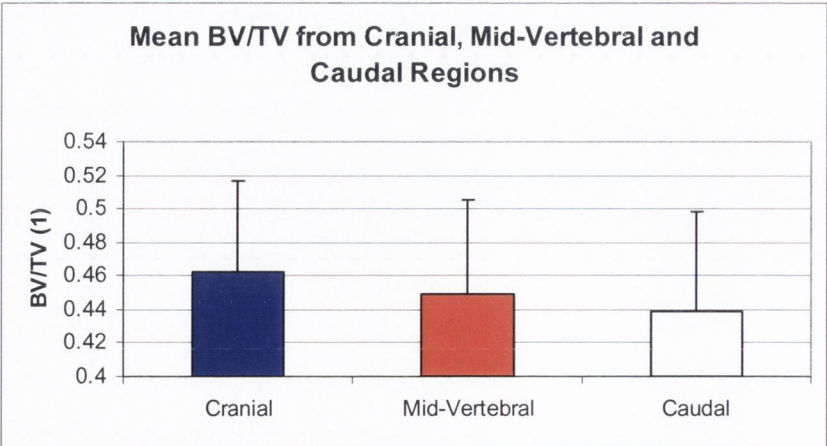


Figure 5.20: Mean BV/TV in three regions of L3, pooled data from both groups.

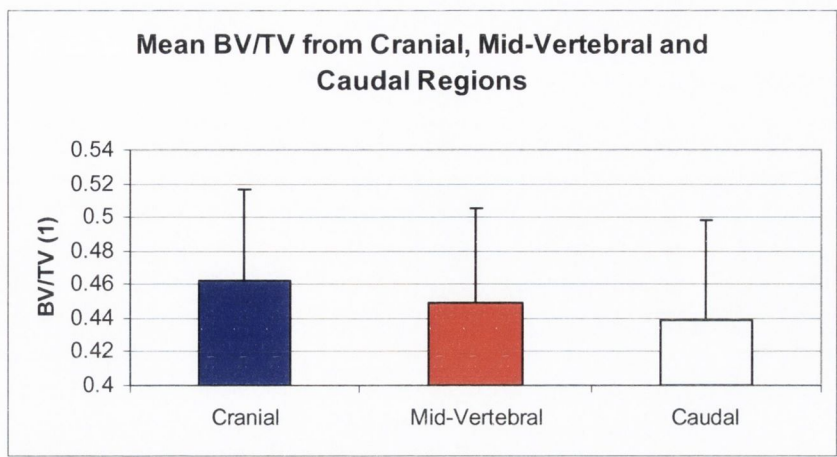


Figure 5.20: Mean BV/TV in three regions of L3, pooled data from both groups.

These data are shown again in Figure 5.21, but here the experimental groups are considered. The same regional trends are apparent and a non-significant trend of reduced BV/TV in the OVX group in each of the three regions is present.

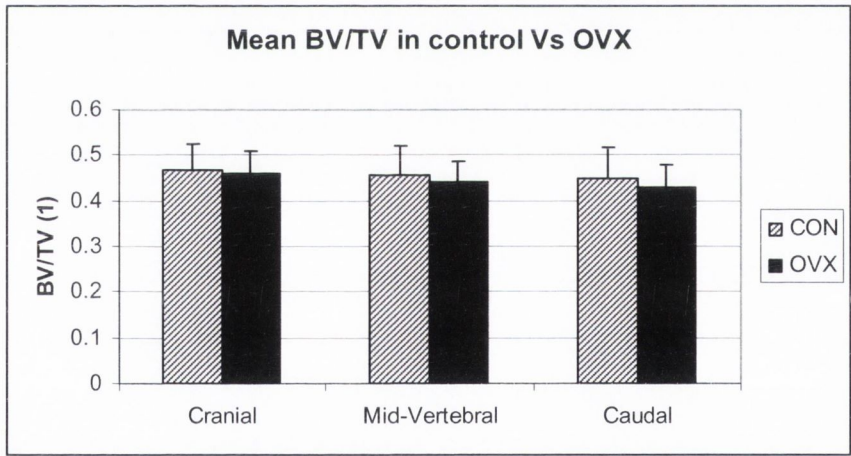


Figure 5.21: Mean BV/TV in three regions of L3, from control and OVX groups.

5.3.4 Biomechanical testing

The vertebral bodies responded characteristically to both the initial and reload cycles as follows: all specimens showed a small toe in the first part of the curve then a linear elastic region followed by an ultimate point which occurred between 3 and 4% strain. The response to the reload cycles was similar with a reduced stiffness and a reduced ultimate point.

Reductions in mechanical properties after the initial cycle were apparent in all cases. Ultimate strength from the initial load cycle was defined as the maximum stress point on the curve. The average ultimate strength in the control and OVX group were 99.03 ± 12.57 and 91.01 ± 7.98 (MPa), respectively (Figure 5.22). This represents a statistically significant reduction in the OVX group ($p=0.036$). The proof stress, taken as the ultimate point on the reload curve, was lower in the OVX group compared to controls but the difference was not significant ($p=0.073$).

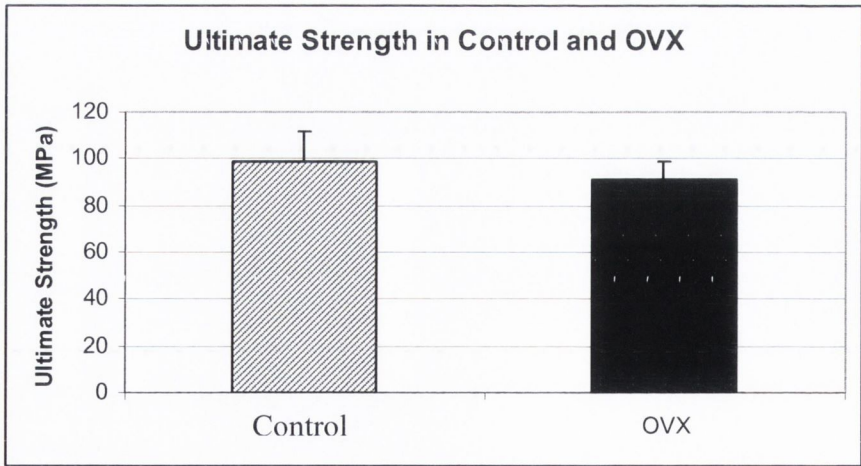


Figure 5.22: Ultimate strength of L3 lumbar vertebrae from control and OVX groups.

The reload stiffness was calculated from the slope of the force displacement curve. The data are presented here as the percentage reduction in structural stiffness between the load and reload cycles, in both groups. The average percent stiffness reduction was higher in the OVX group compared to the controls, but the difference did not quite reach statistical significance ($p=0.09$). These data are illustrated in Figure 5.23. The stiffness from the initial cycle was not significantly different between groups ($p>0.05$)

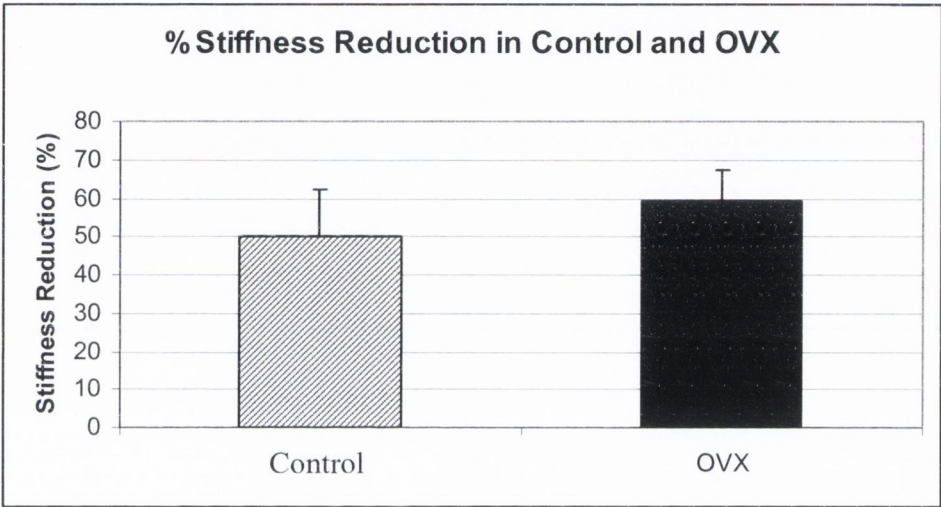


Figure 5.23: Percentage stiffness reduction of L3 lumbar vertebrae from control and OVX groups.

As discussed in Chapter 3 of this thesis, some of the data sets in this study showed marginal significance between experimental groups. Although the desired power of $p<0.05$ was not achieved in some cases, almost all cases displayed trends which were consistent with our stated hypothesis. Thus, in this study, the problem of marginal significant The slope line from the reloading curve was extrapolated back to where it intersected with the x-axis; this point was defined as the residual deformation at a load of 0N. Average residual strain was 1.86 ± 0.51 and 1.55 ± 0.25 (%) in the control and OVX groups, respectively. This represents

a statistically significant reduction in the OVX group compared with controls. These data are illustrated in Figure 5.24.

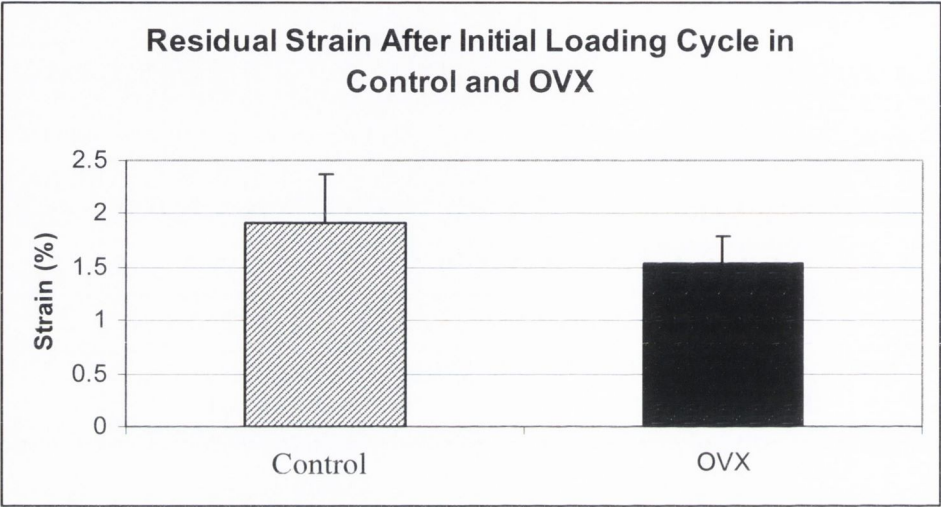


Figure 5.24: Residual strain for L3 lumbar vertebrae from control and OVX groups.

5.4 Discussion

Understanding the relationship between bone quality, osteoporosis and fracture risk is becoming increasingly important as the worlds' elderly population rises. One vertebral fracture is associated with a 4-5 times greater risk of subsequent fracture; two coincident fractures increase the fracture risk nearly 12 times (Ross et al, 1991). In the last decade it has become clear that BMD can only predict fracture with an accuracy of between 40-70% (Bouxsein, 2003).

The role of bone quality in vertebral fracture has been investigated predominantly in terms of the trabecular microarchitecture of the structure. Some studies have considered the influence of bone turnover, however it is typically measured using biochemical bone markers which reflect systemic metabolic activity rather than site specific turnover. The primary aim of this study was to assess the contribution of local bone turnover within the L3 vertebral body to its mechanical behaviour in control and OVX bone. Secondary aims were to investigate the effects of microarchitecture and BMD on strength in the same samples.

BMD in the vertebrae of OVX animals was not statistically different from the controls, although a trend towards reduced BMD in the OVX group was apparent. Our results of 0.799 ± 0.074 and 0.785 ± 0.084 (g/cm^2) in the control and OVX groups, respectively, compare well with others in the literature. Mitton et al (1997) used a similar DEXA scanning machine to evaluate BMD in L5 vertebra from 30 female sheep and found an average value of 0.79 ± 0.11 g/cm^2 . These results confirm those from previous studies which

suggested that DEXA did not detect early changes in BMD of OVX sheep 12 months post-surgery (Turner et al, 1995; Chavassieux et al, 2001). In a more recent study, Sigrist et al (2007) examined the long term effects of ovariectomy on bone density in sheep and found a significant OVX effect on trabecular bone BMD. In their study, density scans were carried out at the distal radius of OVX sheep. A rapid initial phase of trabecular bone loss of 12.7% between 0 and 4 months post-OVX was exhibited ($p=0.008$). Then a period of relative stabilisation occurred between 4 and 12 months followed by minimal increases until sacrifice at 18 months. Possible reasons for the differences between these data and ours are that the site examined was the distal radius and also that the machine used was a Densiscan 1000 (Scanco Medical, Bassersdorf, Switzerland) which has a higher resolution than the scanner we used. This machine uses specific software which considers only trabecular bone which reduces the effect of averaging over cortical and trabecular bone tissue which is inherent in most DEXA scanning systems. Most importantly, however, was that OVX was carried out at a different time of year in these studies, meaning that the seasonal effect would differ in each case.

The rate of bone turnover was measured by calculating the number of sites of bone turnover per measured area at 6 months post-OVX. For cortical bone this was calculated as the number of labelled osteons per bone area, for trabecular bone the number of labelled 'packets' per bone area. In the cortical bone shell, bone turnover was increased approximately 2-fold in the OVX group compared to controls. While there are not many other studies that have measured bone turnover in osteoporosis with this method, our findings compare well with similar studies in the literature.

Schorlemmer et al (2005) studied the effects of steroid treatment on cortical bone in terms of BMD, strength and new bone formation and compared it to trabecular bone. This study used sixteen ovariectomised sheep and divided them into a steroid-treated group (GLU; n=8) and an untreated group (OVX; n=8). Animals were intravenously administered calcein at 4 months post-OVX to label bone turnover, while the same parameter was assessed at 12 months by measuring forming osteons at the time of sacrifice. In the OVX group, compact bone turnover was 7.33 ± 8.55 and 3.86 ± 4.31 (#/mm²) at 4 and 12 months post-OVX, respectively. Our bone turnover data, from 6 months post-OVX, was 3.00 ± 1.11 #/mm² which compares reasonably well. There was no control group, with normal estrogen levels, used in their study with which to compare our control data.

In the same study by Schorlemmer et al (2005), trabecular bone turnover in the femoral condyle was measured. At 4 months post-OVX turnover was 0.48 ± 0.33 , compared with 1.87 ± 0.97 (#/mm²) at 6 months in our study. This difference may be due to the anatomical location of where the samples were taken from, the difference in sheep breed, and also the time of year. The difference in trabecular bone turnover in OVX sheep in these two studies highlights the need for localised information on bone turnover compared with system-wide measures as obtained by biochemical bone markers.

The microarchitecture of the L3 vertebra was analysed in two ways in this study. Firstly, samples were pooled together and parameters of trabecular architecture were measured in three regions, cranial, mid-vertebral and caudal. Then, the animal group was taken into consideration and the parameters of the controls were compared with OVX, in each of the three regions. Tb.N was significantly higher in the cranial compared to the mid-vertebral

and caudal regions, and caudal was also significantly higher than mid-vertebral. There was no difference between control and OVX animals, but our data compared well to the literature. Tb.Th was significantly higher in the mid-vertebral region compared to the cranial and caudal regions. There was no difference between control and OVX, but there was a trend towards reduced Tb.Th in the mid-vertebral region of the OVX compared to controls. Tb.Sp was significantly higher in the mid-vertebral region compared to cranial and caudal regions. There was no group variation between control and OVX animals, but there was a trend towards reduced Tb.Sp in the mid-vertebral region of the OVX group. Our results are compared to others found in the literature in Table 5.2.

Table 5.2: Trabecular parameters Tb.N, Tb.Th and Tb.Sp from our study and others from the literature. Data from the present study are averaged over the cranial, mid-vertebral and caudal regions.

Authors	Site	Tb.N (1/mm)		Tb.Th (mm)		Tb.Sp (mm)		Method
		CON	OVX	CON	OVX	CON	OVX	
<i>Present study</i>	L3	1.72±0.2	1.70±1.3	0.39±0.07	0.38±0.06	0.528±0.08	0.529±0.08	μCT-40
<i>Lill et al (2002)</i>	L4	1.9±0.1	-	0.11±0.03	-	0.395±0.02	-	μCT-20
<i>Schorlemmer et al(2003)</i>	L4	-	2.4±0.2	-	0.17±0.08	-	0.243±0.02	μ-scope
<i>Chavassieux et al (2001)*</i>	Iliac crest	1.40±0.1	1.20±0.1	0.092±0.1	0.09±1.2	0.626±33.3	0.759±50.6	histology
<i>Newton et al (2004)</i>	Iliac crest	2.02±0.1	2.05±0.1	0.135±0.01	0.128±0.01	0.364±0.01	0.370±0.02	histology

* In this experiment animals were sacrificed after 6 months.

The differences between the measured parameters in these studies may be attributable to different scanning techniques (such as using stereological models rather than direct method of calculation in evaluating scans). Differences may also be attributable to the resolution used during scanning, particularly in the case of the Tb.Th measurement. If we consider the case of a set of scans being carried out at a resolution of 40 μm. A vital step in the image

reconstruction process is the application of threshold values. This will dictate the number of voxels from the grayscale image which will become segmented into bone. The thresholding procedure can be somewhat subjective, and this can have important implications on outcome measurements. If the thickness of a given trabecular strut is 100 μ m, a difference of 2 voxels (which may occur by choosing different threshold values) could almost double the value of Tb.Th. However, if threshold values are kept constant during the analysis of a full set of samples, then intra-group comparisons can be made with confidence. Microarchitectural parameters from the lumbar region of sheep may also vary between studies due to the observation of regional differences within vertebrae that was made earlier in this study.

BV/TV was highest in the cranial region, then the mid-vertebral and finally the caudal region, however, differences between regions were not significant. The same trend was apparent when the control and OVX groups were considered separately. Again, a trend towards lower BV/TV in the OVX compared to the controls was apparent at each region. DA was significantly higher in the cranial compared to the mid-vertebral and caudal regions, and caudal was also significantly higher than mid-vertebral. There was no difference between control and OVX animals, however the difference in the caudal region was very close to significance ($p < 0.053$). Our results are compared to some others found in the literature in Table 5.3. The values for BV/TV reported by Lill et al (2002) are considerably lower than what we, and Schorlemmer et al (2003), observed. As before, different resolutions used during scanning may be the cause of these differences. It is also possible that the time of year that their biopsies were taken could influence BV/TV, due to

seasonal effects. It is well recognised that bone loss is greatest, in both sheep and humans, in the winter months.

Table 5.3: Trabecular parameters BV/TV and DA from our study and others from the literature. Data from the present study is averaged over the cranial, mid-vertebral and caudal regions.

Authors	Site	BV/TV (%)		DA (1)		Method
		CON	OVX	CON	OVX	
<i>Present study</i>	L3	45.7±0.9	44.1±1.4	2.16±0.09	2.22±0.08	μCT-40
<i>Lill et al (2002)</i>	L4	27.5±0.09	-	-	-	μCT-20
<i>Schorlemmer et al (2003)</i>	L4	-	40.7±4.4	-	-	μ-scope
<i>Newton et al (2004)</i>	Iliac crest	24.2±1.8	20.4±1.5	-	-	Histology

To our knowledge, this is the first time that these highly significant differences in trabecular microarchitecture in different anatomical locations of the lumbar vertebra have been reported. They show that while the transverse cross-sectional area remains roughly constant from the cranial to the caudal aspect of the vertebra, the mid-vertebral region is made up of fewer thicker trabeculae. The trabeculae towards both end-plates become less thick, but more numerous. This can be explained from a mechanics perspective because more trabeculae are required beneath the joint surfaces in order to dissipate the complex stresses which are imposed there. As the distance from the joint surface increases, load on the trabecular bone compartment decreases while load on the compact bone compartment increases. This agrees with other data in the literature, Eswaran et al (2007) used high-resolution μCT-based finite element models of 13 elderly human vertebrae to determine the role of the cortical shell versus the trabecular centrum in load bearing. They found that the mean maximum load fraction taken by the cortical shell was between 0.38 - 0.54 and always occurred at the narrowest section of the bone, which is in the mid-vertebral region.

Our results also show a regional difference in DA and BV/TV throughout the vertebra. It is known that bone grows in response to the loads applied to it. Gibson (1985) observed that the symmetry of trabecular bone structure depends on the direction of the applied loads. Also, the relative volume of bone in a particular location depends on the magnitude of the applied loads. Thus our results can be explained in terms of the loading on the vertebral bodies. If the loading is greatest in the cranial region, this would result in higher BV/TV, but also more complex stress patterns, which result in a highly asymmetric or anisotropic structure. These results have practical implications in terms of how vertebral bone is sampled and tested *in vitro* to predict whole vertebra behaviour. Samples of trabecular bone are often cored through the vertebral body, in the superior-inferior direction, to be analysed and tested in a variety of ways to predict the whole bone behaviour. For mechanical testing, it is often the case that the proximal and distal ends of the sample are embedded in some way leaving only the mid-section exposed for testing. Our results would suggest that the mid-section of the vertebra is the least appropriate region for testing because the load fraction taken by trabecular bone is lowest in that region. This may explain why that approach has not been highly successful at predicting biomechanically measured vertebral strength (Crawford et al, 2003).

The biomechanical testing procedure used in this study was designed to highlight the effects of increased bone turnover in the OVX group, on the mechanical behaviour of the samples. The average ultimate strength in the OVX group was reduced by approximately 8.25% compared to controls. This compares well to findings by Lill et al (2002) who found a reduction of 11.79 % in failure strength of OVX trabecular bone samples compared to

controls. In their study, testing was carried out on bone biopsies of approximately 10mm diameter and 10mm in height. The reduction in ultimate strength in the OVX group can be explained by the fact that the amount of load-bearing bone present is reduced as a result of the increased bone turnover.

The reduction in structural stiffness on the reload cycle was greater in the OVX group. Although the difference did not quite reach statistical significance there was a strong trend present. In a similar study, Kopperdahl et al (2000) investigated the response of human vertebrae under similar testing conditions to those used in this study. The average reduction in stiffness at strains up to 3-5% was 53.6%. This compares reasonably well to our data which showed stiffness reduction of 49.8 ± 21.79 and 60.4 ± 8.44 (%) in control and OVX, respectively. The larger reduction in stiffness in the OVX group over the two loading cycles can, again, be explained by the reduced amount of load-bearing bone present. The bone which is present takes on increased load in the first cycle and thus becomes more damaged, resulting in a reduced stiffness on the second cycle. This supports the concept from continuum damage mechanics whereby percentage reductions in stiffness can be interpreted as quantitative measures of mechanical damage (Krajcinovic and Lemaitre, 1987).

The residual strains which developed on unloading after the initial cycle were 16.13% lower in the OVX group compared to controls ($p=0.037$). The development of residual strains is indicative of plastic strain as opposed to percentage reductions in stiffness which are direct measures of effective mechanical damage. Our results indicate that after the initial loading cycle the control group experienced more permanent deformation than the

OVX group. This is consistent with the theory that increased remodelling in the OVX bone results in a more compliant structure which experiences less permanent deformation compared to controls under the same loads. This effect is also related to the fact that, in the initial loading cycle, both groups were loaded to the same strain level of 5%. This deformation is comprised of elastic and plastic strain, and also strain due to damage. So, logically if the OVX group experiences more damage, then more of the 5% strain will be due to damage, so less will be due to plastic strain.

Another mechanism by which a change in the mechanical behaviour of the vertebral structure could occur, is through the presence of stress concentrations. Increased remodelling in trabecular bone, as a result of estrogen withdrawal, leads to the presence of more sites of bone resorption. These sites of bone resorption remain temporarily unfilled, due to the delay between the initiation and completion of the bone formation process that is coupled with resorption. This creates stress concentrators that may predispose bone to microdamage formation, thus reducing the mechanical performance of the structure.

The findings from this study indicate that, following OVX, significant changes occur in trabecular and cortical bone turnover in sheep which have an effect on the biomechanical behaviour of the vertebral body. These changes happen despite the fact that there is no change in BMD or the amount of bone present. This also raises the question of whether the sheep has limited use in terms of its ability to serve as a viable model for osteoporosis. However, it can also be said that the sheep is one of the few models that exhibits sustained increases in bone turnover following OVX. Increased bone turnover is one of the major characteristics of osteoporosis and one of the least well understood. Therefore, at 12

months post-OVX, the sheep skeleton may not display advanced bone loss, however it does exhibit increased levels of bone turnover in cortical and trabecular compartments. This is an extremely important parameter which contributes to bone quality and one which is difficult to find in other animal models.

5.5 *Conclusions*

This study demonstrated that:

- 1) DEXA scanning revealed no difference in BMD at L3 between control and OVX groups 12 months post-OVX.
- 2) Histological analyses showed increased bone turnover in compact and trabecular tissue in the OVX group compared to controls at 6 months post-surgery.
- 3) Analyses of the microarchitecture of the vertebral bodies showed that Tb.N, Tb.Th, Tb.Sp, and DA varied between cranial, caudal and mid-vertebral regions, but BV/TV did not.
- 4) While the differences in trabecular parameters between control and OVX groups did not reach significance, trends toward reduced structural integrity were apparent in the OVX group.
- 5) Biomechanical testing revealed a reduced ultimate strength in the OVX group as well as a greater reduction in stiffness. A subtle yet significant reduction in the residual strain in the OVX group was also observed. These data show a significant change in the biomechanical behaviour of OVX bone compared to controls due to increased bone turnover. This effect was present despite the fact that no changes were found in BMD.

Chapter 6

Discussion

6.1	Bone quality and osteoporosis	156
6.2	Ovine animal model	157
6.3	Bone turnover and microarchitecture in compact bone	159
6.4	Fatigue properties and crack behaviour in compact bone	161
6.5	BMD, bone quality and bone strength in the vertebral body	164
6.6	Future work	169
6.7	Conclusions	173

6.1 Bone quality and osteoporosis

The importance of bone quality has become clear in recent years as a result of observations that the traditional way of measuring bone strength in a clinical setting, namely bone densitometry, does not always reliably predict fracture risk (Seeman and Delmas, 2006). This thesis describes a project which used an OVX sheep animal model to the effects of increased bone turnover on bone quality over a 12 month period. During that time, five different fluorochrome dyes were intravenously administered to all animals. Sites that were undergoing turnover within the bone at the time of injection were labelled with a characteristic colour. Following sacrifice, three separate studies were carried out which investigated different aspects of the relationship between bone turnover and other parameters of bone quality.

The unique feature of our OVX sheep model experiment, and the subsequent studies on bone samples from these animals, was the use of five fluorochrome dyes to label bone turnover at stages during the 12 months post-OVX. It has become clear that bone turnover is one of the most important parameters of bone quality, and this study provides extensive information relating to it. The rate of turnover in bone tissue effectively dictates the nature of the material within the structure i.e. high bone turnover results in a higher percentage of new undermineralised, and thus more ductile material compared with low turnover which results in older, and thus more brittle, bone. This raises the question as to whether bone which has experienced high turnover should then begin to display more ductile characteristics under load. However, this is not the case in practice as bone failure (fracture) is inherently brittle in nature. One explanation may be that the new bone, when it is first

laid down during periods of increased remodelling, is too weak to take any load at all, thus overloading the surrounding material, which would explain the brittle fracture. Another mechanism, which is related to the first, may be the role of resorption cavities as stress concentrators, particularly in trabecular bone. Biochemical bone markers are used clinically to measure the rate of bone turnover. In general, however, they are not often used for diagnosis of osteoporosis because levels overlap significantly between those who have the disease, and those who do not. The main clinical use of bone markers at present is to help chart patients' response to therapies; however the results of many large studies carried out have been inconsistent (Stokstad, 2005).

6.2 *Ovine animal model*

Sheep are a practical and economical model for age-related and post-menopausal bone loss and the size and anatomy of their skeleton is comparable to that of humans. The histological appearance and metabolism of ovine bone can also be compared with humans (Pastoureau et al, 1989; Turner and Villanueva, 1994). Other workers have shown that 3 months after OVX, bone-specific alkaline phosphatase, which is a biochemical indicator of bone formation, increases significantly compared with controls while BMD at the spine decreases at 4-6 months following OVX (Turner et al, 1995). The rate at which bone is lost in sheep post-OVX is also comparable to that of post-menopausal women (Lill et al, 2002).

Our experiment used 76 sheep in total, one half of the animals (Group 1) were sacrificed 12 months post-OVX and the remainder (Group 2) after 30 months. Four animals from this group died during the first 12 months of this project; however none of the deaths were

related to our intervention. Analyses on Group 2 are underway in a related study (Brennan et al, 2007) but there was a substantially higher mortality rate in that group, which justifies our decision to increase the calculated sample size as discussed in Chapter 2. The intravenous administration of the 5 fluorochrome dyes in this study proved to be very successful. The analyses of hormonal profiles which were carried out in this study showed a highly significant reduction in the levels of estradiol and progesterone in OVX animals compared with controls. Some other studies have found contradictory data; Sigrist et al (2007) measured estradiol levels in control and OVX sheep monthly up to 12 months post-surgery. They found that there was a clear decline following OVX but the levels had returned to normal 6 months post-OVX, suggesting that the effect of OVX on sheep metabolism is reversible. There are much conflicting data in the literature on this topic, partly because there are many variables to be considered such as breed, weight, time of year, estrous cycles, diet, exercise and environmental conditions. However, our study has shown that, even with mixed breeds of animals, the OVX sheep is a good model for investigating the effect of increased bone turnover on bone quality.

6.3 *Bone turnover and microarchitecture in compact bone*

One feature which is often overlooked in the diagnosis of bone diseases and fracture risk assessment is the contribution of compact bone quantity and quality. Biomechanical studies in the past have clearly demonstrated that the structural behaviour of whole bone specimens is highly determined by the contribution of compact bone (Augat and Schorlemmer, 2006). Also, it has been shown that trabecular at certain sites bone is lost more rapidly than cortical bone following estrogen depletion (Khastgir et al, 2001). It follows then, that the remaining cortical tissue in ageing bone becomes even more important as its load bearing role increases. Generally, women lose 20% of peak compact bone mass and 40-50% of trabecular mass by 90 years of age (Melton et al, 1988).

Chapter 3 of this thesis describes an experiment which was designed to investigate bone turnover and microarchitecture in control and OVX compact bone samples. The number of labelled osteons was measured at five time-points to calculate the level of bone turnover. These data showed an OVX effect taking place at 3 months post-OVX and continuing on to significance at 6, 9 and 12 months. These results illustrated a seasonal effect on bone turnover, while still demonstrating the effect of reduced circulating hormones due to OVX.

Substantial changes in bone turnover were observed in the OVX group compared to the control. We hypothesised that the increase in turnover would result in higher porosity within the bone cortices due to the presence of more Haversian canals and resorption cavities. To investigate this, microarchitecture was measured using μ CT scanning techniques. There was a 2-fold increase in the mean porosity of the OVX group compared

with the controls. This resulted in a significant decrease in Young's modulus, and a slight reduction in compressive strength and work to fracture in the OVX group. The reduction in biomechanical properties was due to two main factors. Firstly, increased intracortical remodelling creates a larger amount of recently formed, undermineralised bone which bears relatively little, if any, load compared with the surrounding tissue. Secondly, and in a more obvious way, increased porosity will also result in a reduced area available to bear the load.

Another potential source of reduction in bone strength is the accumulation of *in vivo* microdamage. Although a full microdamage analysis was not carried out in this study, a full quantitative analysis was carried out in a related study (Brennan et al, 2006) on the metacarpal bones from the same animals, in which very little microdamage was found in either the control or OVX group. This may be because the OVX group, which has increased porosity and would thus be more susceptible to microdamage, conversely has the microdamage removed by the increased bone turnover. Regardless of the mechanism it can be said that there was no significant difference in microdamage levels between groups *in vivo*, and therefore there was no effect on bone strength due to it. Our data showed that compact bone turnover and porosity are significantly increased in OVX animals. This study gives us new insights into the behaviour of some of the parameters which affect compact bone quality. Using this information it may be possible to detect the onset of osteoporosis before significant changes in BMD occur and before fracture risk is increased.

6.4 *Fatigue properties and crack behaviour in compact bone*

In the last decade, it has been shown comprehensively that bone fragility increases with age. Courtney et al (1996) carried out a study of bone samples from a population of elderly adults and from a population of younger adults. This study revealed two major findings. Firstly, the *in vivo* microcrack density was significantly higher in the older bone than in the younger, which one might expect. The second finding was that, when a sub-population of both groups was subjected to *in vitro* fatigue loading, the older bone developed more cracks, again as expected, but the younger bone did not. This indicates that there is inherent fragility of bone as it ages although the precise reason for this is not known.

Zioupos et al (1999) carried out a study on aged human bone and found increasing crack densities and crack lengths with increasing age. These are two standard measures of the microcrack burden of a sample. It was noted recently by Burr (2005) that in many microdamage studies of older Vs younger bone where mean crack length is measured, this parameter does not change between groups. However, the number of longer cracks has been found to increase in older bone. Thus, valuable information may become lost by averaging out crack lengths. Considering frequency distributions may help to address this issue because it is the behaviour of longer cracks which will dictate the ultimate failure of the bone.

Nalla et al (2005) carried out a series of studies on the toughness characteristics of human bone. They found that the toughness for the initiation of cracks declines with age by approximately 40% between the ages of 40-100 years. More importantly however, the

toughness for the propagation of cracks declines even more substantially. Arguably, propagation of cracks in bone is the more important phenomenon because many cracks can be initiated in bone but if they do not grow to a critical size then they will not necessarily have a detrimental effect on the structure. However, a single crack that is allowed to grow to a critical size might result in total failure of the bone. This once again illustrates the similarity between bone and a typical composite material found in the world of engineering which are often designed not to prevent the initiation of cracks but to prevent their propagation.

Chapter 4 in this thesis describes a study which was designed to investigate the accumulation and propagation of microcracks during fatigue testing. In particular the way microcracks behave in relation to newly formed osteons which had been labelled using fluorochrome dyes was assessed. It is known that crack behaviour depends on crack length because this dictates the amount of energy it has. In our study, we observed that cracks of the same length behaved differently on meeting an old osteon compared to a newer (labelled) osteon, indicating the importance of osteonal tissue properties in terms of microcrack propagation. This means that higher bone turnover, which would result in more new osteons, has a direct effect on microcrack behaviour in compact bone. Recently formed osteons were identifiable in our study by the presence of fluorochrome labels within them. They were observed to behave much like pores in the material by attracting propagating cracks towards them and then blunting the crack tip at the point of impingement. One theory as to why osteons tend to arrest microcracks is that when the crack tip reaches the cement-line, which normally has a relatively low mineralisation level, it loses energy and becomes trapped. The mechanical properties of the cement-line are

traditionally very difficult to measure, and thus it is difficult to prove this theory. Our study supports the idea that properties of the osteon itself, as well as its cement-line, dictates its crack-arresting properties. One of the primary factors which defines the properties of an osteon is age and the level of mineralisation.

Burr (2005) posed the question ‘is the increasing fragility of bone tissue with age, which we know occurs, due to accumulated microdamage or of other changes to the matrix properties such as mineralisation?’ In studies on bone samples from dogs, which had been treated with bisphosphonates, they found that toughness in the treated group was reduced by approximately 20% after 12 months. When they correlated these data with microdamage accumulation they found no relationship between the two. They also found a small 2-3% increase in the tissue mineralisation in the treated group. In order to assess the contribution of this mineralisation increase to toughness, they used a relationship which was originally described by Currey et al (1996) which related mineralisation, as measured by ash content, to toughness. Using that equation, they predicted that a 2-3% increase in mineralisation would result in approximately a 20% reduction in toughness, which compared very well with their experimental observations. These findings suggest that changes in bone tissue properties with age or therapies have more to do with matrix mineralisation and collagen, than with microdamage *per se*. It also suggests that microdamage is not the cause of fragility but a consequence of altered bone matrix properties.

6.5 *BMD, bone quality and bone strength in the vertebral body*

Vertebral fractures due to osteoporosis commonly occur under non-traumatic loading conditions. This problem affects more than 1 in 3 women and 1 in 10 men over a lifetime (Kanis, 2000). As discussed in previous chapters, the measurement of BMD does not fully account for the influence of changes in bone quality, such as microarchitecture and tissue properties, on the strength of the vertebra. Studies have shown that deterioration of the vertebral trabecular architecture results in a more anisotropic structure which has a greater susceptibility to fracture. Transverse trabeculae are preferentially thinned and perforated while the remaining vertical trabeculae maintain their thickness (Parfitt et al, 2002). Such a structure is likely to be more susceptible to buckling under normal compressive loads and has a decreased ability to withstand unusual or off-axis loads. Very few studies have addressed the issue of the effect of bone turnover on strength in a whole vertebral body. While some studies have accounted for systemic bone turnover by measuring biochemical bone markers (Stokstad, 2005), to our knowledge none have specifically measured local bone turnover in a whole bone and then assessed its biomechanical properties.

Chapter 5 in this thesis describes a study which was designed to investigate the effect of bone quality in the L3 vertebra in control and OVX sheep. Bone quality of the structure was assessed by measuring bone turnover and microarchitecture using epifluorescence microscopy and microCT techniques respectively, in both cortical and trabecular tissue. The vertebral body was then subjected to a mechanical testing protocol which was designed to identify changes in its mechanical behaviour as a result of altered bone quality.

BMD data from the DEXA scans carried out in this study revealed a non-significant downward trend in the OVX group compared to the controls. Strictly speaking, these data should be called areal BMD values because DEXA scanning measures the amount of mineral per area. This is a 2D measurement of a 3D phenomenon and thus we would not expect to obtain completely accurate diagnostic or predictive answers from this method, however this remains the gold standard in osteoporosis diagnosis. Other workers have suggested that fracture risk variation between individuals may lie in the more subtle sub-regional density differences within the vertebral body. These sub-regional differences are hidden when the whole vertebral body BMD is measured (Legrand et al, 2000).

The number of labelled sites of bone turnover in the L3 vertebra was higher in the OVX group compared to the controls in both compact and trabecular bone tissue. It had been established in the study described in Chapter 3 that bone turnover was highest 6 months post-OVX and that there was an inter-group difference at that time-point. For this reason, this time-point was chosen to evaluate bone turnover in the L3 vertebra. Interestingly, bone turnover was similar in cortical and trabecular tissue. The commonly held belief is that trabecular bone is always more metabolically active than cortical tissue and thus bone turnover is always higher there. A major contributory factor to this belief is that iliac bone biopsy is the primary source for the study of human bone turnover. What is not always recognised is that the ilium is often selected as a biopsy site due to its surgical accessibility, not because it is representative of the entire skeleton (Parfitt, 2002). Other studies have shown that in the beagle dog, trabecular bone turnover throughout the skeleton can vary from 50% higher to 80% lower than in the ilium (Kimmel and Jee, 1982).

Trabecular bone microarchitecture was assessed in this study using μ CT scanning techniques. In terms of the standard microarchitectural parameters, there were very few statistical differences between the control and OVX groups. This may be because scan resolution was relatively low in order to accommodate a large sample like a whole vertebra. However, substantial differences between parameters were observed at different sites within the vertebra. Each bone was divided into a cranial, mid-vertebral and caudal region. Striking differences were observed in some of the measured architectural parameters, particularly trabecular number, thickness and spacing. Trabecular number was higher in the cranial and caudal regions and trabecular thickness was higher in the mid-vertebral region.

This is intuitively correct as the loading at the joint surfaces create complex stress patterns that need to be dissipated efficiently away from the end-plates and out to the surrounding cortical shell. It has been shown that during uniaxial loading, the cortical shell takes the maximum load fraction at the mid-vertebral region (Eswaran et al, 2007). This also agrees with the theory that in areas of complex stress patterns, bone will form in an asymmetric fashion in order to bear those loads most efficiently (Gibson, 1985). This finding has implications in the mechanical testing of standard trabecular samples (such as cylindrical cores) which are often taken from the central part of vertebrae and analysed in order to predict whole bone behaviour. This technique assumes homogeneity of microarchitectural parameters throughout the sample, which as our results show, may not be justified.

The biomechanical consequences of increased remodelling were investigated. Ultimate strength, proof stress, reduction in stiffness and residual strain were quantified after specimens were loaded to a point beyond yield, unloaded briefly, and then reloaded again to approximately 10% strain. OVX bone displayed a reduced ultimate strength, an increased reduction in stiffness and a reduced level of residual strain. Reduction in stiffness is a direct measure of effective mechanical damage, whereas the development of residual strain is indicative of permanent deformations. Our findings can be explained as follows: both groups were loaded to 5% strain, which is made up of elastic, plastic and damage related strains. If the OVX group experienced more damage during initial loading than the controls, and this can be justified by the increased bone turnover and facilitated by the stress concentrating effect of resorption cavities, then it would be expected that the reduction in stiffness would also be greater in that group. So, if more of the 5% strain can be attributed to damage in the OVX group then, logically, less must be attributable to plastic strain. This idea is reinforced by our findings that permanent deformation after the initial cycle was less in the OVX group. This study demonstrates the significant effect of increased remodelling on the biomechanical behaviour of the L3 lumbar vertebra despite the fact that no difference was detected in BMD values. This further supports the hypothesis, which is held by many authors, that more consideration must be given to bone quality to predict bone strength and fracture risk, as BMD determined by DEXA cannot measure all of the relevant parameters.

In conclusion, when taken together, the results from the individual studies in this thesis have provided comprehensive quantitative evidence that changes in bone quality due to increased remodelling effect the mechanical behaviour of bone at various structural levels. Furthermore, our data also supports the idea that 2D bone densitometry provides little information about two important properties that influence bone strength: its material composition and its structural design. In the future, the development of clinical tools which can assess bone quality independent of BMD will be essential in advancing the diagnosis and treatment of osteoporosis.

6.6 *Future work*

The experiment which was designed and implemented as part of this thesis developed an ovine model for post-menopausal osteoporosis, which included the capacity to directly measure bone turnover. Another benefit of this project is that two separate groups of animals were used, Group 1 being sacrificed after 12 months and Group 2 after 30 months, allowing studies to be carried out at different stages in disease progression. A sub-group was also created from the OVX animals within Group 2, these animals received a supra-clinical dose of a bisphosphonate called zoledronic acid. This will also allow us to study the effects of zoledronic acid, a potent and widely used bisphosphonate, on bone tissue over time. Continued work on this project will greatly expand our knowledge of osteoporosis and the real effects of commonly used treatments, such as bisphosphonates, on bone quality.

This study showed that OVX resulted in increased bone turnover in sheep which, in turn, contributed to increased intracortical porosity. The precise effect of having bone at different stages of mineralisation within the cortex could be further developed by assessing precisely how its mechanical properties change with time. This could be achieved by utilising the fluorochrome dyes, which were used in this study to label bone turnover, along with testing procedures such as nanoindentation or scanning acoustic microscopy to measure material properties. Clinically, bone turnover is assessed using biochemical bone markers of resorption and formation; these are normally serum based, and thus give an assessment of predominantly cortical bone, which constitutes about 80% of the skeleton. This technique often produces considerable variation within and between individuals. Bone turnover can

also be assessed by histomorphometric assessment using fluorochrome labelling prior to biopsy. However, as discussed in previous chapters, this may not reflect turnover at all other sites. In order to reconcile these measurement methods, development of other techniques will be required. Two examples of potentially useful techniques like this are: F-fluoride positron emission computed tomography and single photon emission computed tomography using technetium labelled bisphosphonates (Compston, 2006). These may provide new approaches to the assessment of regional bone turnover at sites of clinical relevance.

This study provided new insights into the behaviour of microcracks during propagation, particularly in relation to secondary osteons. Microcrack propagation is an important phenomenon, possibly more so than microcrack accumulation because a lot of accumulation, without propagation, is not necessarily detrimental to a material whereas just one critical length crack is needed to cause failure. We observed that new osteons behaved much like holes in the material insofar as they tended to attract propagating cracks and then blunt them at the point of impingement. It would be of great interest to test osteons of different ages, using the fluorochrome dyes in this study, to assess how osteonal tissue properties change with age. At present, assessment of microdamage can only be made by histological techniques. However, in the future, clinical assessment of microdamage may be possible by using specifically designed agents which have iodine atoms in their molecular structures. These agents chemically bind to calcium on the walls of microcracks, and can be detected radiologically using μ CT. Then, for example, a μ CT scan could quantify microdamage and BMD and combine these indices to give a better prediction of which osteoporosis patients are most at risk of fracture and their treatment could be tailored

accordingly. It is hoped that radiological detection of microdamage will aid fracture prediction and prevention.

This study found that DEXA did not detect changes in BMD in L3 vertebrae 12 months post-OVX. Bone turnover was increased, and microarchitectural changes slightly altered in the OVX group. Biomechanical assessment of these bones showed that increased turnover reduced the yield strength of the bone as well as the residual strain, after one loading cycle, to a point past yield. Further mechanical characterisation of the behaviour of vertebral bodies with high bone turnover would increase our understanding of what the role of new bone, compared to older bone, actually is in terms of load bearing. It would also be interesting to examine the relationship between stress concentrators (resorption sites) and damage initiation during fatigue testing. Alterations in bone microarchitecture make an important contribution to bone strength that is not captured by BMD measurements. In trabecular bone the number, size and shape of trabeculae and their connectivity and orientation (anisotropy) contribute to bone strength while in compact bone, cortical width, porosity and gross bone size and shape are the main determinants. More sophisticated methods are being developed to allow accurate 3D assessment of these parameters. These include high-resolution magnetic resonance imaging (HR-MRI), high-resolution peripheral quantitative computed tomography (HR-pQCT) and synchrotron radiation μ CT. All of these are currently research tools and, *in vivo*, can only be applied to the peripheral skeleton although technological advances may eventually lead to their use in the central skeleton.

In conclusion, this study has illustrated the importance of the relationship between bone turnover and bone quality. To put this into practice and reduce the incidence of osteoporotic fractures will require further improvements in the diagnosis and treatment of the disease

based on a deeper understanding of bone strength and bone quality. Some other factors associated with bone quality which were not considered in this study are nanoscale tissue structure and properties, microporosity, mineralisation profile, collagen status and the chemical composition of the extracellular matrix. These components can be influenced, at some level, by genetic modulation and regulation. For this reason gene therapies, such as gene transfer, offer attractive technology for osteoporosis treatment. Ideally, it would be beneficial to combine all of these factors in one predictive equation to enable the calculation of fracture risk. However, because this is unlikely in the short term, the research community must continue to expand our understanding of these factors and how they relate to fracture risk.

6.7 *Conclusions*

- (1) Compact bone turnover and microarchitecture, two important parameters in bone quality, were altered in OVX bone compared to controls 12 months post-OVX. The small reduction in strength which was observed in the OVX group compared well to our calculations, which were based on the amount of reduced load bearing area. This illustrated important changes in compact bone quality due to increased remodelling.
- (2) Fatigue life was reduced in the OVX group compared to controls. Our data for N_f , bending modulus and bulk crack properties (Cr.Dn, Cr.S.Dn) compared well to the literature. Long cracks ($>300\mu\text{m}$) tended to deflect around older osteons and stop at new osteons indicating that new osteons behave like a hole in the material. This provides novel information regarding the interaction between microdamage and bone microstructure in areas of high turnover.
- (3) Increased turnover was found throughout the L3 vertebrae in the OVX group compared with the controls. This altered the biomechanical behaviour of the vertebral body under load, particularly in terms of yield stress, reduction in stiffness and residual strain. μCT analysis of the L3 vertebra also showed that microarchitectural parameters vary according to site within the bone. These changes were found despite the fact that no difference in BMD was detected.
- (4) When taken together, the results from the individual studies in this thesis have provided comprehensive quantitative evidence that changes in bone quality due to increased remodelling affect the mechanical behaviour of bone at various structural levels.

REFERENCES

- Akkus, O. and Rimnac, C. M. (2001) Cortical bone tissue resists fatigue fracture by deceleration and arrest of microcrack growth. *J Biomech* **34**(6): 757-64.
- An Y, H. and Draughn R, A. (2000). *Mechanical Testing of Bone and the Bone-Implant Interface*, CRC Press.
- Ashizawa, N., Nonaka, K., Michikami, S., Mizuki, T., Amagai, H., Tokuyama, K. and Suzuki, M. (1999) Tomographical description of tennis-loaded radius: reciprocal relation between bone size and volumetric BMD. *J Appl Physiol* **86**(4): 1347-51.
- Augat, P. and Schorlemmer, S. (2006) The role of cortical bone and its microstructure in bone strength. *Age Ageing* **35 Suppl 2**: ii27-ii31.
- Augat, P., Schorlemmer, S., Gohl, C., Iwabu, S., Ignatius, A. and Claes, L. (2003) Glucocorticoid-treated sheep as a model for osteopenic trabecular bone in biomaterials research. *J Biomed Mater Res A* **66**(3): 457-62.
- Bagi, C. M., Hanson, N., Andresen, C., Pero, R., Lariviere, R., Turner, C. H. and Laib, A. (2006) The use of micro-CT to evaluate cortical bone geometry and strength in nude rats: correlation with mechanical testing, pQCT and DXA. *Bone* **38**(1): 136-44.
- Bauss, F., Wagner, M. and Hothorn, L. H. (2002) Total administered dose of ibandronate determines its effects on bone mass and architecture in ovariectomized aged rats. *J Rheumatol* **29**(5): 990-8.
- Bell, G.H. (1956) Bone as a mechanical engineering problem. *The Biochemistry and Physiology of Bone*. Bourne, G.H., Ed., Academic Press, New York, 27.
- Bell, K. L., Loveridge, N., Jordan, G. R., Power, J., Constant, C. R. and Reeve, J. (2000) A novel mechanism for induction of increased cortical porosity in cases of intracapsular hip fracture. *Bone* **27**(2): 297-304.
- Bentolila, V., Boyce, T. M., Fyhrie, D. P., Drumb, R., Skerry, T. M. and Schaffler, M. B. (1998) Intracortical remodeling in adult rat long bones after fatigue loading. *Bone* **23**(3): 275-81.

Borah, B., Dufresne, T. E., Chmielewski, P. A., Gross, G. J., Prenger, M. C. and Phipps, R. J. (2002) Risedronate preserves trabecular architecture and increases bone strength in vertebra of ovariectomized minipigs as measured by three-dimensional microcomputed tomography. *J Bone Miner Res* **17**(7): 1139-47.

Bouxsein, M. L. (2003) Bone quality: where do we go from here? *Osteoporos Int* **14 Suppl 5**: 118-27.

Boyce, R. W., Franks, A. F., Jankowsky, M. L., Orcutt, C. M., Piacquadio, A. M., White, J. M. and Bevan, J. A. (1990) Sequential histomorphometric changes in cancellous bone from ovariectomized dogs. *J Bone Miner Res* **5**(9): 947-53.

Boyce, R. W., Paddock, C. L., Gleason, J. R., Sletsema, W. K. and Eriksen, E. F. (1995) The Effects Of Risedronate On Canine Cancellous Bone Remodeling - Three-Dimensional Kinetic Reconstruction Of the Remodeling Site. *J Bone Miner Res* **10**(2): 211-221.

Boyce, T. M., Fyhrie, D. P., Glotkowski, M. C., Radin, E. L. and Schaffler, M. B. (1998) Damage type and strain mode associations in human compact bone bending fatigue. *J Orthop Res* **16**(3): 322-9.

Brennan, O., Kennedy, O. D., Mahony, N. J., Lee, T. C., Rackard, S. M. and O'Brien, F. J. (2006). BMD measurements do not adequately assess the onset of osteoporosis. *52nd meeting of the Orthopedic Research Society, Chicago, Illinois, USA.* **31** (1795).

Briggs, A. M., Greig, A. M., Wark, J. D., Fazzalari, N. L. and Bennell, K. L. (2004) A review of anatomical and mechanical factors affecting vertebral body integrity. *Int J Med Sci* **1**(3): 170-180.

Burr, D. B. (1997) Bone, exercise, and stress fractures. *Exerc Sport Sci Rev* **25**: 171-94.

Burr, D. B. (2004) Bone quality: understanding what matters. *J Musculoskelet Neuronal Interact* **4**(2): 184-6.

Burr, D. B. (2005). The effects of microdamage on bone strength. *ASBMR Meeting. Bone Quality: What is it, and can we measure it?* Bethesda, Maryland, USA.

- Burr, D. B., Forwood, M. R., Fyhrie, D. P., Martin, R. B., Schaffler, M. B. and Turner, C. H. (1997) Bone microdamage and skeletal fragility in osteoporotic and stress fractures. *J Bone Miner Res* **12**(1): 6-15.
- Burr, D. B., Hirano, T., Turner, C. H., Hotchkiss, C., Brommage, R. and Hock, J. M. (2001) Intermittently administered human parathyroid hormone(1-34) treatment increases intracortical bone turnover and porosity without reducing bone strength in the humerus of ovariectomized cynomolgus monkeys. *J Bone Miner Res* **16**(1): 157-65.
- Burr, D. B. and Hooser, M. (1995) Alterations to the en bloc basic fuchsin staining protocol for the demonstration of microdamage produced in vivo. *Bone* **17**(4): 431-3.
- Burr, D. B. and Stafford, T. (1990) Validity of the bulk-staining technique to separate artifactual from in vivo bone microdamage. *Clin Orthop Rel Res* **260**: 305-8.
- Burstein, A. H., Reilly, D. T. and Martens, M. (1976) Aging of bone tissue: mechanical properties. *J Bone Joint Surg* **58**(1): 82-6.
- Carter, D. R. and Beaupre, G. S. (2001). *Skeletal Form and Function. Mechanobiology of Skeletal Development, Aging and Regeneration.*, Cambridge University Press.
- Carter, D. R., Caler, W. E., Spengler, D. M. and Frankel, V. H. (1981) Fatigue behavior of adult cortical bone: the influence of mean strain and strain range. *Acta Ortho Scan* **52**(5): 481-90.
- Carter, D. R. and Hayes, W. C. (1977) Compact bone fatigue damage II: a microscopic examination. *Clin Orthop Rel Res* **1977**(127): 265-74.
- Carter, D. R., Hayes, W. C. and Schurman, D. J. (1976) Fatigue life of compact bone-- II. Effects of microstructure and density. *J Biomech* **9**(4): 211-8.
- Cefalu, C. A. (2004) Is bone mineral density predictive of fracture risk reduction? *Curr Med Res Opin* **20**(3): 341-9.
- Cerroni, A. M., Tomlinson, G. A., Turnquist, J. E. and Grynepas, M. D. (2003) Effect of parity on bone mineral density in female rhesus macaques from Cayo Santiago. *Am J Phys Anthropol* **121**(3): 252-69.

Chavassieux, P. (1990) Bone effects of fluoride in animal models in vivo. A review and a recent study. *J Bone Miner Res* **5 Suppl 1**: S95-9.

Chavassieux, P., Garnero, P., Duboeuf, F., Vergnaud, P., Brunner-Ferber, F., Delmas, P. D. and Meunier, P. J. (2001) Effects of a new selective estrogen receptor modulator (MDL 103,323) on cancellous and cortical bone in ovariectomized ewes: a biochemical, histomorphometric, and densitometric study. *J Bone Miner Res* **16**(1): 89-96.

Chavassieux, P., Pastoureau, P., Boivin, G., Delmas, P. D., Chapuy, M. C. and Meunier, P. J. (1991) Effects of ossein-hydroxyapatite compound on ewe bone remodeling: biochemical and histomorphometric study. *Clin Rheumatol* **10**(3): 269-73.

Cheng, X. G., Nicholson, P. H., Boonen, S., Lowet, G., Brys, P., Aerssens, J., Van der Perre, G. and Dequeker, J. (1997) Prediction of vertebral strength in vitro by spinal bone densitometry and calcaneal ultrasound. *J Bone Miner Res* **12**(10): 1721-8.

Choi, K. and Goldstein, S. A. (1992) A comparison of the fatigue behavior of human trabecular and cortical bone tissue. *J Biomech* **25**(12): 1371-1381.

Cody, D. D., Goldstein, S. A., Flynn, M. J. and Brown, E. B. (1991) Correlations between vertebral regional bone mineral density (rBMD) and whole bone fracture load. *Spine* **16**(2): 146-154.

Cohen, J. and Harris, W. H. (1958) The three-dimensional anatomy of haversian systems. *J Bone Joint Surg Am* **40-A**(2): 419-34.

Compston, J. (2006) Bone quality: what is it and how is it measured? *Arq Bras Endocrinol Metabol* **50**(4): 579-85.

Compston, J. E. (2004) The risks and benefits of HRT. *J Musculoskelet Neuronal Interact* **4**(2): 187-90.

Cooper, C., Atkinson, E. J., O'Fallon, W. M. and Melton, L. J., 3rd (1992) Incidence of clinically diagnosed vertebral fractures: a population-based study in Rochester, Minnesota, 1985-1989. *J Bone Miner Res* **7**(2): 221-7.

- Courtney, A. C., Hayes, W. C. and Gibson, L. J. (1996) Age-related differences in post-yield damage in human cortical bone. Experiment and model. *J Biomech* **29**(11): 1463-71.
- Cowin, S. C. (1995) On the minimization and maximization of the strain energy density in cortical bone tissue. *J Biomech* **28**(4): 445-7.
- Crawford, R. P., Cann, C. E. and Keaveny, T. M. (2003) Finite element models predict in vitro vertebral body compressive strength better than quantitative computed tomography. *Bone* **33**(4): 744-50.
- Cummings, S. R., Black, D. M., Nevitt, M. C., Browner, W. S., Cauley, J. A., Genant, H. K., Mascioli, S. R., Scott, J. C., Seeley, D. G., Steiger, P. and et al. (1990) Appendicular bone density and age predict hip fracture in women. The Study of Osteoporotic Fractures Research Group. *JAMA* **263**(5): 665-8.
- Cummings, S. R., Nevitt, M. C., Browner, W. S., Stone, K., Fox, K. M., Ensrud, K. E., Cauley, J., Black, D. and Vogt, T. M. (1995) Risk factors for hip fracture in white women. Study of Osteoporotic Fractures Research Group. *N Engl J Med* **332**(12): 767-73.
- Currey, J. D. (1988) The effect of porosity and mineral content on the Young's modulus of elasticity of compact bone. *J Biomech* **21**(2): 131-9.
- Currey, J. D. (2004). The state of art of knowledge of bone mechanics, and our main areas of ignorance. *14th Meeting of the European Society of Biomechanics. 's-Hertogenbosch, The Netherlands*.
- Currey, J. D., Brear, K. and Zioupos, P. (1996) The effects of ageing and changes in mineral content in degrading the toughness of human femora. *J Biomech* **29**(2): 257-60.
- Dai, R. C., Liao, E. Y., Yang, C., Wu, X. P. and Jiang, Y. (2004) Microcracks: an alternative index for evaluating bone biomechanical quality. *J Bone Miner Metab* **22**(3): 215-23.
- Davidson, M. K., Lindsey, J. R. and Davis, J. K. (1987) Requirements and selection of an animal model. *Isr J Med Sci* **23**(6): 551-5.

- Delmas, P. D. (2000) Markers of bone turnover for monitoring treatment of osteoporosis with antiresorptive drugs. *Osteoporos Int* **11 Suppl 6**: S66-76.
- Delmas, P. D., Confavreux, E., Garnero, P., Fardellone, P., de Vernejoul, M. C., Cormier, C. and Arce, J. C. (2000) A combination of low doses of 17 beta-estradiol and norethisterone acetate prevents bone loss and normalizes bone turnover in postmenopausal women. *Osteoporos Int* **11**(2): 177-87.
- Diab, T., Condon, K. W., Burr, D. B. and Vashishth, D. (2006) Age-related change in the damage morphology of human cortical bone and its role in bone fragility. *Bone* **38**(3): 427-31.
- Diab, T. and Vashishth, D. (2005) Effects of damage morphology on cortical bone fragility. *Bone* **37**(1): 96-102.
- Donahue, S. W., Sharkey, N. A., Modanlou, K. A., Sequeira, L. N. and Martin, R. B. (2000) Bone strain and microcracks at stress fracture sites in human metatarsals. *Bone* **27**(6): 827-33.
- Duboeuf, F., Jergas, M., Schott, A. M., Wu, C. Y., Gluer, C. C. and Genant, H. K. (1995) A comparison of bone densitometry measurements of the central skeleton in post-menopausal women with and without vertebral fracture. *Br J Radiol* **68**(811): 747-53.
- Ebihara, H., Ito, M., Abumi, K., Taneichi, H., Kotani, Y., Minami, A. and Kaneda, K. (2004) A biomechanical analysis of metastatic vertebral collapse of the thoracic spine: a sheep model study. *Spine* **29**(9): 994-9.
- Eriksen, E. F., Axelrod, D. W. and Melsen, F. (1994). *Bone Histomorphometry*. New York, Raven Press.
- Eswaran, S. K., Bayraktar, H. H., Adams, M. F., Gupta, A., Hoffmann, P. F., Lee, D. C., Papadopoulos, P. and Keaveny, T. M. (2007) The micromechanics of cortical shell removal in the human vertebral body. *Comp Meth App Mech Eng* **In submission**.
- Eswaran, S. K., Gupta, A., Adams, M. F. and Keaveny, T. M. (2006) Cortical and trabecular load sharing in the human vertebral body. *J Bone Miner Res* **21**(2): 307-14.

- Fleisch, H. (1991) Bisphosphonates. Pharmacology and use in the treatment of tumour-induced hypercalcaemic and metastatic bone disease. *Drugs* **42**(6): 919-44.
- Follet, H., Boivin, G., Rumelhart, C. and Meunier, P. J. (2004) The degree of mineralization is a determinant of bone strength: a study on human calcanei. *Bone* **34**(5): 783-9.
- Forwood, M. R., Burr, D. B., Takano, Y., Eastman, D. F., Smith, P. N. and Schwardt, J. D. (1995) Risedronate treatment does not increase microdamage in the canine femoral neck. *Bone* **16**(6): 643-50.
- Forwood, M. R. and Parker, A. W. (1989) Microdamage in response to repetitive torsional loading in the rat tibia. *Calcif Tissue Int* **45**(1): 47-53.
- Frost, H. M. (1958) Preparation of thin undecalcified bone sections by rapid manual method. *Stain Technol* **33**(6): 273-7.
- Frost, H. M. (1960) Presence of microscopic cracks in vivo in bone. *Bull Henry Ford Hospital* **8**: 27-35.
- Frost, H. M. (1969) Tetracycline-based histological analysis of bone remodeling. *Calcif Tissue Res* **3**(3): 211-37.
- Frost, H. M. (1973) Metabolism of bone. *N Engl J Med* **289**(16): 864-5.
- Frost, H. M. (1991) A new direction for osteoporosis research: a review and proposal. *Bone* **12**(6): 429-37.
- Frost, H. M. (1992) Perspectives: bone's mechanical usage windows. *Bone Mineral* **19**(3): 257-71.
- Garnero, P., Jamin, C., Benhamou, C. L., Pelissier, C. and Roux, C. (2002) Effects of tibolone and combined 17beta-estradiol and norethisterone acetate on serum C-reactive protein in healthy post-menopausal women: a randomized trial. *Hum Reprod* **17**(10): 2748-53.
- Geusens, P., Nijs, J., Van der Perre, G., Van Audekercke, R., Lowet, G., Goovaerts, S., Barbier, A., Lacheretz, F., Remandet, B., Jiang, Y. and et al. (1992) Longitudinal effect

of tiludronate on bone mineral density, resonant frequency, and strength in monkeys. *J Bone Miner Res* **7**(6): 599-609.

Gibson, L. J. (1985) The mechanical behavior of cancellous bone. *J Biomech* **18**(5): 317-328.

Goldstein, S. A. (1987) The mechanical properties of trabecular bone: dependence on anatomic location and function. *J Biomech* **20**(11/12): 1055-1061.

Goodman, R. L., Gibson, M., Skinner, D. C. and Lehman, M. N. (2002) Neuroendocrine control of pulsatile GnRH secretion during the ovarian cycle: evidence from the ewe. *Reprod Suppl* **59**: 41-56.

Goodship, A. E., Lanyon, L. E. and McFie, H. (1979) Functional adaptation of bone to increased stress. An experimental study. *J Bone Joint Surg Am* **61**(4): 539-46.

Goulet, R. W., Goldstein, S. A., Ciarelli, M. J., Kuhn, J. L., Brown, M. B. and Feldkamp, L. A. (1994) The relationship between the structural and orthogonal compressive properties of trabecular bone. *J Biomech* **27**(4): 375-389.

Green, J. R. (2002) Preclinical pharmacology of zoledronic acid. *Semin Oncol* **29**(6 Suppl 21): 3-11.

Greenspan, S. L., Harris, S. T., Bone, H., Miller, P. D., Orwoll, E. S., Watts, N. B. and Rosen, C. J. (2000) Bisphosphonates: safety and efficacy in the treatment and prevention of osteoporosis. *Am Fam Physician* **61**(9): 2731-6.

Gunji, H., Hosaka, K., Huffman, M. A., Kawanaka, K., Matsumoto-Oda, A., Hamada, Y. and Nishida, T. (2003) Extraordinarily low bone mineral density in an old female chimpanzee (*Pan troglodytes schweinfurthii*) from the Mahale Mountains National Park. *Primates* **44**(2): 145-9.

Guo, X. E. and Kim, C. H. (2002) Mechanical consequence of trabecular bone loss and its treatment: a three-dimensional model simulation. *Bone* **30**(2): 404-11.

Haddock, S. M., Yeh, O. C., Mummaneni, P. M., Rosenberg, W. S. and Keaveny, T. M. (2000) Fatigue behavior of human vertebral trabecular bone. *34th Annual Meeting ORS, Feb. 1-4, Atlanta* **25**: 733.

- Hardiman, D. A., O'Brien, F. J., Prendergast, P. J., Croke, D. T., Staines, A. and Lee, T. C. (2005) Tracking the changes in unloaded bone: Morphology and gene expression. *Eur J Morphol* **42**(4-5): 208-16.
- Hazenbergh, J. G., Taylor, D. and Lee, T. C. (2007) The role of osteocytes and bone microstructure in preventing osteoporotic fractures. *Osteoporos Int* **18**(1): 1-8.
- Hirano, T., Burr, D. B., Turner, C. H., Sato, M., Cain, R. L. and Hock, J. M. (1999) Anabolic effects of human biosynthetic parathyroid hormone fragment (1-34), LY333334, on remodeling and mechanical properties of cortical bone in rabbits. *J Bone Miner Res* **14**(4): 536-45.
- Hirano, T., Turner, C. H., Forwood, M. R., Johnston, C. C. and Burr, D. B. (2000) Does suppression of bone turnover impair mechanical properties by allowing microdamage accumulation? *Bone* **27**(1): 13-20.
- Hodgen, G. D., Goodman, A. L., O'Connor, A. and Johnson, D. K. (1977) Menopause in rhesus monkeys: model for study of disorders in the human climacteric. *Am J Obstet Gynecol* **127**(6): 581-4.
- Hornby, S. B., Ford, S. L., Mase, C. A. and Evans, G. P. (1995) Skeletal changes in the ovariectomised ewe and subsequent response to treatment with 17 beta oestradiol. *Bone* **17**(4 Suppl): 389S-394S.
- Hui, S. L., Slemenda, C. W. and Johnston, C. C., Jr. (1988) Age and bone mass as predictors of fracture in a prospective study. *J Clin Invest* **81**(6): 1804-9.
- Innui, K., Takaoka K. (2003) Etidronate. *Nippon Rinsho* **61**:2, 226-30.
- Ito, M., Hayashi, K., Ishida, Y., Uetani, M., Yamada, M., Ohki, M. and Nakamura, T. (1997) Discrimination of spinal fracture with various bone mineral measurements. *Calcif Tissue Int* **60**(1): 11-5.
- Ito, M., Nishida, A., Koga, A., Ikeda, S., Shiraishi, A., Uetani, M., Hayashi, K. and Nakamura, T. (2002) Contribution of trabecular and cortical components to the mechanical properties of bone and their regulating parameters. *Bone* **31**(3): 351-8.

Jacobsen, S. J., Cooper, C., Gottlieb, M. S., Goldberg, J., Yahnke, D. P. and Melton, L. J. (1992) Hospitalization with vertebral fracture among the aged: a national population-based study, 1986-1989. *Epidemiology* **3**(6): 515-8.

Jaworski, Z. F., Liskova-Kiar, M. and Uhthoff, H. K. (1980) Effect of long-term immobilisation on the pattern of bone loss in older dogs. *J Bone Joint Surg Br* **62-B**(1): 104-10.

Jerome, C. P., Carlson, C. S., Register, T. C., Bain, F. T., Jayo, M. J., Weaver, D. S. and Adams, M. R. (1994) Bone functional changes in intact, ovariectomized, and ovariectomized, hormone-supplemented adult cynomolgus monkeys (*Macaca fascicularis*) evaluated by serum markers and dynamic histomorphometry. *J Bone Miner Res* **9**(4): 527-40.

Jerome, C. P., Lees, C. J. and Weaver, D. S. (1995) Development of osteopenia in ovariectomized cynomolgus monkeys (*Macaca fascicularis*). *Bone* **17**(4 Suppl): 403S-408S.

Johnell, O. and Kanis, J. A. (2006) An estimate of the worldwide prevalence and disability associated with osteoporotic fractures. *Osteoporos Int* **17**(12): 1726-33.

Johnson, R. B., Gilbert, J. A., Cooper, R. C., Parsell, D. E., Stewart, B. A., Dai, X., Nick, T. G., Streckfus, C. F., Butler, R. A. and Boring, J. G. (2002) Effect of estrogen deficiency on skeletal and alveolar bone density in sheep. *J Periodontol* **73**(4): 383-91.

Junqueira L, C. and J, C. (1998). *Basic Histology, a Text and Atlas*. McGraw-Hill Publishing Co.

Kalu, D. N. (1991) The ovariectomized rat model of postmenopausal bone loss. *Bone Miner* **15**(3): 175-91.

Kanis, J. A. (2000) An update on the diagnosis of osteoporosis. *Curr Rheumatol Rep* **2**(1): 62-6.

Kaplan, S. J., Hayes, W. C., Stone, J. L. and Beaupre, G. S. (1985) Tensile strength of bovine trabecular bone. *J Biomech* **18**(9): 723-7.

- Kaplan, S. J., Hayes, W. C., Stone, J. L. and Beaupre, G. S. (1985) Tensile strength of bovine trabecular bone. *J Biomech* **18**(9): 723-7.
- Katz, J. L. (1980) The structure and biomechanics of bone. *Symp Soc Exp Biol* **34**: 137-68.
- Keaveny, T. M., Wachtel, E. F., Cutler, M. J. and Pinilla, T. P. (1994) Yield strains for bovine trabecular bone are isotropic but asymmetric. *34th Annual Meeting ORS, Feb. 1-4, Atlanta* **19**: 428.
- Keaveny, T. M., Wachtel, E. F., Ford, C. M. and Hayes, W. C. (1994) Differences between the tensile and compressive strengths of bovine tibial trabecular bone depend on modulus. *J Biomech* **27**: 1137-1146.
- Keaveny, T. M., Wachtel, E. F. and Kopperdahl, D. L. (1999) Mechanical behavior of human trabecular bone after overloading. *J Orthop Res* **17**: 346-53.
- Khastgir, G., Studd, J., Holland, N., Alaghband-Zadeh, J., Fox, S. and Chow, J. (2001) Anabolic effect of estrogen replacement on bone in postmenopausal women with osteoporosis: histomorphometric evidence in a longitudinal study. *J Clin Endocrinol Metab* **86**(1): 289-95.
- Kimmel, D. B. and Jee, W. S. (1982) A quantitative histologic study of bone turnover in young adult beagles. *Anat Rec* **203**(1): 31-45.
- Klibanski A, B. T., Blair SN, Boden SD, Dickersin K, Gifford DR, Glasse L, Goldring SR, Hruska K, Johnson SR, McCauley LK, Russell WE (2001) Osteoporosis prevention, diagnosis, and therapy. *JAMA* **285**(6): 785-95.
- Kopperdahl, D. L., Pearlman, J. L. and Keaveny, T. M. (2000) Biomechanical consequences of an isolated overload on the human vertebral body. *Journal of Orthopaedic Research* **18**: 685-690.
- Krajcinovic, D. and Lemaitre, J. (1987). *Continuum Damage Mechanics: Theory and Applications*. New York, Springer Verlag.
- Laib, A., Barou, O., Vico, L., Lafage-Proust, M. H., Alexandre, C. and Rugseger, P. (2000) 3D micro-computed tomography of trabecular and cortical bone architecture

with application to a rat model of immobilisation osteoporosis. *Med Biol Eng Comput* **38**(3): 326-32.

Lalla, S., Hothorn, L. A., Haag, N., Bader, R. and Bauss, F. (1998) Lifelong administration of high doses of ibandronate increases bone mass and maintains bone quality of lumbar vertebrae in rats. *Osteoporos Int* **8**(2): 97-103.

Lang, T. F., Guglielmi, G., van Kuijk, C., De Serio, A., Cammisa, M. and Genant, H. K. (2002) Measurement of bone mineral density at the spine and proximal femur by volumetric quantitative computed tomography and dual-energy x-ray absorptiometry in elderly women with and without vertebral fractures. *Bone* **30**(1): 247-50.

Lanyon, L. E. and Bourn, S. (1979) The influence of mechanical function on the development and remodeling of the tibia. An experimental study in sheep. *J Bone Joint Surg Am* **61**(2): 263-73.

Lanyon, L. E., Goodship, A. E., Pye, C. and McFie, H. (1982) Mechanically adaptive bone remodeling: a quantitative study on functional adaption in the radius following ulna osteotomy in sheep. *J Biomech* **15**: 141-154.

Lee, T. C., Myers, E. R. and Hayes, W. C. (1998) Fluorescence-aided detection of microdamage in compact bone. *J Anat* **193** (Pt 2): 179-84.

Lee, T. C., Staines, A. and Taylor, D. (2002) Bone adaptation to load: microdamage as a stimulus for bone remodelling. *J Anat* **201**(6): 437-46.

Lee, T. C. and Taylor, D. (2003) Quantification of ovine bone adaptation to altered load: morphometry, density, and surface strain. *Eur J Morphol* **41**(3-4): 117-25.

Legrand, E., Chappard, D., Pascaretti, C., Duquenne, M., Krebs, S., Rohmer, V., Basle, M. F. and Audran, M. (2000) Trabecular bone microarchitecture, bone mineral density, and vertebral fractures in male osteoporosis. *J Bone Miner Res* **15**(1): 13-9.

Les, C. M., Spence, C. A., Vance, J. L., Christopherson, G. T., Patel, B., Turner, A. S., Divine, G. W. and Fyhrie, D. P. (2004) Determinants of ovine compact bone viscoelastic properties: effects of architecture, mineralization, and remodeling. *Bone* **35**(3): 729-38.

- Lill, C. A., Fluegel, A. K. and Schneider, E. (2002) Effect of ovariectomy, malnutrition and glucocorticoid application on bone properties in sheep: a pilot study. *Osteoporos Int* **13**(6): 480-6.
- Lindsay, R. (1990) Fluoride and bone--quantity versus quality [editorial; comment]. *N Engl J Med* **322**(12): 845-6.
- Macleay, J. M., Olson, J. D. and Turner, A. S. (2004) Effect of dietary-induced metabolic acidosis and ovariectomy on bone mineral density and markers of bone turnover. *J Bone Miner Metab* **22**(6): 561-8.
- Malpaux, B. and Karsch, F. J. (1990) A role for short days in sustaining seasonal reproductive activity in the ewe. *J Reprod Fertil* **90**(2): 555-62.
- Martin, R., Burr, D. and Sharkey, N. (1998). *Skeletal Tissue Mechanics*. New York, Springer Verlag.
- Martin, R. B. (2000) Toward a unifying theory of bone remodeling. *Bone* **26**(1): 1-6.
- Martin, R. B. and Burr, D. B. (1982) A hypothetical mechanism for the stimulation of osteonal remodelling by fatigue damage. *J Biomech* **15**(3): 137-9.
- Mashiba, T., Turner, C. H., Hirano, T., Forwood, M. R., Jacob, D. S., Johnston, C. C. and Burr, D. B. (2001,a) Effects of high-dose etidronate treatment on microdamage accumulation and biomechanical properties in beagle bone before occurrence of spontaneous fractures. *Bone* **29**(3): 271-8.
- Mashiba, T., Turner, C. H., Hirano, T., Forwood, M. R., Johnston, C. C. and Burr, D. B. (2001,b) Effects of suppressed bone turnover by bisphosphonates on microdamage accumulation and biomechanical properties in clinically relevant skeletal sites in beagles. *Bone* **28**(5): 524-31.
- McCubbrey, D. A., Cody, D. D., Peterson, E. L., Kuhn, J. L., Flynn, M. J. and Goldstein, S. A. (1995) Static and fatigue failure properties of thoracic and lumbar vertebral bodies and their relation to regional density. *J Biomech* **28**(8): 891-9.

- McLain, R. F., Yerby, S. A. and Moseley, T. A. (2002) Comparative morphometry of L4 vertebrae: comparison of large animal models for the human lumbar spine. *Spine* **27**(8): E200-6.
- Meier, C., Nguyen, T. V., Center, J. R., Seibel, M. J. and Eisman, J. A. (2005) Bone resorption and osteoporotic fractures in elderly men: the dubbo osteoporosis epidemiology study. *J Bone Miner Res* **20**(4): 579-87.
- Melton, L. J. (1995) How many women have osteoporosis now? *J Bone Miner Res* **10**(2): 175-177.
- Melton, L. J., 3rd, Wahner, H. W. and Riggs, B. L. (1988) Bone density measurement. *J Bone Miner Res* **3**(1): ix-x.
- Meunier, P. J. and Boivin, G. (1997) Bone mineral density reflects bone mass but also the degree of mineralization of bone: therapeutic implications. *Bone* **21**(5): 373-7.
- Meurman, K. O. and Elfving, S. (1980) Stress fracture in soldiers: a multifocal bone disorder. A comparative radiological and scintigraphic study. *Radiology* **134**(2): 483-7.
- Mitton, D., Rumelhart, C., Hans, D. and Meunier, P. J. (1997) The effects of density and test conditions on measured compression and shear strength of cancellous bone from the lumbar vertebrae of ewes. *Med Eng Phys* **19**(5): 464-74.
- Mohsin, S., O'Brien, F. J. and Lee, T. C. (2006) Microcracks in compact bone: a three-dimensional view. *J Anat* **209**(1): 119-24.
- Mosekilde, L. (1989) Sex differences in age-related loss of vertebral trabecular bone mass and structure--biomechanical consequences. *Bone* **10**(6): 425-32.
- Mosekilde, L. and Mosekilde, L. (1986) Normal vertebral body size and compressive strength: relations to age and to vertebral and iliac trabecular bone compressive strength. *Bone* **7**: 207-212.
- Mosekilde, L., Weisbrode, S. E., Safron, J. A., Stills, H. F., Jankowsky, M. L., Ebert, D. C., Danielsen, C. C., Sogaard, C. H., Franks, A. F., Stevens, M. L. and et al. (1993) Calcium-restricted ovariectomized Sinclair S-1 minipigs: an animal model of osteopenia and trabecular plate perforation. *Bone* **14**(3): 379-82.

- Nalla, R. K., Kruzic, J. J., Kinney, J. H. and Ritchie, R. O. (2005) Aspects of in vitro fatigue in human cortical bone: time and cycle dependent crack growth. *Biomaterials* **26**(14): 2183-95.
- Newman, E., Turner, A. S. and Wark, J. D. (1995) The potential of sheep for the study of osteopenia: current status and comparison with other animal models. *Bone* **16**(4 Suppl): 277S-284S.
- Newton, B. I., Cooper, R. C., Gilbert, J. A., Johnson, R. B. and Zardiackas, L. D. (2004) The ovariectomized sheep as a model for human bone loss. *J Comp Pathol* **130**(4): 323-6.
- Noble, B. S., Stevens, H., Loveridge, N. and Reeve, J. (1997) Identification of apoptotic changes in osteocytes in normal and pathological human bone. *Bone* **20**(3): 273-82.
- Norman, T. L. and Wang, Z. (1997) Microdamage of human cortical bone: incidence and morphology in long bones. *Bone* **20**(4): 375-9.
- Nuzzo, S., Peyrin, F., Cloetens, P., Baruchel, J. and Boivin, G. (2002) Quantification of the degree of mineralization of bone in three dimensions using synchrotron radiation microtomography. *Med Phys* **29**(11): 2672-81.
- O'Brien F, J., Hardiman, D. A., Hazenberg, J. G., Mercy, M. V., Mohsin, S., Taylor, D. and Lee, T. C. (2005) The behaviour of microcracks in compact bone. *Eur J Morphol* **42**(1-2): 71-9.
- O'Brien, F. J., Taylor, D. and Clive Lee, T. (2005) The effect of bone microstructure on the initiation and growth of microcracks. *J Orthop Res* **23**(2): 475-80.
- O'Brien, F. J., Taylor, D. and Lee, T. C. (2003) Microcrack accumulation at different intervals during fatigue testing of compact bone. *J Biomech* **36**(7): 973-80.
- O'Brien, F. J., Taylor, D. and Lee, T. C. (2002) An improved labelling technique for monitoring microcrack growth in compact bone. *J Biomech* **35**: 523-26.
- O'Brien, F. J., Taylor, D., Dickson G.R., and Lee, T. C. (2000) Visualisation of three-dimensional microcracks in compact bone. *J Anat* **197**: 413-420.

- Owan, I., Burr, D. B., Turner, C. H., Qiu, J., Tu, Y., Onyia, J. E. and Duncan, R. L. (1997) Mechanotransduction in bone: osteoblasts are more responsive to fluid forces than mechanical strain. *Am J Physiol* **273**(3 Pt 1): C810-5.
- Parfitt, A. M. (1983). The physiologic and clinical significance of bone histomorphometric data. Bone histomorphometry: techniques and interpretation. R. R. Recker. Boca Raton, FL, CRC Press: 143-223.
- Parfitt, A. M. (1992) Implications of architecture for the pathogenesis and prevention of vertebral fracture. *Bone* **13**: S41-S47.
- Parfitt, A. M. (1996). The skeletal heterogeneity and the purposes of bone remodeling: implications for the understanding of osteoporosis. Osteoporosis. R. Marcus, D. Feldman and J. Kelsey. San Diego, Academic Press: 1672.
- Parfitt, A. M. (2002) High bone turnover is intrinsically harmful: two paths to a similar conclusion. The Parfitt view. *J Bone Miner Res* **17**(8): 1558-9; author reply 1560.
- Parfitt, A. M. (2002) Misconceptions (2): turnover is always higher in cancellous than in cortical bone. *Bone* **30**(6): 807-9.
- Parfitt, A. M., Drezner, M. K., Glorieux, F. H., Kanis, J. A., Malluche, H., Meunier, P. J., Ott, S. M. and Recker, R. R. (1987) Bone histomorphometry: standardization of nomenclature, symbols, and units. Report of the ASBMR Histomorphometry Nomenclature Committee. *J Bone Miner Res* **2**(6): 595-610.
- Parkesh, R., Clive Lee, T. and Gunnlaugsson, T. (2007) Highly selective 4-amino-1,8-naphthalimide based fluorescent photoinduced electron transfer (PET) chemosensors for Zn(II) under physiological pH conditions. *Org Biomol Chem* **5**(2): 310-7.
- Pastoureau, P., Charrier, J., Blanchard, M. M., Boivin, G., Dulor, J. P., Theriez, M. and Barenton, B. (1989) Effects of a chronic GRF treatment on lambs having low or normal birth weight. *Domest Anim Endocrinol* **6**(4): 321-9.
- Pattin, C. A., Caler, W. E. and Carter, D. R. (1996) Cyclic mechanical property degradation during fatigue loading of cortical bone. *J Biomech* **29**(1): 69-79.

- Prendergast, P. J. and Huiskes, R. (1996) Microdamage and osteocyte-lacuna strain in bone: a microstructural finite element analysis. *J Biomech Eng* **118**(2): 240-6.
- Rahn, B. A. (1977) Polychrome fluorescence labelling of bone formation, instrumental aspects and experimental use. *Zeiss Information* **22**(85): 36-39.
- Reid, I. R., Brown, J. P., Burckhardt, P., Horowitz, Z., Richardson, P., Trechsel, U., Widmer, A., Devogelaer, J. P., Kaufman, J. M., Jaeger, P., Body, J. J., Brandi, M. L., Broell, J., Di Micco, R., Genazzani, A. R., Felsenberg, D., Happ, J., Hooper, M. J., Ittner, J., Leb, G., Mallmin, H., Murray, T., Ortolani, S., Rubinacci, A., Saaf, M., Samsioe, G., Verbruggen, L. and Meunier, P. J. (2002) Intravenous zoledronic acid in postmenopausal women with low bone mineral density. *N Engl J Med* **346**(9): 653-61.
- Reifenstein, E. C. and Albright, F. (1947) The Metabolic Effects Of Steroid Hormones In Osteoporosis. *J Clin Invest* **26**(1): 24-56.
- Reilly, D. T. and Burstein, A. H. (1974) Review article. The mechanical properties of cortical bone. *J Bone Joint Surg* **56**(5): 1001-22.
- Reisz, R. R. and Muller, J. (2004) Molecular timescales and the fossil record: a paleontological perspective. *Trends Genet* **20**(5): 237-41.
- Rice, J. C., Cowin, S. C. and Bowman, J. A. (1988) On the dependence of the elasticity and strength of cancellous bone on apparent density. *J Biomech* **21**(2): 155-168.
- Riggs, B. L. and Melton, L. J., 3rd (2002) Bone turnover matters: the raloxifene treatment paradox of dramatic decreases in vertebral fractures without commensurate increases in bone density. *J Bone Miner Res* **17**(1): 11-4.
- Riggs, B. L. and Parfitt, A. M. (2005) Drugs used to treat osteoporosis: the critical need for a uniform nomenclature based on their action on bone remodeling. *J Bone Miner Res* **20**(2): 177-84.
- Rigotti, N. A., Neer, R. M., Skates, S. J., Herzog, D. B. and Nussbaum, S. R. (1991) The clinical course of osteoporosis in anorexia nervosa. A longitudinal study of cortical bone mass. *JAMA* **265**(9): 1133-8.

Rosen, C. J. (2000) Pathogenesis of osteoporosis. *Baillieres Best Pract Res Clin Endocrinol Metab* **14**(2): 181-93.

Ross M, H. and Romrell L, J. (1989). *Histology - A Text and Atlas.*, Williams and Wilkins, Baltimore.

Ross, P. D., Davis, J. W., Epstein, R. S. and Wasnich, R. D. (1991) Pre-existing fractures and bone mass predict vertebral fracture incidence in women. *Ann Intern Med* **114**(11): 919-23.

Ross, P. D., He, Y. F., Davis, J. W., Epstein, R. S. and Wasnich, R. D. (1994) Normal ranges for bone loss rates. *Bone Miner* **26**(2): 169-80.

Salter R, B. (1970). *Textbook of Disorders and Injuries of the Musculoskeletal System*, Lippincott Williams and Wilkins.

Sanderlin, B. W. and Raspa, R. F. (2003) Common stress fractures. *Am Fam Physician* **68**(8): 1527-32.

Sansom, I. J., Smith, M. P., Armstrong, H. A. and Smith, M. M. (1992) Presence of the earliest vertebrate hard tissue in conodonts. *Science* **256**(5061): 1308-11.

Schaffler, M. B., Choi, K. and Milgrom, C. (1995) Aging and matrix microdamage accumulation in human compact bone. *Bone* **17**(6): 521-525.

Schapira, D. and Schapira, C. (1992) Osteoporosis: the evolution of a scientific term. *Osteoporos Int* **2**(4): 164-7.

Scheuer, L. and Black, S. (2004). *The Juvenile Skeleton*, Elsevier Academic Press.

Schmidt-Nielsen, K. (1977). The physiology of wild animals. Proceedings of the Royal Society of London Biological Society. **199** (1136):345-60

Schorlemmer, S., Gohl, C., Iwabu, S., Ignatius, A., Claes, L. and Augat, P. (2003) Glucocorticoid treatment of ovariectomized sheep affects mineral density, structure, and mechanical properties of cancellous bone. *J Bone Miner Res* **18**(11): 2010-5.

Schorlemmer, S., Ignatius, A., Claes, L. and Augat, P. (2005) Inhibition of cortical and cancellous bone formation in glucocorticoid-treated OVX sheep. *Bone* **37**(4): 491-6.

- Schultheis, L., Ruff, C. B., Rastogi, S., Bloomfield, S., Hogan, H. A., Fedarko, N., Thierry-Palmer, M., Ruiz, J., Bauss, F. and Shapiro, J. R. (2000) Disuse bone loss in hindquarter suspended rats: partial weightbearing, exercise and ibandronate treatment as countermeasures. *J Gravit Physiol* **7**(2): P13-4.
- Seeman, E. and Delmas, P. D. (2006) Bone quality--the material and structural basis of bone strength and fragility. *N Engl J Med* **354**(21): 2250-61.
- Sevostianov, I. and Kachanov, M. (2000) Impact of the porous microstructure on the overall elastic properties of the osteonal cortical bone. *J Biomech* **33**(7): 881-8.
- Shen, V., Dempster, D. W., Birchman, R., Mellish, R. W., Church, E., Kohn, D. and Lindsay, R. (1992) Lack of changes in histomorphometric, bone mass, and biochemical parameters in ovariectomized dogs. *Bone* **13**(4): 311-6.
- Sigrist, I. M., Gerhardt, C., Alini, M., Schneider, E. and Egermann, M. (2007) The long-term effects of ovariectomy on bone metabolism in sheep. *J Bone Miner Metab* **25**(1): 28-35.
- Silva, M. J., Brodt, M. D. and Uthgenannt, B. A. (2004) Morphological and mechanical properties of caudal vertebrae in the SAMP6 mouse model of senile osteoporosis. *Bone* **35**(2): 425-31.
- Smith, S. Y., Recker, R. R., Hannan, M., Muller, R. and Bauss, F. (2003) Intermittent intravenous administration of the bisphosphonate ibandronate prevents bone loss and maintains bone strength and quality in ovariectomized cynomolgus monkeys. *Bone* **32**(1): 45-55.
- Soderman, K., Bergstrom, E., Lorentzon, R. and Alfredson, H. (2000) Bone mass and muscle strength in young female soccer players. *Calcif Tissue Int* **67**(4): 297-303.
- Sparidans, R. W., Twiss, I. M. and Talbot, S. (1998) Bisphosphonates in bone diseases. *Pharm World Sci* **20**(5): 206-13.
- Stokstad, E. (2005) Bone quality fills holes in fracture risk. *Science* **308**(5728): 1580.
- Taylor, D. (1998) Fatigue of bone and bones: an analysis based on stressed volume. *J Orthop Res* **16**(2): 163-9.

Taylor, D. (2000) Scaling effects in the fatigue strength of bones from different animals. *J Theor Biol* **206**(2): 299-306.

Taylor, D., O'Brien, F., Prina-Mello, A., Ryan, C., O'Reilly, P. and Lee, T. C. (1999) Compression data on bovine bone confirms that a "stressed volume" principle explains the variability of fatigue strength results. *J Biomech* **32**(11): 1199-203.

Thomsen, J. S., Ebbesen, E. N. and Mosekilde, L. (2002) Predicting human vertebral bone strength by vertebral static histomorphometry. *Bone* **30**(3): 502-8.

Turner, A. S. (2001) Animal models of osteoporosis--necessity and limitations. *Eur Cell Mater* **1**: 66-81.

Turner, A. S., Alvis, M., Myers, W., Stevens, M. L. and Lundy, M. W. (1995) Changes in bone mineral density and bone-specific alkaline phosphatase in ovariectomized ewes. *Bone* **17**(4 Suppl): 395S-402S.

Turner, A. S., Mallinckrodt, C. H., Alvis, M. R. and Bryant, H. U. (1995) Dose-response effects of estradiol implants on bone mineral density in ovariectomized ewes. *Bone* **17**(4 Suppl): 421S-427S.

Turner, A. S., Mallinckrodt, C. H., Alvis, M. R. and Bryant, H. U. (1995) Dual-energy X-ray absorptiometry in sheep: experiences with in vivo and ex vivo studies. *Bone* **17**(4 Suppl): 381S-387S.

Turner, A. S. and Villanueva, A., R. (1994) Static and dynamic histomorphometric data in 9- to 11-year old ewes. *Vet Comp Ortho Traum* **7**: 101-109.

Turner, C. H. (2002) Determinants of skeletal fragility and bone quality. *J Musculoskelet Neuronal Interact* **2**(6): 527-8.

Turner, R. T., Evans, G. L. and Wakley, G. K. (1995) Spaceflight results in depressed cancellous bone formation in rat humeri. *Aviat Space Environ Med* **66**(8): 770-4.

Verborgt, O., Gibson, G. J. and Schaffler, M. B. (2000) Loss of osteocyte integrity in association with microdamage and bone remodeling after fatigue in vivo. *J Bone Miner Res* **15**(1): 60-7.

- Waarsing, J. H., Day, J. S., van der Linden, J. C., Ederveen, A. G., Spanjers, C., De Clerck, N., Sasov, A., Verhaar, J. A. and Weinans, H. (2004) Detecting and tracking local changes in the tibiae of individual rats: a novel method to analyse longitudinal in vivo micro-CT data. *Bone* **34**(1): 163-9.
- Weinbaum, S., Cowin, S. C. and Zeng, Y. (1994) A model for the excitation of osteocytes by mechanical loading-induced bone fluid shear stresses. *J Biomech* **27**(3): 339-60.
- Wilke, H. J., Kettler, A., Wenger, K. H. and Claes, L. E. (1997) Anatomy of the sheep spine and its comparison to the human spine. *Anat Rec* **247**(4): 542-55.
- Wolff, J. (1892). *Das Gesetz der Transformation der Knochen*. Berlin, Hirschwald.
- Wronski, T. J., Lowry, P. L., Walsh, C. C. and Ignaszewski, L. A. (1985) Skeletal alterations in ovariectomized rats. *Calcif Tissue Int* **37**(3): 324-8.
- Wronski, T. J., Yen, C. F. and Scott, K. S. (1991) Estrogen and diphosphonate treatment provide long-term protection against osteopenia in ovariectomized rats. *J Bone Miner Res* **6**(4): 387-94.
- Yoshitake, K., Yokota, K., Kasugai, Y., Kagawa, M., Sukamoto, T. and Nakamura, T. (1999) Effects of 16 weeks of treatment with tibolone on bone mass and bone mechanical and histomorphometric indices in mature ovariectomized rats with established osteopenia on a low-calcium diet. *Bone* **25**(3): 311-9.
- Zioupos, P. (2001) Ageing human bone: factors affecting its biomechanical properties and the role of collagen. *J Biomater Appl* **15**(3): 187-229.
- Zioupos, P., Currey, J. D. and Hamer, A. J. (1999) The role of collagen in the declining mechanical properties of aging human cortical bone. *J Biomed Mater Res* **45**(2): 108-16.

APPENDICES

Appendix 3.1: Data from mechanical testing of control and OVX metatarsal samples

	CONTROL		
	Strength[MP]	Modulus[GP]	Work to Fracture [kJ/mm^2]
1	158.9	19.6725	2.92
2	153.73	20.93	2.11
3	118.25	14.2295	1.03
4	0	0	0
5	131.41	17.368	2.7
6	104.65	14.563	1.52
7	172.13	10.489	2.91
8	0	0	0
9	0	0	0
10	0	0	0
11	0	0	0
12	121.36	18.764	2.56
13	89.16	11.7405	2.46
14	0	0	0
15	0	0	0
16	134.99	21.543	2.21
17			
18	0	0	0
19		0	0
20	153.8	21.914	2.97
21	0	0	0
22	144.09	17.2815	3.54
23	0	0	0
24	0	0	0
25	0	0	0
26	0	0	0
27	143.05	16.263	3.6
28	149.88	17.2635	3.86
29	108.13	14.668	2.35
30			
31	133.07	17.14	2.83
32	0	0	0
33	0	0	0
34	120.62	16.719	2.62
Mean	133.57625	16.90928125	2.636875
SD	22.24851512	3.269939571	0.728255621

OVX			
	Strength[MPa/]	Modulus[GPa]	Work to Fracture [kJ/mm^2]
1	0	0	0
2	0	0	0
3	0	0	0
4	102.65	10.325	1.38
5	0	0	0
6	0	0	0
7	0	0	0
8	146.76	16.5935	2.45
9	80.8	10.5915	2.1
10	74.18	10.491	1.28
11	107.49	18.9165	2.36
12	0	0	0
13	0	0	0
14	93.7	19.3505	1.11
15	125.3	19.096	1.15
16	0	0	0
17			
18	147.27	12.1155	3.91
19	160.8	13.84	2.78
20	0	0	0
21	144.9	11.272	3.54
22	0	0	0
23	146.59	15.7905	3.936
24	135.64	11.872	2.72
25	132.57	18.744	2.58
26	86.15	6.204	2.11
27	0	0	0
28	0	0	0
29	0	0	0
30			
31	0	0	0
32	154.57	17.3045	3.84
33	123.97	15.671	2.101
34	0	0	0
Mean	122.70875	14.26109375	2.4591875
SD	28.1741361	3.979861401	0.966945239